AUTOMATIC DEVELOPMENT OF GLOBAL PHASE DIAGRAMS FOR BINARY SYSTEMS IN PRESSURE-TEMPERATURE SPACE

A Thesis Submitted to the

College of Graduate Studies and Research

in Partial Fulfillment of the Requirements

for the Degree of Master of Science

in the

Department of Chemical Engineering

University of Saskatchewan

Saskatoon, Canada

By

Quan Yang

PERMISSION TO USE

In presenting this thesis in partial fulfillment of the requirements for a Postgraduate degree from the University of Saskatchewan, I agree that the Libraries of this University may make it freely available for inspection. I further agree that permission for copying of this thesis in any manner, in whole or in part, for scholarly purposes may be granted by the professor who supervised my thesis work or, in his absence, by the Head of the Department or the Dean of the College in which my thesis work was done. It is understood that any copying, publication, or use of this thesis or parts thereof for financial gain shall not be allowed without my written permission. It is also understood that due recognition shall be given to me and to the University of Saskatchewan in any scholarly use which may be made of any material in my thesis.

Requests for permission to copy or to make other use of material in this thesis in whole or part should be addressed to:

Head of the Department of Chemical Engineering

University of Saskatchewan

Saskatoon, Saskatchewan S7N 5A9

Canada

ABSTRACT

Global phase diagrams of binary systems in pressure-temperature (*PT*) space are very useful. In this project the techniques to automatically develop global phase diagrams in *PT* space were created. The codes to compute different components of a global phase diagram in *PT* space were developed. These codes were then successfully incorporated into a single functional program.

To generate the binary *PT* phase diagram, the overall composition was varied from pure component 2, the least volatile component (LVC) to pure component 1, the most volatile component (MVC). The step size for changing mole fraction was varied in the calculation of different parts of a global phase diagram. When the points near the joining points between different parts were computed, the step size was set to a rather small value. The step size was then increased to twice of the last value for each subsequent point computed. When the MVC mole fraction was approaching one, the step size was set to a small value to obtain enough points needed to minimize the chances of missing important phenomena.

The techniques to set initial guesses for evaluation of different components of a global phase diagram were discussed. The code performance, including the number of iterations for different convergence criteria and the sensitivity of the algorithm were presented. Using the code developed, phase diagrams of type I, type II, type III and type V were generated using representative binary systems from the petroleum processing field.

The boundary states between different types of phase behaviour were also explored. It was observed that with the increase of the binary interaction parameters, the phase behaviour of the ethane + ethanol binary system changes from type I to type II to type III while the methane + n-hexane binary system changes from type V to type III. These conclusions matched the results of van Konynenburg and Scott (1980). It was also concluded that with the increase of the binary interaction parameter for a binary system, the system showed a trend to exhibit more liquid-liquid immiscibility.

ACKNOWLEDGEMENTS

I would like to show my gratitude to Professor Phoenix for his support and assistance throughout the research. I would like to thank Professor Peng for his help and advice. I would also like to acknowledge the committee members for their valuable work.

I am also grateful to my colleagues and friends. With them, I enjoy the time spent at the laboratory.

DEDICATED TO,

My Family.

TABLE OF CONTENTS

LIST OF TABLES

LIST OF FIGURES

NOMENCLATURE

a .....Temperature dependant energy parameter of equation of state (Pa.m^6/mol^2)

A .....Helmholtz free energy (J/mol)

b ..... Co-volume parameter of equation of state (m^3/mol)

C .....Cubic term of the Taylor series expansion of Helmholtz energy

f_{ij} .....Fugacity of component i in phase j (Pa)

f .....Fugacity (Pa)

F .....Tangent plane distance (J.mol)

g.....Function used in phase equilibrium computation

G .....Gibbs free energy (J/mol)

H .....Helmholtz free energy (J/mol)

$H(\bar{x},t)$ .....Function for Newton homotopy

ΔH_v .....Enthalpy for vapourization of liquid (J/mol)

J .....Jacobian matrix

K.....Tangent plane distance at stationary point (J/mol)

K_{ij} .....Binary interaction parameter of component i, j

M.....Number of components in a phase

n.....Mole number

N.....Number of components

P .....Pressure (bar)

P_{vp} .....Vapour pressure of pure component (bar)

q_{ij} .....Element of matrix Q in i th column and j th row

Q.....Matrix derived from the quadratic form of the Taylor series expansion of the Helmholtz free energy

R.....Universal gas constant (J/(mol • K))

S.....Entropy of a system (J/mol/K)

t .....Scalar homotopy parameter

T.....Temperature (K)

u, w .....Parameters used in common cubic equation of state

U.....Internal energy of a system (J/mol)

v.....Molar volume (l/mol)

x.....Mole fraction of component

$\bar{x}$ .....Composition vector

y.....Mole fraction of component

$\bar{y}$ .....Composition vector

Y.....Un-normalized mole fraction

z.....Mole fraction of component

$\bar{z}$ .....Composition vector

ΔZ_v .....Difference of compressibility factor after and before vapourization

Greek Symbols

ε .....Number of moles (mol)

ζ .....Parameter showing the difference between the energy parameters of the two components

θ .....Dimensionless tangent plane distance

κ .....Characteristic constant of a substance

Λ .....Parameter showing the contribution of the interaction between molecules of different components

μ .....Chemical potential (J/mol)

ξ .....Parameter showing the size ratio of molecules of different components

ϕ_i .....Fugacity coefficient of component *i*

ω .....Acentric factor

Subscripts

c.....Critical phase

i,*j*,*k*.....Component or phase indices

L .....Liquid phase

n.....Number of iterations

ref .....Reference phase

T .....Total

V .....Vapour phase

1. INTRODUCTION

1.1 Background

Binary systems are systems composed of two components. Phase diagrams of binary systems are very useful from both a theoretical standpoint and an industrial standpoint. For example, phase diagrams in pressure-temperature (*PT*) space can be employed to correlate the binary interaction parameter of an equation of state. Industrially, the importance of phase diagrams can be seen in the example of carbon dioxide in a supercritical state space (the critical pressure is 7.38 MPa and critical temperature is 304.2 K). Supercritical carbon dioxide is a common solvent in many processes, such as polymer manufacturing, pharmaceuticals and soil remediation because it is non-toxic, non-flammable and inexpensive (Suleimenov et al., 2003). The design of such processes must require knowledge of the vapour-liquid equilibrium for pure components and mixtures (Choi and Yeo, 1998). Such knowledge can be obtained from phase diagrams in *PT* space.

Many researchers have studied phase diagrams (Christov and Dohrn, 2002). A significant improvement in experimental methods and theoretical modeling of the vapour-liquid equilibrium data has been achieved. However, there are still some

unresolved problems coming from the chemical industry that need to be solved, like the design of the catalytic cracking of bitumen and heavy oil where the knowledge of liquid-liquid-vapour phase behaviour is essential.

1.2 Critical Points, Critical Endpoints and Three-Phase Lines

In a global phase diagram in pressure-temperature (*PT*) space, there are critical points, critical endpoints and three-phase points. A critical point of a pure component is a point in phase space where two or more phases become identical.

A pressure-volume diagram for a pure component is shown in Figure 1-1. Four isotherms are indicated in the diagram by the dotted lines. It is observed that when the temperature of a system is less than the critical temperature, T_c, and the pressure is increased to the corresponding vapour pressure at that temperature, there will be vapour-liquid (VL) coexisting. When the temperature of a system is higher than the critical temperature, T_c, no matter how the pressure of the system is increased, there will be no point where a liquid phase and a vapour phase coexit. Thus, the critical point for a pure component can also be defined as the point with the highest temperature and pressure where a liquid phase and a vapour phase coexist.

The critical points of a mixture are points where the properties of two or more coexisting phases become identical. A more precise definition for critical points will be given in chapter three. At a critical point of a binary system, the degree of freedom for the system is one, so in a global *PT* phase diagram, different critical points corresponding to different pressures make up critical lines. At a

three-phase point of a binary system or a vapour pressure point of a pure component, the degree of freedom is also one. Thus three-phase lines and vapour pressure lines are observed. For some binary systems, the critical line joins with a three-phase line. The point joining the critical line and the three-phase line is named the critical endpoint. At a critical endpoint within a binary system, the degree of freedom is zero, therefore it is represented by a single point in a *PT* phase diagram. At the critical endpoint, an additional phase is in equilibrium with a critical phase.

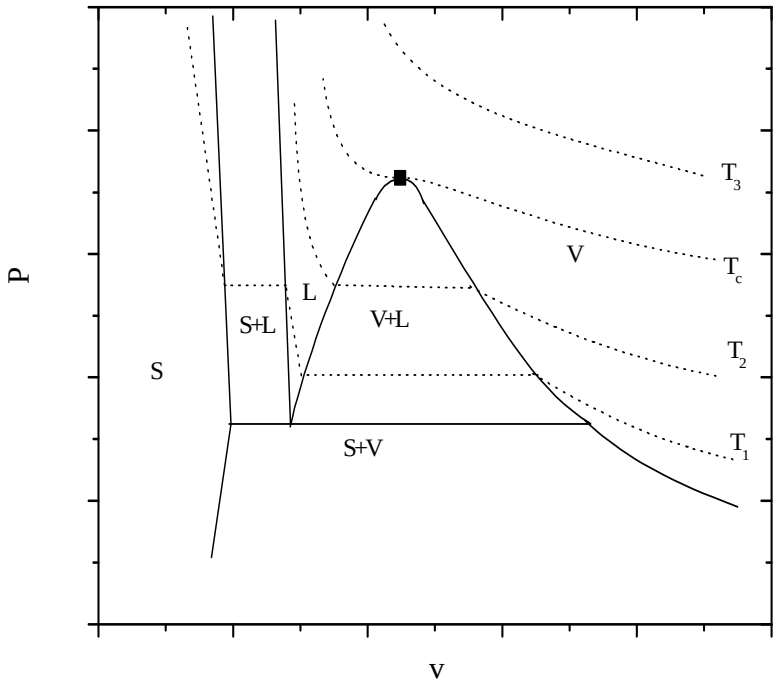

Figure 1-1 Typical pressure-volume phase digram for a pure component showing the critical point (■) and four isotherms. ($T_3 > T_c > T_2 > T_1$). S, L and V represent solid, liquid and vapour phases, respectively.

A three-phase line is composed of three-phase points, indicating where three phases coexist. At a three-phase point, the same component has equal fugacity in all three phases.

Figure 1-2 is an example global phase diagram in *PT* space for a binary system where phase behaviours including pure component vapour-liquid curves, critical phenomena and liquid-liquid-vapour coexisting curves over a large pressure and temperature range are presented.

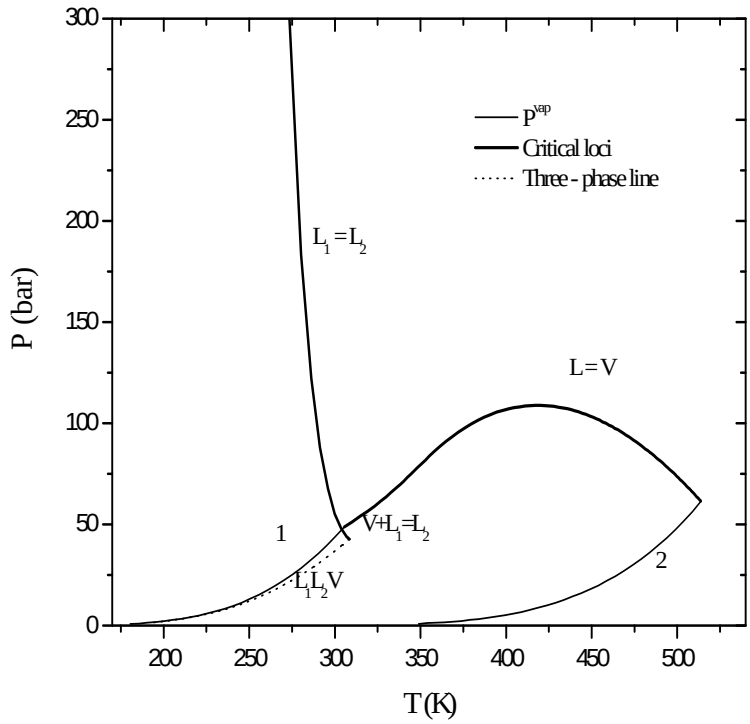

Figure 1-2 Example figure showing global phase diagram in *PT* space. $L_1=L_2$ and L = V stand for critical line. L_1L_2V stands for three-phase line and $V+L_1=L_2$ represents critical endpoint.

1.3 Equation of State

To predict the global phase diagram, an equation of state needs to be used. An equation of state is employed to relate the pressure, temperature, composition and molar volume of a system. Some equations of state are given as pressure-explicit and some are written as volume-explicit. Some equations are empirical correlations (for example, two- and three-parameter correlations of compressibility factor) while some other equations are analytic equations with a theoretical basis (for example, the Ideal Gas Law, the virial equation and cubic equations of state).

The Ideal Gas Law ($P = RT / v$) is not applicable to a liquid phase. For the virial equation, it is usually difficult to correlate or compute the virial coefficients and the commonly used virial equation only contains the second virial coefficient ($Pv / RT = 1 + B / v$). As a result, the deviation from experimental results may not be small. At a certain pressure, only one molar volume satisfies the virial equation containing only the second virial coefficient. The cubic equations of state have a relatively simple form and can also be used to evaluate thermodynamic properties, such as *G*, *H*, *S* and *A*, which represent Gibbs free energy, enthalpy, entropy and Helmholtz free energy, respectively. Using these computed properties, a cubic equation of state can be used to evaluate chemical potentials and fugacities, which may then be employed to predict complex phase behaviour.

The common cubic equation of state can be expressed as (Reid et al., 1987):

$$P = \frac{RT}{v - b} - \frac{a}{v^2 + ubv + wb^2} \tag{1.1}$$

where *P*, *v* and *T* represents pressure molar volume and temperature of the system, respectively.

The parameters *a* and *b* in equation (1.1) are the energy parameter and the size parameter, respectively. *b* is also called the co-volume parameter (Wang and Sadus, 2003). For a mixture, the following van der Waals mixing rules are employed in the project to evaluate *a* and *b*:

$$a = \sum_i \sum_j x_i x_j (1 - K_{ij}) a_i^{1/2} a_j^{1/2} \tag{1.2}$$

$$b = \sum_i x_i b_i \tag{1.3}$$

K_{ij} stands for the binary interaction parameter for the binary mixture. a_i and b_i are the energy parameter and size parameter for pure component *i*, respectively. a_i and b_i are determined by matching vapour pressure and liquid densities data for a pure component or through a generalized correlation. x_i is the mole fraction of species *i* in the mixture. It is observed that with the decrease of K_{ij}, the parameter *a* increases and the pressure of the system at a fixed volume, temperature and composition decreases.

In this project, the Peng-Robinson equation of state (Peng and Robinson, 1976) has been employed, for which the values for *u* and *w* are 2 and -1, respectively.

An isotherm plotted using the Peng-Robinson equation of state is shown in Figure 1-3. In the figure, it is observed that at pressure p_1, three molar volumes are obtained. Among them, v_2 is discarded because $\left(\frac{\partial p}{\partial v}\right)_T > 0$; This value, the mechanical compressibility, should be negative because the volume of an isolated

system decreases when the pressure on it increases. Thus two molar volumes, v_1 for a vapour phase, and v_3 for a liquid phase, are obtained.

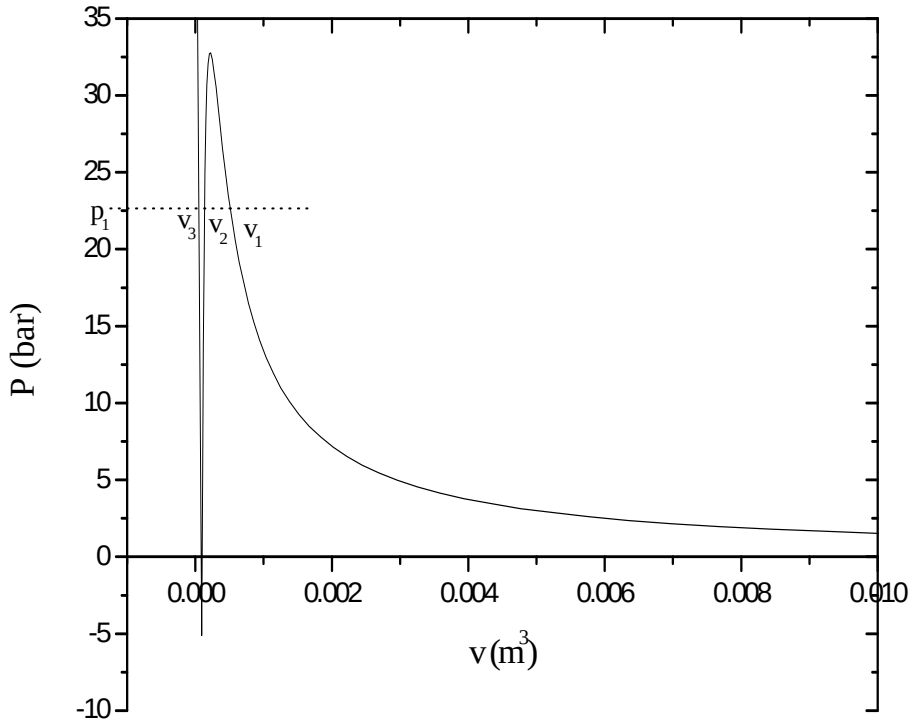

Figure 1-3 Isotherm for pure methane at 185.4 K plotted according to the Peng-Robinson equation of state. At pressure p_1, three molar volumes are obtained. Among them, v_2 is discarded because here $\left(\frac{\partial p}{\partial v}\right)_T > 0$.

1.4 Objective and Scope

Global phase diagrams are very important from both a theoretical and industrial standpoint. Development of an algorithm to compute global phase diagrams is essential to the study of the relationships between equation of state parameters and phase behaviour.

The objectives of the project are set as:

- To code algorithms for computing critical lines and three-phase lines of binary systems, and for computing the vapour pressure line of pure components;
- To compute global phase diagrams of different types of phase behaviour. An algorithm to automatically predict the whole global phase diagram will be developed using the individual codes developed in the first objective;
- To explore the transition between different types of phase behaviour. The phase behaviour of two binary systems will be explored when the binary interaction parameters of the corresponding binary mixture increase;
- To analyze the performance of the code. The developed code should be able to evaluate global phase diagrams automatically. It should be able to determine the type of phase behaviour of the explored binary system precisely and automatically. The iteration times and sensitivity of the algorithms with respect to different convergence criterions will be analyzed.

The project focuses on the systems used in, or representative of, the petroleum processing field. Methane + alkane binaries, ethane + alkanol binaries and a binary mixture of propane + phenanthrene are explored in this project because these mixtures show types I, II, III and V binary phase behaviour according to van

Konynenburg and Scott's (1980) classification scheme. The deviation of the computed results from the experimental data will not be taken into consideration.

1.5 Thesis Overview

A literature review on the classification schemes of phase behaviour and the global phase diagram is presented in Chapter 2. The mathematical framework for locating phase behaviour phenomena is presented in Chapter 3. The algorithms based on the mathematical framework are discussed in Chapter 4. The calculated results, discussion and analysis of the code performance are in Chapter 5 and the conclusions and recommendations are in Chapter 6. In the Appendix, the properties of the explored systems in the project are shown.

2. LITERATURE REVIEW

2.1 Introduction

In this chapter, the classification scheme of phase behaviour as developed by van Konynenburg and Scott (1980) is presented. The global phase diagrams proposed by different researchers are then discussed and the research to explore different parts of a phase diagram in *PT* space is summarized. Algorithms for predicting a single element of a global phase diagram are then presented. Finally, the Newton-Raphson method and the successive substitution methods are discussed to provide the necessary backgrounds in numerical methods.

2.2 van Konynenburg and Scott's Phase Behaviour Classification Scheme

Van Konynenburg and Scott (1980) developed a classification scheme for the phase behaviour of binary mixtures. The scheme was based on the nature of the phase diagrams in pressure-temperature (*PT*) space: the shape of critical lines and the presence or absence of three-phase lines and critical endpoints. Example global phase diagrams for type I to type VII phase behaviour of binary systems according to van Konynenburg and Scott's classification scheme are presented in Figure 2-1 to Figure 2-7. In the phase diagrams, VL(1) and VL(2) stand for the vapour

pressure lines of component 1 and 2, respectively. L = V represents the vapour-liquid critical line, and L_1L_2V stands for the liquid-liquid-vapour (L_1L_2V) three-phase line. The liquid phases are identified as having a smaller molar volume compared to the vapour phase in equilibrium with the liquid phase. $L_1 = L_2$ represents the liquid-liquid ($L_1 = L_2$) critical line. UCEP and LCEP stand for upper critical endpoint and lower critical endpoint, respectively.

Figure 2-1 shows a *PT* phase diagram for type I phase behaviour of a binary mixture. It is observed that besides the two pure component vapour pressure lines, only one continuous critical line joining the two pure component critical points is present. Experiments have shown that the phase behaviour of a binary mixture of ethane + n-heptane is an example of type I phase behaviour (van Konynenburg and Scott, 1980).

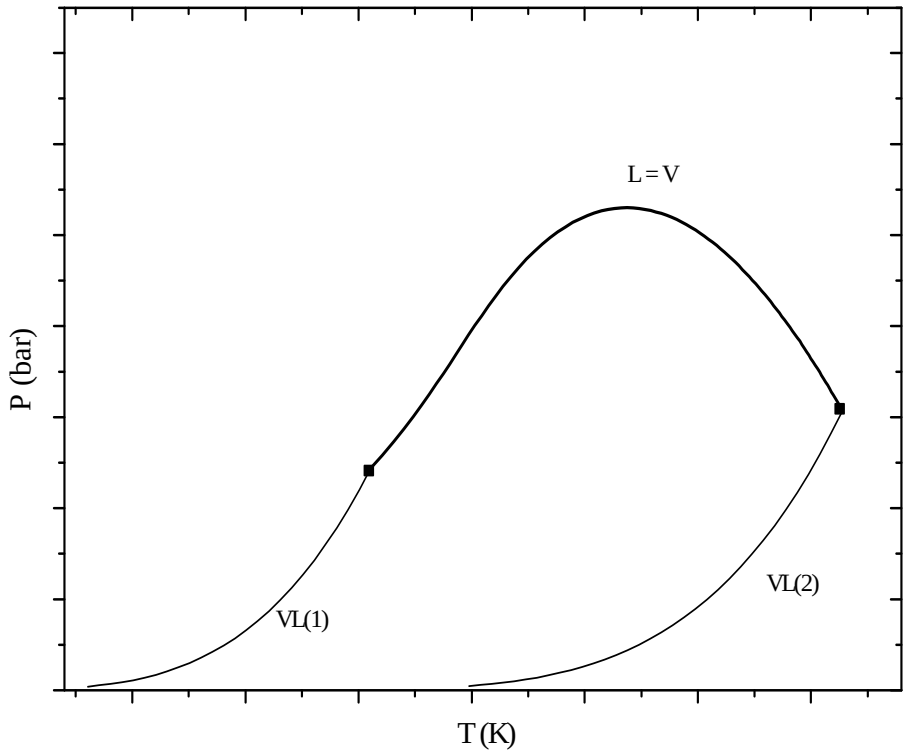

Figure 2-1 Example global phase diagram in *PT* space for type I phase behaviour of binary systems: (■) pure component critical point.

When the attraction interaction between unlike molecules decreases, a binary mixture may show type II phase behaviour. Figure 2-2 is the phase diagram for a type II binary system. Two critical lines are present. The L = V critical line connects the two pure component critical points and the $L_1 = L_2$ critical line starts from an upper critical endpoint (UCEP) and extends to high pressure. A UCEP usually lies at a position with higher pressure and temperature in *PT* space than a lower critical endpoint (LCEP). When only one critical endpoint is present for a three-phase line, if the endpoint has larger pressure than any other three-phase

points in the three-phase line, the endpoint is a UCEP and if the pressure of the endpoint is lower than any other points in the three-phase line, the endpoint is a LCEP. In type II phase behaviour, a three-phase line also commences from the UCEP and extends to lower pressure. It is observed that there is one additional $L_1 = L_2$ critical line and one additional three-phase line in type II global phase diagrams compared to the lines in type I systems. The carbon dioxide + n-octane system is an example of a type II binary system (van Konynenburg and Scott, 1980).

Figure 2-3a shows type III binary phase behaviour. Two critical lines are present. One starts from the pure solute (less volatile component) critical point and extends to very high pressure. The other one commences from the pure MVC (most volatile component) critical point and ends at an UCEP. A three-phase line is observed to start from the UCEP and extends to lower pressure. The continuous L = V critical line in type I and type II phase diagrams becomes two separate parts in a type III phase diagram. If the critical line starting from the critical point of the pure solute shows a local minimum, such phase behaviour belongs to type IIIm (Figure 2-3b) according to van Konynenburg and Scott's classification scheme. The systems methane + n-heptane (Chang et al., 1966) and carbon dioxide + n-tridecane are examples of type III and type IIIm binary systems, respectively.

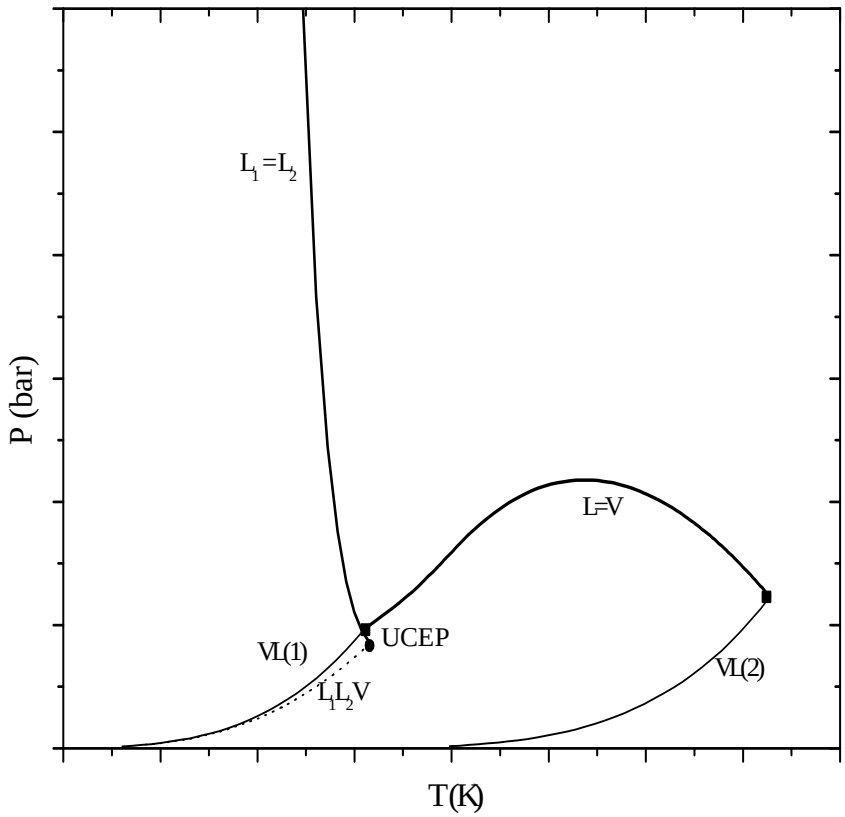

Figure 2-2 Example global phase diagram in *PT* space for type II phase behaviour of binary systems: (■) pure component critical point, (●) critical endpoint.

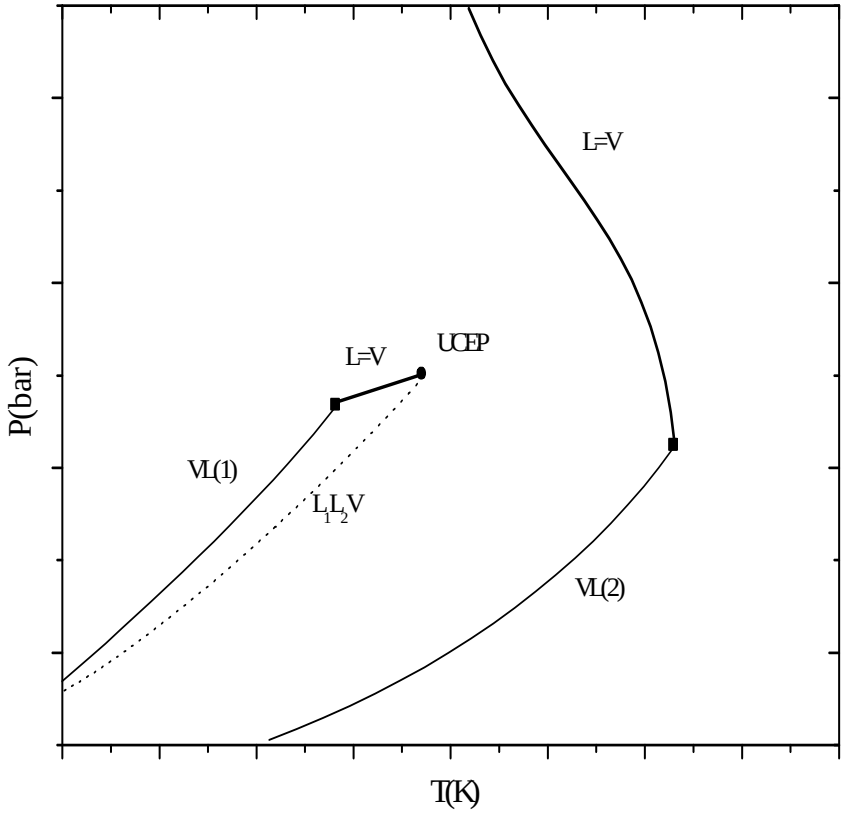

Figure 2-3a Example global phase diagram in *PT* space for type III phase behaviour of binary mixtures: (■) pure component critical point, (●) critical endpoint.

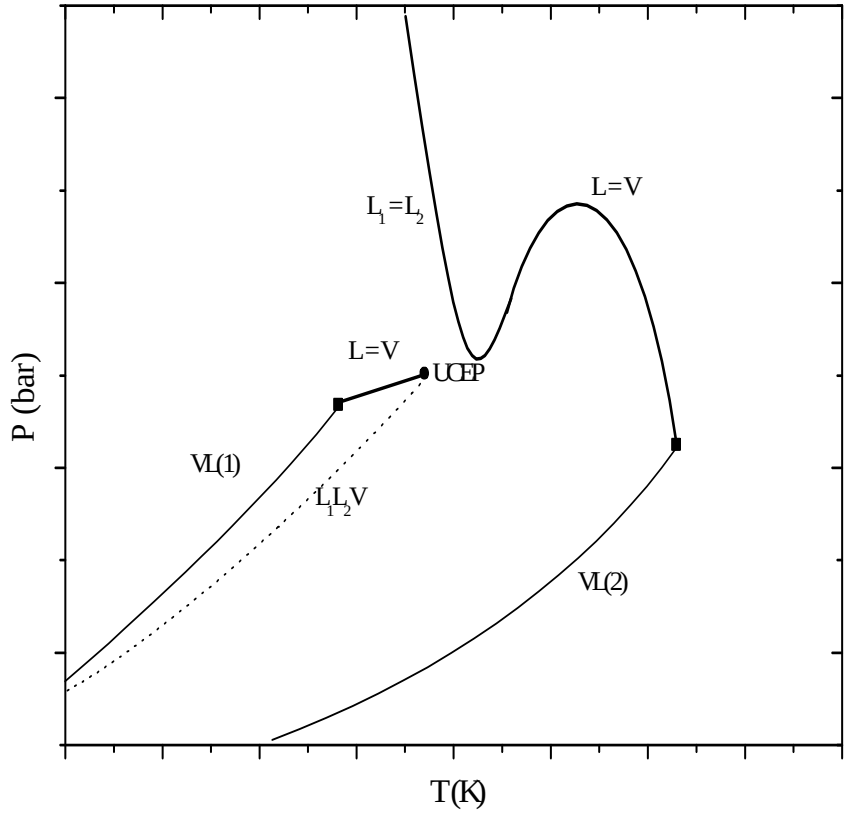

Figure 2-3b Example global phase diagram in *PT* space for type IIIm phase behaviour of binary mixtures: (■)pure component critical point, (●) critical endpoint.

Figure 2-4 is a phase diagram showing type IV phase behaviour. Three critical lines are present in the phase diagram of such a type. Two are L = V critical lines and another one is a $L_1 = L_2$ critical line. The two L = V critical lines, commencing from pure component critical points, both end at a critical endpoint, one UCEP and one LCEP. Between the two critical endpoints, a three-phase line is bounded. Another critical endpoint, a UCEP, exists in the phase diagram. From this second UCEP, a $L_1 = L_2$ critical line extends to very high pressure. A three-

phase line commencing from the second UCEP is observed as well. It extends to lower pressure. The methane + 1-hexene and methane + 3, 3-dimethlpentane (van Konynenburg and Scott, 1980) systems are examples of type IV binary systems.

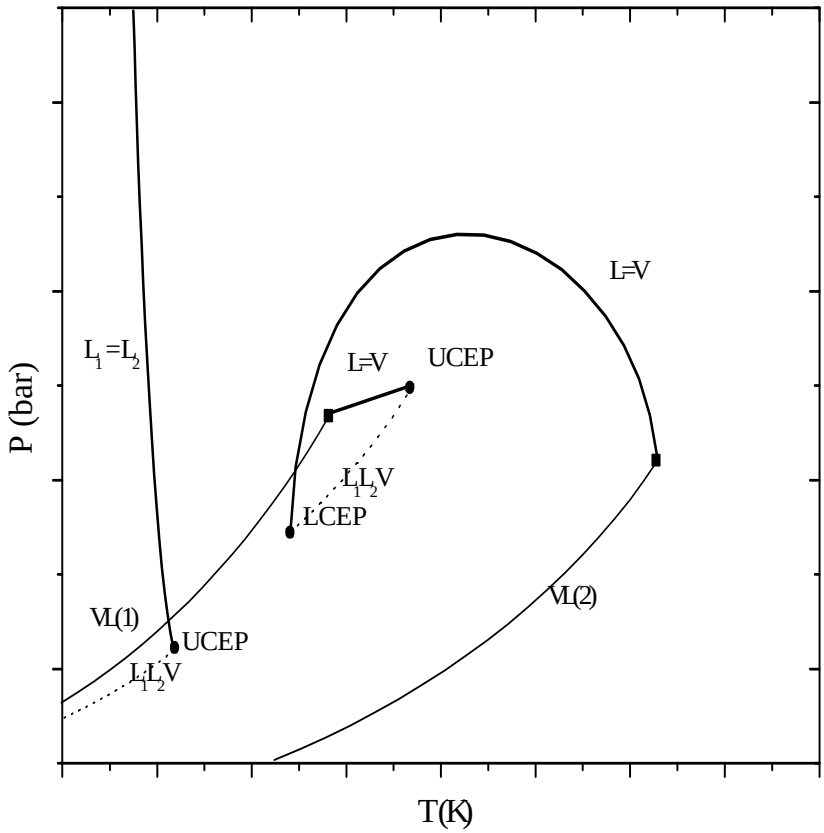

Figure 2-4 Example global phase diagram in *PT* space for type IV phase behaviour of binary mixtures: (■)pure component critical point, (●)critical endpoint.

When the difference in attraction interaction between like molecules of the two components becomes larger, a binary mixture may show type V phase behaviour. Figure 2-5 is a phase diagram showing type V binary phase behaviour. Compared to type IV behaviour, type V behaviour has no $L_1 = L_2$ critical line or

low pressure three-phase line. The two critical lines commencing from pure component critical points both end at a critical endpoint, one UCEP and one LCEP. A three-phase line is bounded between the two critical endpoints. The methane + n-hexane and carbon dioxide + nitrobenzene systems are examples of type V binary systems (van Konynenburg and Scott, 1980).

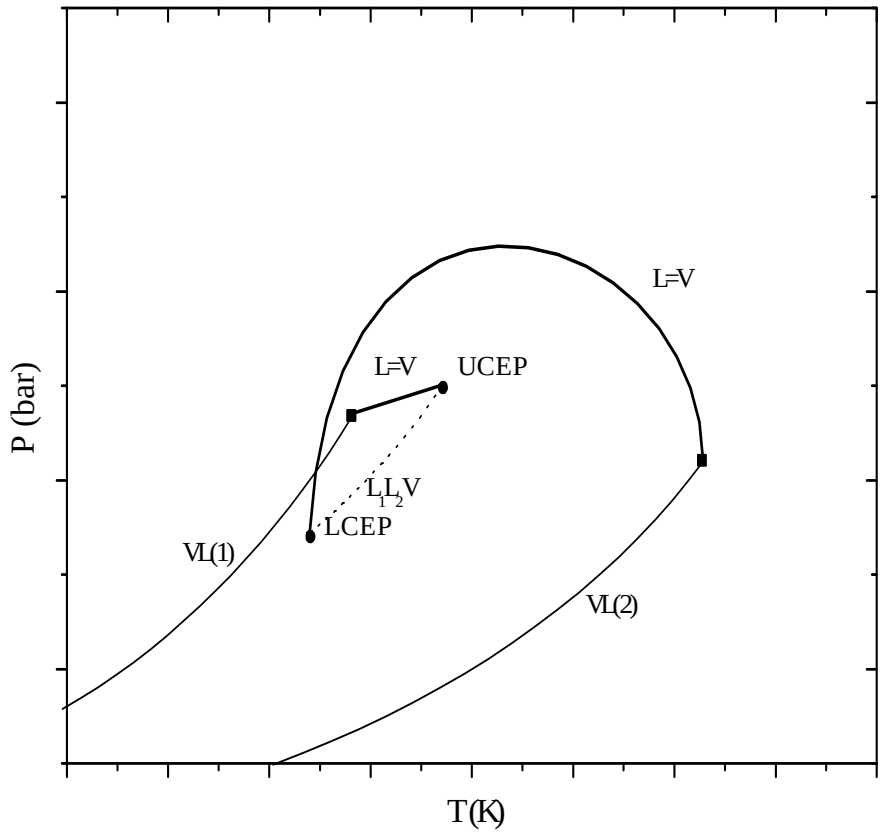

Figure 2-5 Example global phase diagram in *PT* space for type V phase behaviour of binary mixture: (■)pure component critical point, (●)critical endpoint.

Figure 2-6 is a phase diagram for type VI binary phase behaviour. It is observed that such phase behaviour has one additional closed-loop $L_1 = L_2$ critical

line and one additional three-phase line when compared with the phase diagram of type II phase behaviour. The two endpoints of the closed-loop $L_1 = L_2$ critical line are one LCEP and one UCEP. A three-phase line is bounded between the two critical endpoints. Type VI phase behaviour is observed in some aqueous or strongly polar systems (Kraska and Deiters, 1992); for example, the binary mixture D_2O + 2- methyl-pyridine (Gubblns et al., 1983).

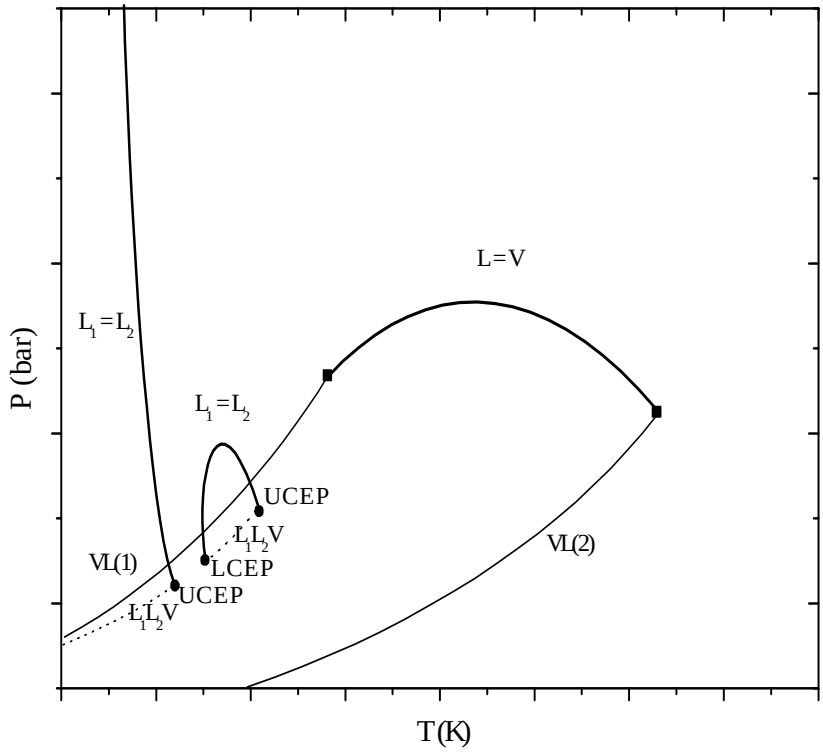

Figure 2-6 Example global phase diagram in *PT* space for type VI phase behaviour of binary mixture: (■) pure component critical point, (●) critical endpoint.

Figure 2-7 is a phase diagram showing type VII binary phase behaviour. It is observed that such a phase diagram has one additional closed-loop $L_1 = L_2$

critical line and one additional three-phase line when compared with the phase diagram of type IV phase behaviour. The two endpoints of the additional $L_1 = L_2$ critical line are one LCEP and one UCEP. A three-phase line is bounded between the two critical endpoints.

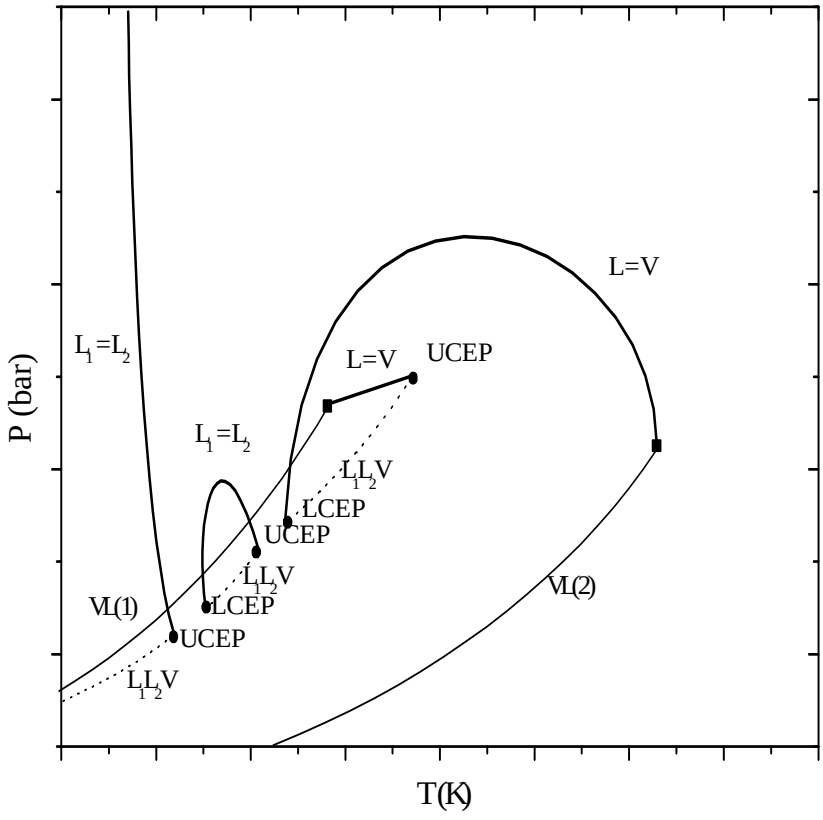

Figure 2-7 Example global phase diagram in *PT* space for type VII phase behaviour of binary mixtures: (■) pure component critical point, (●) critical endpoint.

From the above global phase diagrams for the seven types of binary phase behaviour, it is observed that vapour pressure lines, critical lines, three-phase lines

and critical endpoints are the four major parts of global phase diagrams. From the examples of different phase behaviours, it is observed that the binary mixture of methane + n-hexane is type V binary system, while the binary systems of methane + n-heptane and methane + 1-hexene are type III and type IV binary systems, respectively. The similarity and differences between molecules play an important role in phase behaviour, resulting in different types of phase behaviours and the corresponding phase diagrams.

2.3 Global Phase Diagrams

2.3.1 Global Phase Diagrams Developed by van Konynenburg and Scott

The global phase diagrams to be developed in this project are *PT* projections. The $\zeta - \Lambda$ projections developed by van Konynenburg and Scott (1980) using the van der Waals equation of state are also called global phase diagrams (Deiters and Pegg, 1989). In the calculation of the $\zeta - \Lambda$ projections, three parameters are defined:

$$\xi = (b_{22} - b_{11})/(b_{11} + b_{22}), \tag{2.1}$$

$$\zeta = (\frac{a_{22}}{b_{22}^2} - \frac{a_{11}}{b_{11}^2})/(\frac{a_{11}}{b_{11}^2} + \frac{a_{22}}{b_{22}^2}), \text{ and} \tag{2.2}$$

$$\Lambda = (\frac{a_{11}}{b_{11}^2} - \frac{2a_{12}}{b_{11}b_{22}} + \frac{a_{22}}{b_{22}^2})/(\frac{a_{11}}{b_{11}^2} + \frac{a_{22}}{b_{22}^2}). \tag{2.3}$$

In the above equations, *a* is the energy parameter and *b* is the size parameter for the equation of state. ξ shows the size ratio of molecules of different

components. Λ shows the contribution of the attraction interaction between molecules of different components. If a_{ij} is defined for a mixture as

$$a_{ij} = (1 - K_{ij}) a_{ii}^{1/2} a_{jj}^{1/2} \tag{2.4}$$

then if a binary interaction parameter K_{ij} increases, Λ increases as well, and corresponds to a decrease in the attraction between molecules of different components. ζ shows the difference between the energy parameters of the two components.

Figure 2-8 and Figure 2-9 are the global phase diagrams developed by van Konynenburg and Scott. It was observed that when ξ increases, most of the lines in the global phase diagram move right. As mentioned above, with the increase of a binary interaction parameter, the parameter Λ increases. When the size difference between the molecules of two components increases, for example, in the case when one component of a binary mixture with methane changes from n-hexane to n-heptane, the parameter Λ will increase. With the increase of Λ, the phase behaviour may transfer from type I to type II to type III or from type V to type III.

Besides the increase of Λ, the variation of ζ can also result in changes of the types of phase behaviour of binary systems. For a type I binary system, from the global phase diagrams (Figure 2-8 and 2-9), one can see that with the increase of ζ, when the difference in the attraction between like molecules of the two components increases, the phase behaviour may vary from type I to type V. The larger difference in attraction between like molecules of the two components results in additional critical endpoints and three-phase lines of a global phase diagram corresponding to type V phase behaviour.

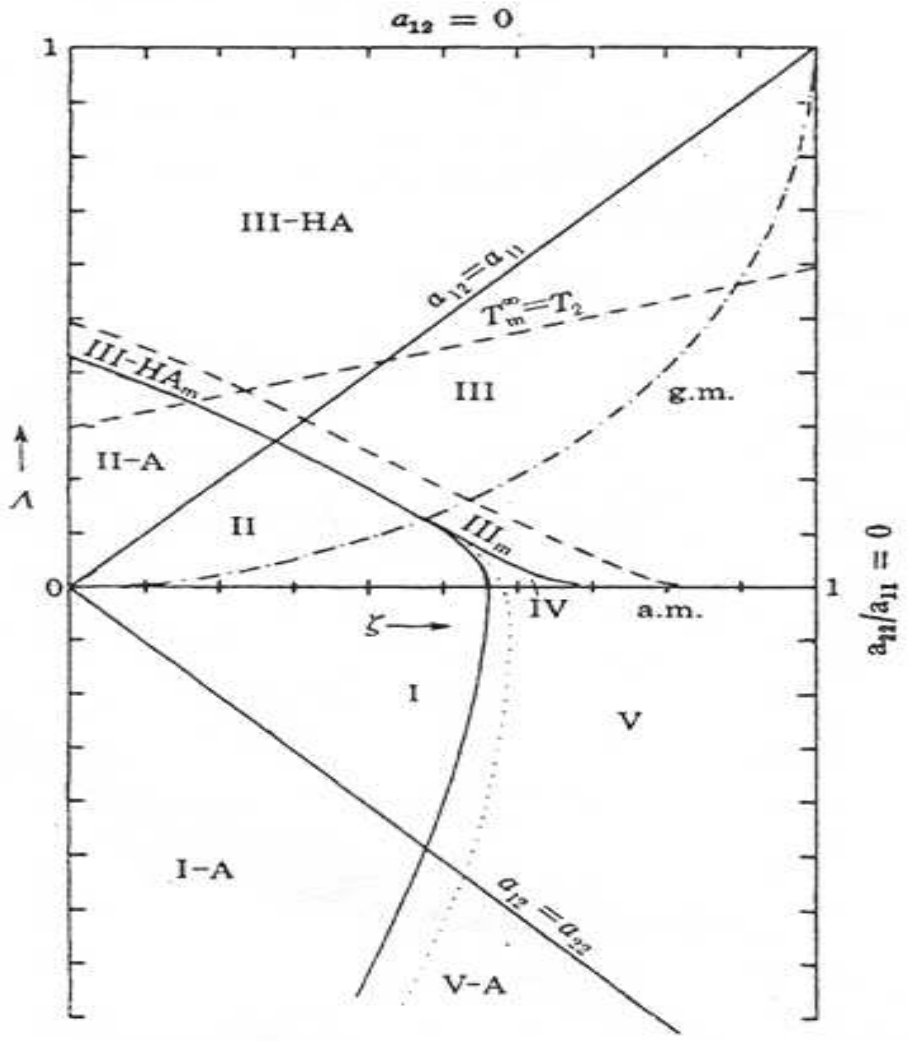

Figure 2-8: A global phase diagram for equal-sized molecules ($\xi = 0$) predicted by van Konynenburg and Scott (1980). The figure is symmetric so only the right side is presented.

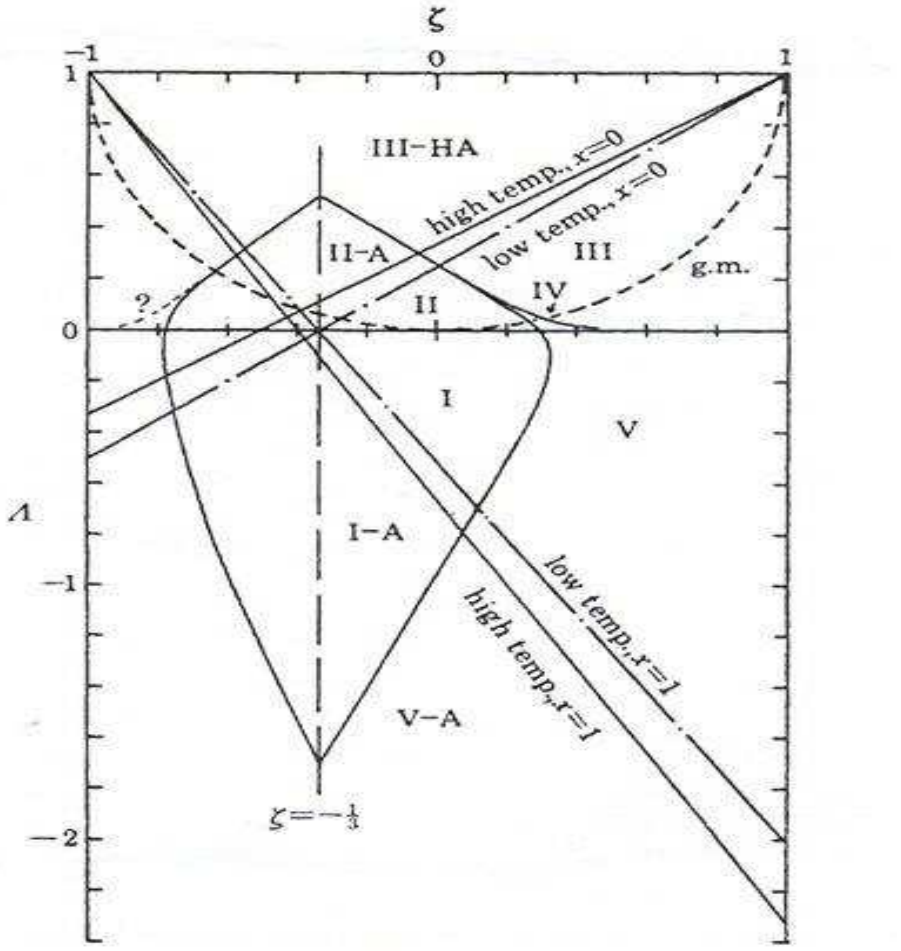

Figure 2-9: A global phase diagram for unequal-sized molecules ($\xi = 0.333$) predicted by van Konynenburg and Scott (1980).

Deiters and Pegg (1989) developed $\zeta - \Lambda$ projections using the Redlich-Kwong equation of state (Redlich and Kwong, 1949). For equal-sized molecules, the global phase diagrams developed employing the Redlich-Kwong equation of state are very similar to those obtained using the van der Waals equation of state. For molecules of unequal sizes, the phase diagrams obtained become topologically different. Type VI and type VII phase behaviour, which were not observed in the global phase diagrams developed by van Konynenburg and Scott (1980), could

instead be predicted with the Redlich-Kwong equation of state because this equation contains a temperature related term.

Wang and Sadus (2003) also developed global phase diagrams using the Carnahan-Starling-van der Waals equation of state. Their global phase diagrams are presented in terms of pure component properties. The abscissa and ordinate of the developed global phase diagrams are the ratio of the critical temperatures and the ratio of the critical volumes of pure components, respectively. The regions for type VI and VII phase behaviour, which the van der Waals equation of state is unable to predict, are observed in the global phase diagrams they developed.

2.4 Global Phase Diagram for Binary Systems in PT Space

Phase behaviours of different systems have been explored by many researchers. Suleimenov et al. (2003) evaluated the phase behaviour of pure tetrachloride and its binary mixture with carbon dioxide using the grand canonical histogram-reweighting Monte Carlo method. Huckaby et al. (1986) used the Guggenheim approximation technique to compute the phase behaviour of the mixture of the two enantiomeric forms of a tetrahedral molecule. The equation employed was derived from the theories of statistical thermodynamics. Stryjek (1993) used the Soave-Redlich-Kwong equation of state to compute the phase behaviour of the binary systems composed of N_2, CH_4 and C_2H_6 with alkanes. Scalise et al. (1989) explored the azeotropic states and phase equilibrium of the binary mixture of CO_2 and C_2H_6 by employing the thermodynamic perturbation theory. Luszczyk (2002) did experiments to explore the vapour-liquid equilibrium

near the upper critical end point for the specific system 3-methoxypropionitrile and water. Ribeiro and Aguiar-Ricardo (2001) used an acoustic technique to explore the critical behaviour of CO_2 and $N(C_2H_5)_3$. The system exhibited type I phase behaviour according to van Konynenburg and Scott's classification scheme. Straver et al. (1993) used a Cailletet apparatus to measure the three-phase equilibrium in binary mixtures of propane + triglycerides. Kordikowski et al. (1997) used a simple acoustic method to explore the phase behaviour of the ternary systems CO_2 + CH_2F_2 + CF_3CH_2F and CO + C_2H_4 + CH_3CHCH_2, as well as their binary subsystems. Kordikowski et al. (1996) used a simple acoustic method to explore the phase behaviour of pure components (CO_2, C_2H_6, and CF_3CH_2F, refrigerant R134a) and binary mixtures of CF_3CH_2F with CO_2 or C_2H_6. Specovius et al. (1981) measured the temperatures and pressures at the upper and lower critical end points of binary mixtures of ethane + n-octadecane, n-nonadecane and n-eicosane. Straver et al. (1998) reported the experimental data of the phase behaviour of binary mixtures of propane + tristearin, which can be represented as "SSS". Gauter et al. (1999) proposed methods to model multiphase equilibrium in ternary systems composed of near-critical carbon dioxide and two solutes. Algorithms for computing critical lines and critical endpoints were developed.

It is observed that the researchers mentioned above only explore phase behaviour of specific one or two binary systems or only propose algorithms to predict separate parts of a global phase diagram in *PT* space, for example, a critical line, a three-phase line, a VL equilibrium line, etc. After different parts of a global phase diagram for binary mixtures in *PT* space are obtained, they are combined in a

single plot to get a global phase diagram. It is usually difficult to set initial guesses for evaluation of different parts because prediction of one part usually needs the computed results of another part as its initial guess. For example, when the code transfers from the evaluation of a critical line to the computation of a three-phase line, the data of the computed critical endpoint needs to be used to set initial estimates for the computation of the first three-phase point. For these reasons, it is beneficial to develop an algorithm capable of automatically calculating whole global phase diagrams for binary mixtures in *PT* space. If such a code is developed successfully, the problem of setting initial guesses encountered in other techniques for developing global phase diagrams of binary mixtures in *PT* space can be settled easily.

The following sections outline some of the methods used to compute phase behaviour relevant to *PT* phase diagrams.

2.4.1 Computation of Vapour Pressure Line

The degree of freedom for a pure component in vapour-liquid equilibrium is one. When the temperature or pressure of the system is specified, the state of the system is certain. Thus a line will represent the vapour-liquid equilibrium of pure components in global phase diagrams.

When the vapour and liquid phases of the system are in equilibrium, the fugacities of both phases are identical. Many methods are available for evaluating the vapour pressure curves (Reid, et al. 1987). The equality of chemical potential, temperature and pressure in both phases in equilibrium leads to the Clausius-Clapeyron equation, a theoretical equation:

$$\frac{d \ln P_{vp}}{d(1/T)} = -\frac{\Delta H_{vp}}{R \Delta Z_{vp}}, \tag{2.5}$$

where

$$\Delta Z_{vp} = \frac{P_{vp} \Delta V_{vp}}{RT}, \tag{2.6}$$

and where P_{vap} represents vapour pressure, ΔH_{vp} stands for the enthalpy change in the process of vapourization and ΔZ_{vp} represents compressibility factor change in the vapourization process.

Antoine (1888) proposed a simple empirical equation which has been widely used over limited temperature ranges:

$$\ln P_{vp} = A - \frac{B}{T + C} \tag{2.7}$$

where *A*, *B* and *C* are constants and can be specified using experimental data. The Antoine equation should never be used outside the applicable temperature limits. Vapour pressure evaluation for temperatures beyond these limits may lead to absurd results.

Wagner et al. (1976) proposed an empirical equation which had the following form:

$$\ln P_{vp} = \frac{a\tau + b\tau^{1.5} + c\tau^{3} + d\tau^{6}}{T_r}, \tag{2.8}$$

with

$$\tau = 1 - T_r, \tag{2.9}$$

where $T_r = T / T_c$. Values of the constants *a*, *b*, *c* and *d* were obtained by regression analysis.

The Frost-Kalkwarf-Thodos (Reid et al., 1987) equation is also widely used:

$$\ln P_{vp} = A - \frac{B}{T} + C \ln T + \frac{DP_{vp}}{T^2}. \tag{2.10}$$

Values of the constants *A*, *B*, *C* and *D* were obtained by regression analysis.

Though these empirical equations are easy to use, they should not be used beyond the corresponding temperature and pressure limits because constants have been correlated with limited experimental data.

In this project, the Peng-Robinson equation of state is employed to calculate vapour pressure of pure components. When the vapour and liquid phases of the system of a pure component are in equilibrium, the fugacities of both phases are identical. This criterion is employed to compute the vapour pressure line.

2.4.2 Computation of a Critical Line

Many researchers have developed methods for calculating the critical properties of mixtures. For mixtures with *n* components, Peng and Robinson (1977) stated that at a critical point the following two equations should be satisfied:

$$\begin{vmatrix} \dfrac{\partial^2 G}{\partial x_1^{\,2}} & \dfrac{\partial^2 G}{\partial x_1 \partial x_2} & \cdots & \dfrac{\partial^2 G}{\partial x_1 \partial x_{n-1}} \\ \dfrac{\partial^2 G}{\partial x_2 \partial x_1} & \dfrac{\partial^2 G}{\partial x_2^{\,2}} & \cdots & \dfrac{\partial^2 G}{\partial x_2 \partial x_{n-1}} \\ \cdot & \cdot & & \cdot \\ \cdot & \cdot & \cdots & \cdot \\ \dfrac{\partial^2 G}{\partial x_{n-1} \partial x_1} & \dfrac{\partial^2 G}{\partial x_{n-1} \partial x_2} & \cdots & \dfrac{\partial^2 G}{\partial x_{n-1}^{\,2}} \end{vmatrix} = 0 , \tag{2.11}$$

and

$$\begin{vmatrix} \dfrac{\partial U}{\partial x_1} & \dfrac{\partial U}{\partial x_2} & \cdots & \dfrac{\partial U}{\partial x_{n-1}} \\ \dfrac{\partial^2 G}{\partial x_2 \partial x_1} & \dfrac{\partial^2 G}{\partial x_2^{\,2}} & \cdots & \dfrac{\partial^2 G}{\partial x_2 \partial x_{n-1}} \\ \cdot & \cdot & & \cdot \\ \cdot & \cdot & \cdots & \cdot \\ \dfrac{\partial^2 G}{\partial x_{n-1} \partial x_1} & \dfrac{\partial^2 G}{\partial x_{n-1} \partial x_2} & \cdots & \dfrac{\partial^2 G}{\partial x_{n-1}^{\,2}} \end{vmatrix} = 0 , \tag{2.12}$$

where G and U represent Gibbs free energy and internal energy of the system, respectively.

Peng and Robinson (1977) then developed a method to calculate the critical point of a multi-component mixture using the Peng-Robinson equation of state. Their method was more reliable and more applicable than previous methods, for example, the technique proposed by Chueh and Prausnitz (1967), whose simple correlations computed critical points merely using the critical properties of pure components.

Michelsen (1984) presented a method to calculate critical points. It was based on the tangent plane criteria. The critical temperature and pressure were determined by direct Newton-Raphson iteration, but a close initial guess was required. However, considering the evaluation of thermodynamic properties, the

method was still cost-efficient. The partial derivatives required by the algorithm were those normally used in calculations of phase equilibrium.

Heidemann and Khalil (1980) presented their method to calculate critical points. The authors stated that the form of the critical condition most frequently used was calculated by considering the pressure, temperature and mole fractions as independent variables. But when one dealt with pressure explicit equations of state ($P = f(v,T)$), the most convenient variables to consider as independent were the temperature, the volume and the mole fractions. In their research those variables were taken as independent.

Heidemann and Khalil (1980) presented that a given phase with N components would be stable if for every isothermal variation in the state, the following condition was satisfied:

$$\left[\Delta A + P_0 \Delta V - \sum_{i=1}^{N} \mu_{i0} \Delta n_{i0}\right]_{T_0} > 0. \qquad (2.13)$$

ΔA, ΔV and Δn_{i0} are differences in Helmholtz free energy, volume of the phase and mole number of the i th component between the varied state and the initial state of the given phase, respectively. P_0 and μ_{i0} are the initial pressure and chemical potential of the given phase, respectively.

In the project, this method is employed. The technique will be discussed in detail in Chapter 3.

2.4.3 Tangent Plane Criterion

A phase will not be stable if it does not satisfy the minimum energy criterion. To ensure stability of a system, the Gibbs energy of the system should be

at the global minimum. Geometrically, if the tangent plane to the Gibbs energy surface at the composition of a test phase does not extend above the Gibbs energy surface over the entire accessible composition range, the system is stable. Otherwise, the system is unstable and the overall free energy can be reduced by splitting the test phase into two or more phases of different compositions. This, simply, is the tangent plane criterion. Baker et al. (1982) gave a mathematical proof of this tangent plane theory. Michelsen (1982) developed the following practical implementation of the tangent plane criterion:

At a given temperature and pressure (T_0, P_0), the component mole fractions of an *M*-component mixture are $z_1, z_2, ..., z_M$ and the Gibbs energy of the mixture is

$$G_0 = \sum_i n_i \mu_i^{\,0} \,. \tag{2.14}$$

If this mixture is separated into two phases, the mole numbers of the two phases are $N - \varepsilon$ and ε, respectively, ε being infinitesimal, and the mole fractions of different components in phase II are $y_1, y_2, ..., y_M$. The variation of Gibbs energy is as follows:

$$\Delta G = G_I + G_{II} - G_0 = G(N - \varepsilon) + G(\varepsilon) - G_0 \,. \tag{2.15}$$

G_I can be expanded in a Taylor series. If the second and higher order terms in ε are discarded, the following expression is yielded:

$$G(N - \varepsilon) = G(N) - \varepsilon \sum_i y_i \left(\frac{\partial G}{\partial n_i}\right)_N = G_0 - \varepsilon \sum_i y_i \mu_i^0 \tag{2.16}$$

or

$$\Delta G = G(\varepsilon) - \varepsilon \sum_i y_i \mu_i^0 = \varepsilon \sum_i y_i (\mu_i(\bar{y}) - \mu_i^0) \,. \tag{2.17}$$

The Gibbs energy of the original mixture should be at the global minimum to ensure stability. Hence a criterion for stability of the phase is:

$$F(\bar{y}) = \sum_i y_i(\mu_i(\bar{y}) - \mu_i^0) \geq 0 \tag{2.18}$$

for all trial compositions $\bar{y}$.

$F(\bar{y})$ is the distance from the tangent plane to the molar Gibbs energy surface at composition *z* to the energy plane at composition $\bar{y}$, as shown in Figure 2-10. To ensure the stability of the system, the tangent plane should at no point extend above the energy surface over the accessible composition range.

For a multiphase system the system is stable if equation (2.18) is satisfied for all possible compositions. Instead of scanning the entire composition domain, specific stationary points are sought. In Figure 2-10, the point A_{sp} is a stationary point. A stationary point is a point on the Gibbs free energy surface where a tangent plane to the energy surface is parallel to the tangent plane to the energy surface at the composition of the tested phase. Michelsen's algorithm works well, but the stability of the system will remain uncertain unless all stationary points are determined.

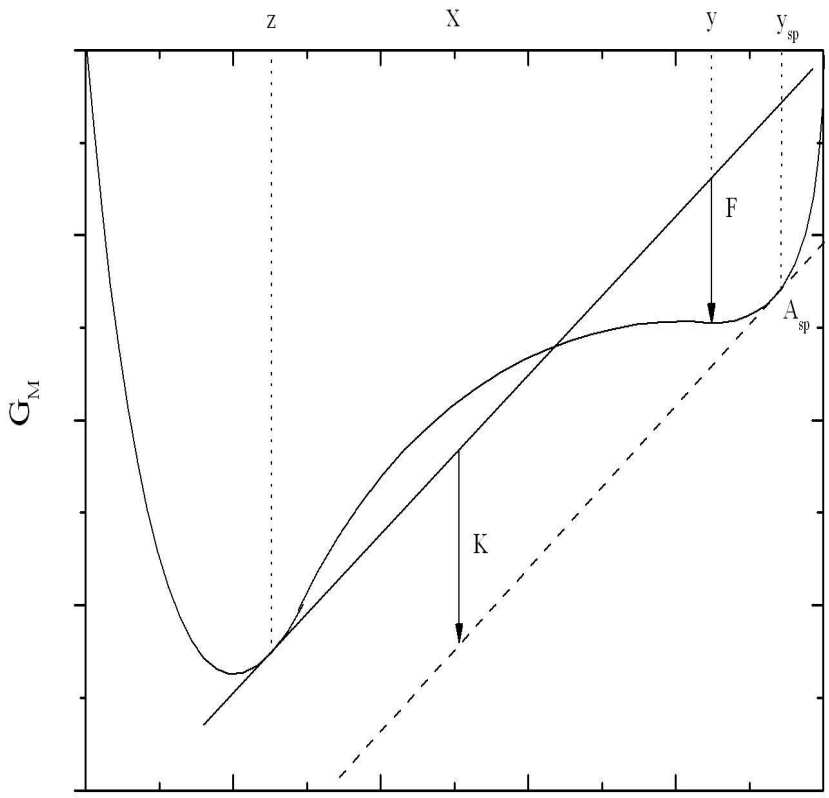

Figure 2-10 Molar Gibbs' energy of system for binary systems showing the tangent at mole fraction *z* and tangent distance *F* at mole fraction *y* (Michelsen, 1982a)

Sun and Seider (1995) proposed a technique using the homotopy-continuation method to determine the stability of the system. Homotopy-continuation is widely used in the calculation of separation processes (Lin and Seader, 1987), flash calculation (Degance, 1993), etc. Homotopy continuation provides a technique to explore the true solutions of an equation ($W(x) = 0$)

starting from an initial guess (x_0) by using a scalar homotopy parameter, *t*. The Newton homotopy function is as follows:

$$H(x,t) = W(x) - (1-t)W(x_0). \tag{2.19}$$

Starting from the point $t = 0$, where $H(x_0,0) = 0$, when *t* is increased to one, where $H(x,1) = W(x) = 0$, along the homotopy path, the true solution for the equation is obtained. To find stationary points in Michelsen's algorithm, the $W(\bar{x})$ and $H(\bar{x},t)$ equations are set as follows:

$$W(\bar{x}) = F(\bar{x}) = \sum_i x_i(\mu_i(\bar{x}) - \mu_i^0), \tag{2.20}$$

and

$$H(\bar{x},t) = F(\bar{x}) - (1-t)F(\bar{x}). \tag{2.21}$$

Nevertheless, the homotopy-continuation method is complex and many computations are needed. To avoid this complexity, Michelsen's algorithm for performing a phase stability test is used in this work.

2.5 Newton-Raphson Method and Successive Substitution Method

2.5.1 Newton-Raphson Method

For an equation, $f(x) = 0$, if x_0 is an initial guess of the root of the equation, x_r, and $f(x)$ is differentiable in an interval containing x_0 and x_r, the mean value theorem for derivatives gives (Plybon, 1992):

$$f(x) = f(x_0) + f'(\xi)(x - x_0) \tag{2.22}$$

where ξ is a value between x_0 and x_r.

When $x = x_r$, the following equation is obtained:

$$f(x_r) = f(x_0) + f'(\xi)(x_r - x_0). \tag{2.23}$$

That is,

$$-f(x_0) = f'(\xi)(x_r - x_0). \tag{2.24}$$

So,

$$x_r = x_0 - \frac{f(x_0)}{f'(\xi)}. \tag{2.25}$$

When x_0 is close to x_r, $f'(x_0) \cong f'(\xi)$, and

$$x_r \cong x_0 - \frac{f(x_0)}{f'(x_0)} \tag{2.26}$$

when $f'(x_0)$ is not zero. So the equation to be used for a single variable Newton-Raphson method is:

$$x_{n+1} = x_n - \frac{f(x_n)}{f'(x_n)}. \tag{2.27}$$

If a system of equations is to be solved and $\bar{x}_0$ is close to $\bar{x}_r$, equation (2.23) becomes:

$$\bar{f}(\bar{x}_r) = \bar{f}(\bar{x}_0) + \overline{\overline{DF}}\Big|_{\bar{x}_0} \cdot (\bar{x}_r - \bar{x}_0) \tag{2.28}$$

where

$$\overline{\overline{DF}} = \begin{bmatrix} \frac{\partial f_1}{\partial x_1} & \frac{\partial f_1}{\partial x_2} & \cdots & \frac{\partial f_1}{\partial x_n} \\ \frac{\partial f_2}{\partial x_1} & \frac{\partial f_2}{\partial x_2} & \cdots & \frac{\partial f_2}{\partial x_n} \\ \cdot & \cdot & \cdots & \cdot \\ \cdot & \cdot & & \cdot \\ \frac{\partial f_n}{\partial x_1} & \frac{\partial f_n}{\partial x_2} & \cdots & \frac{\partial f_n}{\partial x_n} \end{bmatrix}. \tag{2.29}$$

Finally the corresponding equation to be used for the Newton-Raphson method is obtained:

$$\bar{x}_{n+1} = \bar{x}_n - \overline{\overline{DF}}^{-1}\Big|_{\bar{x}_n} \cdot \bar{f}(\bar{x}_n). \tag{2.30}$$

The algorithm for the Newton-Raphson method is presented in Figure 2-11. The order of convergence for the method is two. It should be noted that only after $\bar{x}_n$ is close enough to the root, will the method converge quadratically.

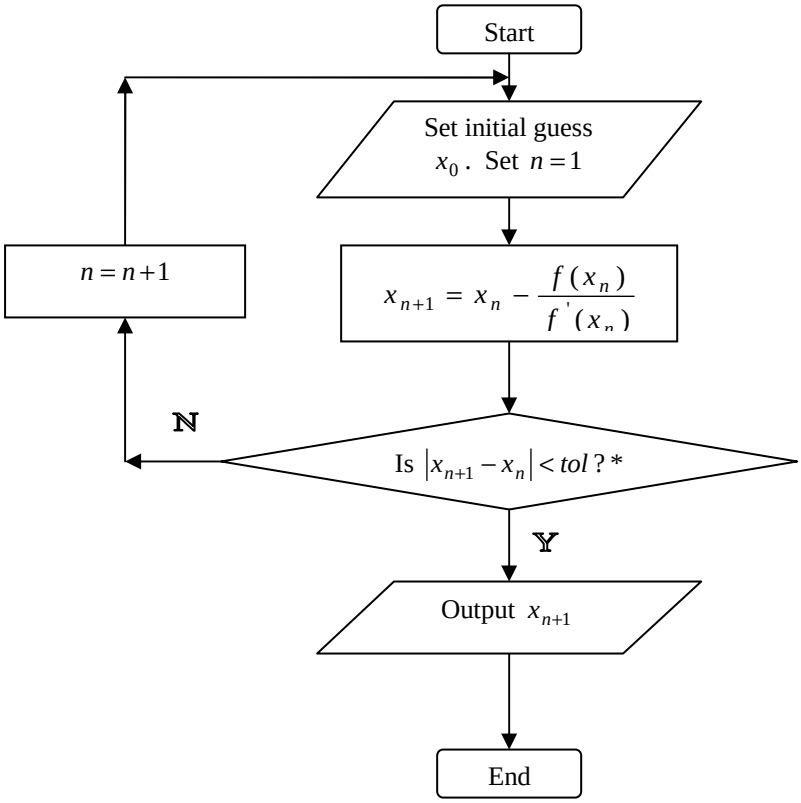

Figure 2-11 Algorithm for Newton-Raphson method. * other convergence criteria can also be employed.

In some cases, for example, when $f''(x_r) = 0$ or derivatives near the root varies rapidly, the method may not converge. In such cases, a good initial guess is essential. When $f'(x_r) = 0$, the method does not converge.

If the initial guess is properly set, the algorithm converges rapidly.

2.5.2 Successive Substitution Method

If an equivalent equation, $x = g(x)$, (Plybon, 1992) is found for an equation $f(x) = 0$, the function $g(x)$ can be used to estimate roots of $f(x)$. The algorithm is simple compared to the Newton-Raphson method.

If x_0 is an initial guess for the equation, because $x_1 = g(x_0)$, x_1 is then used for the second iteration and the process is continued according to $x_{n+1} = g(x_n)$ until a convergence criterion is satisfied.

The order of convergence is less than two. The convergence is not so rapid compared to the Newton-Raphson method near to the roots.

From the mean value theorem, the following equation is obtained:

$$\left|x_{n+1} - x_r\right| = \left|g(x_n) - g(x_r)\right| = \left|g'(\xi_n)(x_n - x_r)\right|, \tag{2.31}$$

where ξ_n is between x_n and x_r. Then

$$\frac{\left|x_{n+1} - x_r\right|}{\left|x_n - x_r\right|} = \left|g'(\xi_n)\right|. \tag{2.32}$$

Because

$$\lim_{n\to\infty}\left|g'(\xi_n)\right| = \left|g'(x_r)\right|, \tag{2.33}$$

the following result is obtained:

$$\lim_{n\to\infty}\frac{\left|x_{n+1} - x_r\right|}{\left|x_n - x_r\right|} = \left|g'(x_r)\right| = k. \tag{2.34}$$

For a system of equations, when $\bar{x}_n$ is rather close to $\bar{x}_r$, equation (2.31) becomes:

$$\left\|\bar{x}_{n+1} - \bar{x}_r\right\| = \left\|\bar{g}(\bar{x}_n) - \bar{g}(\bar{x}_r)\right\| = \left\|\overline{\overline{g'}}(\bar{x}_r)\cdot(\bar{x}_n - \bar{x}_r)\right\|, \tag{2.35}$$

where the norm is the magnitude of the largest eigenvalue for the matrix $\overline{\overline{g'}}(\bar{x}_r)$. The eigenvalues can be calculated from their standard mathematical definition, and from the features of a norm, the following equation is obtained:

$$\left\| \overline{\overline{g'}}(\bar{x}_r) \cdot (\bar{x}_n - \bar{x}_r) \right\| \le \left\| \overline{\overline{g'}}(\bar{x}_r) \right\| \cdot \left\| \bar{x}_n - \bar{x}_r \right\|. \tag{2.36}$$

Thus,

$$\lim_{n\to\infty} \frac{\left\| \bar{x}_{n+1} - \bar{x}_r \right\|}{\left\| \bar{x}_n - \bar{x}_r \right\|} \le \left\| \overline{\overline{g'}}(\bar{x}_r) \right\| = k\,. \tag{2.37}$$

Therefore if *k* is larger than one, the method will not converge. The errors will become larger and larger as the iteration count, *n*, increases. Thus, the function $\bar{g}(x)$ should be chosen carefully. Damping the successive substitution method can also work. For example, in Heidemann and Michelsen's work (1995), the system of equations employed in flash calculations is:

$$\ln K_i^{(k+1)} = \ln K_i^k - \ln(f_i^{II} / f_i^{I})^{(k)}. \tag{2.38}$$

To ensure convergence, the following system of equations is used:

$$\ln K_i^{(k+1)} = \ln K_i^k - m \ln(f_i^{II} / f_i^{I})^{(k)}. \tag{2.39}$$

From the features of a eigenvalue, one can observe that the eigenvalues of the Jacobian matrix of the corresponding system of equations for the above two methods have the following relationship:

$$\lambda^* = 1 - m(1-\lambda), \tag{2.40}$$

where λ^* and λ are the eigenvalues corresponding to equations system (2.39) and (2.38), respectively. It is observed that when *m* is set carefully, the norm of the

Jacobian matrix of the system of equations may be less than 1 and convergence will then be ensured.

As presented in Section 2.5.1, for the Newton-Raphson method, when $f'(x_r)$ is zero, it cannot work properly. Because when x_n is approaching x_r, the derivative is close to zero, the ratio of $f(x_n)$ and $f'(x_n)$ begins to change erratically. As a result, the x_{n+1} value changes erratically.

If a root lies at a point where $f'(x_n) = 0$, the Newton-Raphson method should not be employed. For an equation or a system of equations, because only after $\bar{x}_n$ is close enough to the root, will the method converge quadratically. If the initial guesses are not so close to the root, the iteration count for the Newton-Raphson method may not differ much with that for the successive substitution method. In the calculation of an equilibrium phase in the project, both methods have been tried and the corresponding numbers of iteration for convergence of both methods do not differ much. Because the successive substitution method is simple compared with the Newton-Raphson method. The successive substitution method was employed.

2.6 Summary

In this chapter, van Konynenburg and Scott's classification scheme is shown. Then the global phase diagrams proposed by van Konynenburg and Scott (1980), Deiter and Pegg (1989), Wang and Sadus (2003) are discussed and an overview of the published techniques for exploring different parts of a phase diagram in PT space are given. Different algorithms for predicting single parts of a

global phase diagram are then presented. Finally, the Newton-Raphson method and the successive substitution method are presented. In chapter three, the algorithms to be employed in the project will be discussed in detail.

3. MATHEMATICAL FRAMEWORK

3.1 Introduction

In Chapter 2, different methods for determining different parts of a global phase diagram in *PT* space were presented. In this chapter, the Peng-Robinson equation of state, which is employed throughout the project, is presented, and then specific techniques selected for the project to calculate vapour pressure lines of pure components, critical lines, equilibrium phases and three-phase lines are shown in detail.

3.2 The Peng-Robinson Equation of State

In this project, the Peng-Robinson equation of state (Peng and Robinson, 1976) is employed. It can be presented in the following form,

$$P = \frac{RT}{(v-b)} - \frac{a(T)}{v(v+b)+b(v-b)}, \tag{3.1}$$

where a and b are the energy parameter and size parameter of the Peng-Robinson equation of state, respectively. The criterion for a pure component critical point is:

$$\left(\frac{\partial P}{\partial V}\right)_T = \left(\frac{\partial^2 P}{\partial V^2}\right)_T = 0 \tag{3.2}$$

Applying the above criterion at a critical point to equation (3.1), the following parameters are obtained:

$$a(T_c) = 0.45724 \frac{R^2 T_c^2}{P_c}, \tag{3.3}$$

$$b(T_c) = 0.07780 \frac{R\ T_c}{P_c}, \tag{3.4}$$

and

$$Z_c = 0.307. \tag{3.5}$$

At temperatures other than the critical temperature, the energy and size parameters are computed using the following equations:

$$a(T) = a(T_c) \cdot \alpha(T_r, \omega), \tag{3.6}$$

and

$$b(T) = b(T_c). \tag{3.7}$$

In equation (3.6), $\alpha(T_r, \omega)$ is a dimensionless function of reduced temperature and acentric factor. The relationship between α and T_r is given by the following equation

$$\alpha^{1/2} = 1 + \kappa(1 - T_r^{1/2}), \tag{3.8}$$

where κ is the characteristic constant of a component. It is given by the equation:

$$\kappa = 0.37464 + 1.54226\omega - 0.26992\omega^2. \tag{3.9}$$

When the equation of state is applied to mixtures, the parameters for the mixture systems are evaluated using the van der Waals mixing rules:

$$a = \sum_i \sum_j x_i x_j a_{ij} \tag{3.10}$$

where

$$a_{ij} = (1 - K_{ij}) a_i^{1/2} a_j^{1/2}, \tag{3.11}$$

and

$$b = \sum_i x_i b_i . \tag{3.12}$$

In equation (3.11), K_{ij} is the binary interaction parameter for the binary system composed of components i and j. Here $K_{ij} = K_{ji}$.

3.3 Computing Vapour Pressure of Pure Components

For a liquid phase and vapour phase in equilibrium, the fugacity of a component is the same in both of the two phases. The vapour-liquid (VL) equilibrium for the pure components can be calculated at a specified temperature or pressure using equation (3.13).

$$g = \ln f_V - \ln f_L = 0 \tag{3.13}$$

The fugacity of a pure component is evaluated using equation (3.14), which is derived from the departure function for Gibbs free energy (Reid et al. 1987):

$$\ln(f / P) = \frac{\sqrt{2}a}{4bRT} \cdot \ln \frac{z + B(1 - \sqrt{2})}{z + B(1 + \sqrt{2})} - \ln(z - B) + z - 1 \tag{3.14}$$

where

$$B = \frac{bP}{RT} \tag{3.15}$$

and

$$z = \frac{Pv}{RT} . \tag{3.16}$$

The molar volumes are obtained at a specified pressure and temperature from solving equation (3.1) using a cubic solver.

The Newton-Raphson method was used to solve equation (3.13) for the vapour pressure at a fixed temperature. From the relationships

$$\left(\frac{\partial \ln f}{\partial P}\right)_T = \frac{v}{RT} \tag{3.17}$$

and

$$\left(\frac{\partial g}{\partial P}\right)_T = \frac{v_V - v_L}{RT}, \tag{3.18}$$

the following equations used for the Newton-Raphson method can be derived:

$$\Delta P = \frac{-g}{\left(\frac{\partial g}{\partial P}\right)_T} = \frac{[\ln(f_V / f_L)]RT}{v_L - v_V}, \tag{3.19}$$

and

$$P_{n+1} = P_n + \Delta P\ . \tag{3.20}$$

P_{n+1} and P_n are the computed vapour pressures of the current iteration and the last iteration, respectively.

3.4 Calculating Critical Points of Mixtures

As mentioned in chapter two, Heidemann and Khalil (1980) presented a method to calculate critical points of mixtures. It was stated that a given phase with N components would be stable if for every isothermal variation in the state, the following condition was satisfied:

$$\left[\Delta A + P_0 \Delta V - \sum_{i=1}^{N} \mu_{i0} \Delta n_{i0}\right]_{T_0} > 0\,. \tag{2.13}$$

ΔA, ΔV and Δn_{i0} are differences in Helmholtz free energy, volume of the phase and mole number of the *i* th component between the varied state and the initial state of the given phase respectively. P_0 and μ_{i0} are the initial pressure and chemical potential of the given phase respectively.

If the volume and mole number of components of the explored phase change as follows:

$$\Delta V = kV_0 \text{ and} \tag{3.21}$$

$$\Delta n_i = kn_{i0}, i = 1,2,....., N, \tag{3.22}$$

the mole fraction, molar volume, pressure, chemical potential, etc., remain constant. To avoid such variation, set

$$\Delta V = 0. \tag{3.23}$$

Equation (2.13) becomes:

$$\left[\Delta A - \sum_{i=1}^{N} \mu_{i0} \Delta n_{i0}\right]_{T_0, V_0} > 0. \tag{3.24}$$

The Helmholtz free energy in equation (3.24) can be expanded in a Taylor series. The following equation is obtained:

$$\begin{aligned}\left[\Delta A - \sum_{i=1}^{N} \mu_{i0} \Delta n_{i0}\right]_{T_0, V_0} &= \frac{1}{2!} \sum_j \sum_i (\partial^2 A / \partial n_j \partial n_i) \Delta n_i \Delta n_j + \\ \frac{1}{3!} \sum_i \sum_j \sum_k (\partial^3 A / \partial n_i \partial n_j \partial n_k) \cdot \Delta n_i \cdot \Delta n_j \cdot \Delta n_k + 0(\Delta n^4) &> 0.\end{aligned} \tag{3.25}$$

Stability can be ensured if the quadratic term in equation (3.25) is positive-definite. When the quadratic term equals zero, the limit of stability has been obtained.

To calculate the limit of stability, the quadratic term in equation (3.25) can be presented in the following form:

$$\overline{\Delta n}^{T} \cdot Q \cdot \overline{\Delta n} = 0 \tag{3.26}$$

where Q is a matrix with elements $q_{ij} = (\partial^2 A / \partial n_j \partial n_i)$. For equation (3.26), to have a non-zero solution, the matrix Q should have a zero determinant:

$$|Q| = 0 . \tag{3.27a}$$

Equivalently, there should be a non-zero vector $\overline{\Delta n}$, which satisfies the equation:

$$Q \cdot \overline{\Delta n} = 0 . \tag{3.27b}$$

To solve equation (3.27b), the mole number change of the N^{th} component is set to one. That is, $\Delta n_N = 1$. The solution obtained from equation (3.27b) is inserted into equation (3.25). To ensure that equation (3.25) is positive-definite, the first non-vanishing term in the Taylor series must be of even order. That is, the cubic term must be zero:

$$C = \sum_i \sum_j \sum_k (\partial^3 A / \partial n_i \partial n_j \partial n_k) \cdot \Delta n_i \cdot \Delta n_j \cdot \Delta n_k = 0 . \tag{3.28}$$

The derivatives within equations (3.27b) and (3.28) may be replaced with

$$\frac{\partial^2 A}{\partial n_i \partial n_j} = RTn_T \cdot \frac{\partial \ln f_i}{\partial n_j} \tag{3.29}$$

and

$$\frac{\partial^3 A}{\partial n_i \partial n_j \partial n_k} = RTn_T^2 \cdot \frac{\partial^2 \ln f_i}{\partial n_j \partial n_k} \tag{3.30}$$

where n_T is the total number of moles in the system and f_i is the fugacity of the i^{th} component.

With equations (3.27) and (3.28) a critical point can be found.

To test the stability of the system when small changes of the composition of components occur, the following condition is assessed:

$$d = \sum_i \sum_j \sum_k \sum_l (\partial^4 A / \partial n_i \partial n_j \partial n_k \partial n_l) \cdot \Delta n_i \cdot \Delta n_j \cdot \Delta n_k \cdot \Delta n_l > 0 \,. \quad (3.31)$$

If the condition is satisfied, local stability is verified. To test the global phase stability of the system, the tangent plane criterion presented in the following section is employed.

3.5 Evaluation of Equilibrium Phases – the Tangent Plane Criterion

In the calculation of a critical line, one should learn if a critical endpoint exists for the specific binary system. At a critical endpoint, an equilibrium phase coexists with a critical phase. Mathematically, this phase can be located using Michelsen's stability test (1982) that was introduce in Chapter 2. The stability test is done after finding a critical point, using the critical point as the reference phase. If all stationary points found using equation (2.18) result in $F(\bar{y})$ being larger than zero, the critical point is stable. If $F(\bar{y}) < 0$ for any stationary point, the critical point is unstable with respect to the stationary point trial composition. If $F(\bar{y}) = 0$, the trial composition is in equilibrium with the critical point and a critical endpoint has been located.

In Section 2.4.3, the tangent plane criterion and stationary points are described graphically. In this section, the mathematical definition of stationary points will be presented.

Finding the maxima and minima of equation (2.18) gives the stationary points. Using the the Lagrangian multiplier method of finding extrema, constraining $\sum_i y_i = 1$, yields the following stationary condition for an *M*-component system:

$$\mu_i(\bar{y}) - \mu_i^0 = K, i = 1,2,.....M \tag{3.32}$$

where *K* is a constant. The corresponding tangent plane distance is

$$F_{SP} = \sum_i y_i K = K . \tag{3.33}$$

So when $K > 0$ at all stationary points, the system is stable.

For convenience, fugacity coefficients can be employed and

$$\mu_i(\bar{y}) - \mu_i^0 = RT(\ln y_i + \ln \phi_i - \ln z_i - \ln \phi_i(\bar{z})), \tag{3.34}$$

where

$$h_i = \ln z_i + \ln \phi_i(\bar{z}) . \tag{3.35}$$

From equations (3.32), (3.34) and (3.35), the stationary criterion is obtained:

$$\ln y_i + \ln \phi_i - h_i = \theta \tag{3.36}$$

where

$$\theta = K / RT \tag{3.37}$$

If the following new variables are introduced:

$$Y_i = \exp(-\theta) y_i \tag{3.38}$$

the final set of equations can be obtained:

$$\ln Y_i + \ln \phi_i - h_i = 0 \tag{3.39}$$

giving M equations for M unknowns, the unnormalized mole fractions, Y_i. From the equation (3.38), y_i can be computed using the following equation:

$$y_i = Y_i / \sum_j Y_j \ . \tag{3.40}$$

When the solution of equation group (3.39) is obtained, if

$$\sum_j Y_j \le 1 \tag{3.41}$$

or

$$\theta > 0 \tag{3.42}$$

where

$$\theta = -\ln \sum_j Y_j \tag{3.43}$$

for all stationary points, the stability of the system is verified. Otherwise, the system is unstable.

The fugacity coefficient of a component of a mixture is calculated using equations (3.44)-(3.47) (Reid et al., 1987), which is derived using departure functions and the Peng-Robinson equation of state. Equations (3.10) and (3.12) show the corresponding mixing rules.

$$\ln \phi_i = \frac{b_i}{b} \cdot (z-1) - \ln(z-B) + \frac{\sqrt{2}A}{4B} \cdot (\frac{b_i}{b} - \delta_i) \cdot \ln \frac{z + B(1+\sqrt{2})}{z + B(1-\sqrt{2})} \tag{3.44}$$

$$\delta_i = \frac{2a_i^{1/2}}{a} \sum_j x_j a_j^{1/2} (1 - K_{ij}) \tag{3.45}$$

$$A = \frac{aP}{(RT)^2} \tag{3.46}$$

$$B = \frac{bP}{RT} \tag{3.47}$$

z is calculated using equation (3.16). The fugacity of a pure component can also be determined employing equation (3.44) if the divide by zero errors are handled properly. These errors occur when the numerator of an expression equals zero. The corresponding quotient is set with a pre-defined constant to indicate the divide by zero error occurs.

A critical endpoint, where a critical phase is in equilibrium with a non-critical phase, is important for the computation of a global phase diagram. At a critical endpoint, a critical line and a three-phase line join. The results for a critical endpoint are essential for the computation of the three-phase line computation, which is described in Section 3.6, because the initial estimates for the first three-phase point are set using compositions near to those of the critical endpoint.

3.6 Calculation of Three-Phase Line

Here the condition of equal fugacity for the same component in different phases at equilibrium is used to evaluate the three-phase line. That is:

$$\text{and} \qquad \begin{aligned} \ln f_{11} &= \ln f_{21} = \ln f_{31}, \\ \ln f_{12} &= \ln f_{22} = \ln f_{32}. \end{aligned} \tag{3.48}$$

For f_{ij}, i represents the phase index and j represents the component index.

From equation (3.48), four simultaneous equations are obtained to determine the three-phase points for a binary system.

$$
\begin{aligned}
g_1 &= \ln f_{11} - \ln f_{ref1} = 0 \\
g_2 &= \ln f_{12} - \ln f_{ref2} = 0 \\
g_3 &= \ln f_{31} - \ln f_{ref1} = 0 \\
g_4 &= \ln f_{32} - \ln f_{ref2} = 0,
\end{aligned}
\tag{3.49}
$$

where

$$
\begin{aligned}
\ln f_{ref1} &= \ln f_{21} \\
\ln f_{ref2} &= \ln f_{22}
\end{aligned}
\tag{3.50}
$$

The four independent variables are the temperature and pressure of the system and the MVC (most volatile component) compositions of phase I and phase III at the three-phase point.

In Chapter 4, an algorithm based on this theory will be developed to predict three-phase lines.

3.7 Summary

In this chapter, the mathematical framework of the algorithm is presented. The Peng-Robinson equation of state and theories for evaluating vapour pressure lines of pure components, the critical lines, the equilibrium phases and the three-phase lines are presented. In the next chapter, algorithms based on the corresponding theories in this chapter are developed to predict different parts of a global phase diagram.

4. ALGORITHM DEVELOPMENT

The mathematical framework for predicting different parts of a global phase diagram in *PT* space has been presented in Chapter 3. The algorithms, based on the mathematical framework, for evaluating a global phase diagram will be shown in this chapter. It has been mentioned that a global phase diagram in *PT* space is made up of vapour pressure lines, critical lines, critical endpoints and three-phase lines except that only a vapour pressure line and a critical line are present in a type I global phase diagram in *PT* space. In this chapter, the algorithm to automatically develop global phase diagrams will be presented first. Then, based on the algorithm, algorithms for computing different parts of a global phase diagram are discussed.

With the developed code, the vapour pressure lines of the two pure components are computed first. Then, evaluation of the critical lines starts from the point where the MVC (most volatile component) mole fraction is 0.001. The MVC mole fraction is increased with a step size, which is varied according to the number and position of the points to be predicted. In the calculation of critical lines, global stability of the obtained critical points is tested to find any existing critical endpoints. If any critical endpoints are obtained, the code will transfer to the

evaluation of a three-phase line automatically. Different algorithms are applied for different types of phase behaviour.

4.1 Automatic Development of Global Phase Diagrams

4.1.1 Flowchart for Development of Global Phase Diagram

The algorithm for computing a global phase diagram in *PT* space automatically has been developed. The algorithm changes the value of the step size for changing the MVC (most volatile component) mole fraction according to the evaluated component parts of the global phase diagram and the value of the composition itself. This technique makes it easier for different parts of the global phase diagrams to connect with each other and to calculate phase diagrams for different types of binary systems. All the necessary features on a global phase diagram can be captured with the algorithm. The flowchart is shown in Figures 4-1 and 4-2.

Initially, from the data file, the program reads the property data of pure components, data for the binary interaction parameter, and data for control and choice in the code, which include the number of components. The code also reads data for temperature limits and pressure limits used in the computation of vapour pressure lines of pure components.

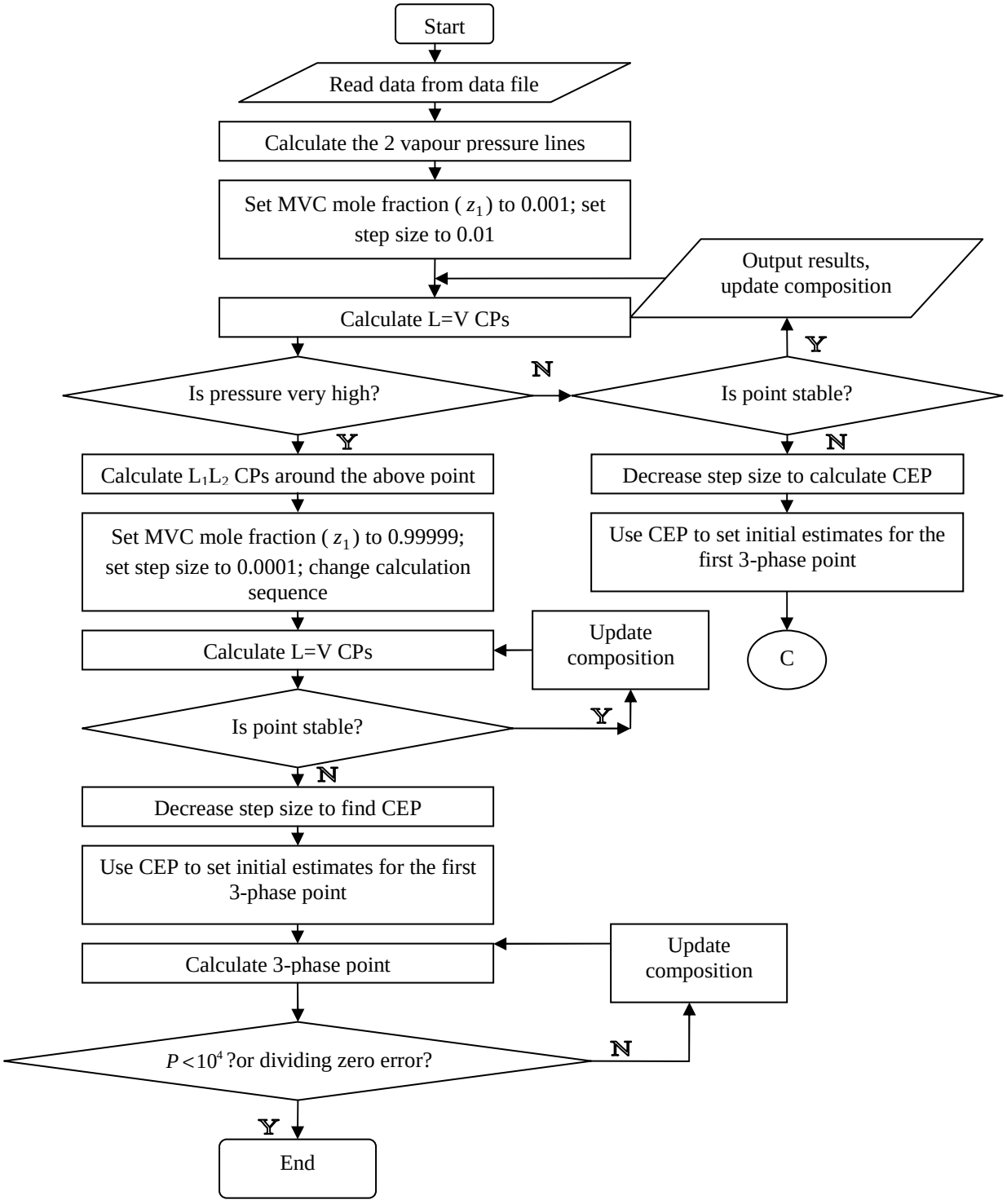

Figure 4-1 One part of the flowchart for the algorithm to evaluate global phase diagram. *P* represents pressure of the three-phase points obtained. (Algorithm for calculating CEP is presented in Figure 4-7.)

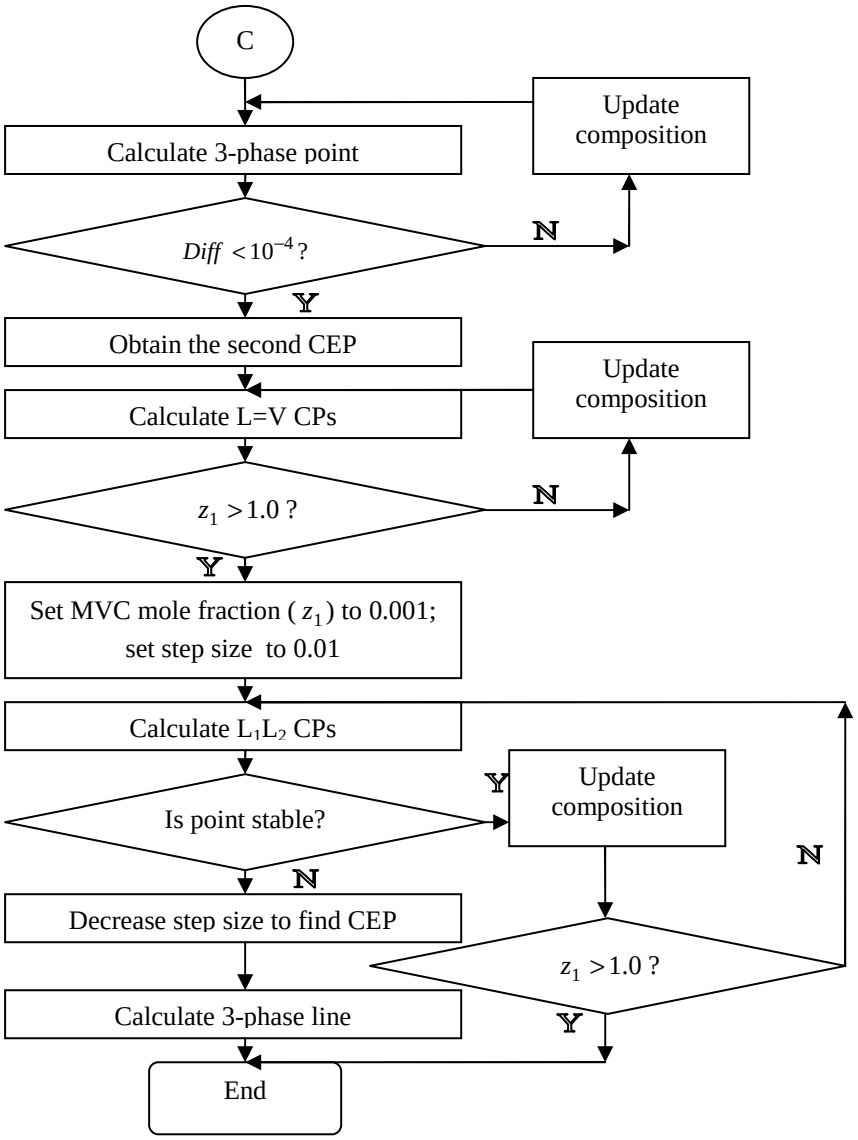

Figure 4-2 The other part of the flowchart for the global phase diagram evaluation algorithm. CEP stands for critical endpoint CP represents critical point and z_1 is the MVC mole fraction. *Diff* represents the difference between the MVC mole fraction of the reference phase and the third phase of the three-phase point. MVC stands for most volatile component.

The code then commences the calculation of the vapour pressure of the pure components. The algorithms to determine the different component parts of a global phase diagram will be described in detail in subsequent sections. After the determination of vapour pressure lines of pure components, the control of the program commences the evaluation of the critical line. The MVC mole fraction (z_1) of the first critical points is 0.001. The following points all have MVC mole fractions larger by the value of the step size (Δz) than the last evaluated point. The code evaluates the critical temperature and critical pressure of these points and determines if the point is stable using the tangent plane criterion. If the critical temperature and critical pressure are obtained successfully and the critical point is stable according to the tangent plane criterion, the control will output the evaluated results. If the evaluation obtains the critical temperature and pressure successfully but the point is unstable, then the program will determine if the value of the θ satisfies the condition $\theta > tol$, tol being a pre-defined tolerance. If it does, the current critical point is a critical endpoint. If it does not, the control restores the compositions and values of other variables with the corresponding values of the last stable point computed and decreases the step size by half for each of the following points to be calculated. The program then determines if the latest point is stable and if θ satisfies the convergence criterion $\theta > tol$. When an unstable point where $\theta > tol$ is obtained, the point is a critical endpoint. The program then records the compositions of the obtained equilibrium phase and stores the critical temperature and pressure and the compositions of the critical phase. These stored values will be

employed as the initial estimates for the evaluation of the first three-phase point. After the control launches the calculation of the three-phase line, the evaluation of other three-phase points takes the computed results of the last three-phase point as the initial guess.

Three-phase points corresponding to different compositions of the reference phase are calculated one after one. The difference in composition between the reference phase and the third phase is compared to determine if it is less than a tolerance. If it is not, the calculation of three-phase points continues. If it is, the second critical endpoint has been found because in such a case phase II and phase III become one critical phase and phase I are in equilibrium with the critical phase. Such three-phase lines have two critical endpoints. They belong to a type IV or type V system according to van Konynenburg and Scott's (1980) classification scheme. If necessary, the control of the code decreases the step size for changing the z_1 by half as a pure component mole fraction is approached to determine the second critical endpoint. If the phase diagram does not belong to type IV or type V, the algorithm for type II or type III will be employed.

After finding the second critical endpoint, the code sets the step size to a small value and restarts the evaluation of the critical points. The step size is increased to twice of the last value for each of the subsequent points to be evaluated until it reaches a pre-defined maximum value. ` The step size is a very important variable in the code. When the MVC mole fraction of the next point to be computed is larger than 1.0, the control of the code terminates the evaluation of L = V critical points. Because in binary systems, $L_1 = L_2$ critical points may exist, the

$L_1 = L_2$ critical points have to be explored thoroughly, and the code then commences the calculation of $L_1 = L_2$ critical points from the point with the MVC mole fraction being 0.001. The control repeats the above procedure for L = V critical lines. In the above calculation, it should be noted that the points to be evaluated are increasing in MVC mole fraction (z_1).

If in the evaluation of L = V and $L_1 = L_2$ critical points, no critical endpoints or no critical points with very high pressure are found, the binary system belongs to a type I system. If a critical endpoint and thus a three-phase line are obtained in the $L_1 = L_2$ critical point evaluations, the system is a type II system. If two critical endpoints are obtained in the L = V critical point computations and no critical endpoint is found in the $L_1 = L_2$ critical point calculation, the corresponding system belongs to type V according to van Konynenburg and Scott's (1980) classification scheme.

In the above computation, the points are evaluated by increasing the MVC mole fraction. When a critical point with very high pressure ($P > 4.2\sum_i P_{ci}$) is obtained, P_{ci} being the critical pressure of pure component *i*, the control of the code suspends the current L = V critical points calculation, and evaluates the $L_1 = L_2$ critical equilibrium around the point with very high pressure. The value $4.2\sum_i P_{ci}$ was obtained after many calculations of critical points (see Chapter 5). The control of the code then changes the MVC mole fraction of the next critical point to 0.99999 and changes the calculation sequence such that the points to be computed have decreasing MVC mole fractions. Because the critical line on the right side of

the global phase diagram extends to very high pressure and there is no three-phase line connecting it with the left side critical line, the global phase diagram cannot be evaluated continuously from the right side and evaluation of critical point has to be restarted from the left side until a critical endpoint is obtained. The three-phase line is then evaluated and a global phase diagram for a type III system is obtained.

The step size for changing the MVC mole fraction is important for the algorithm. It controls the number of points to be evaluated for different parts of a global phase diagram. When the points near the connecting points, including critical points for pure components and critical endpoints are computed, the step size is set to a rather small value, for example, 10^{-4}. Then the step size is increased to twice the previous value for each point computed until it reaches the maximum value of the step size. When the MVC mole fraction is larger than a pre-defined value, for example, 0.995, the step size is set to a small value to obtain enough points needed to plot the corresponding part of the global phase diagram.

In the following sections, the algorithms for computing different parts of a global phase diagram will be presented.

4.2 Vapour Pressure of Pure Components

Based on the mathematical framework to evaluate vapour pressure in Section 3.3, the algorithm for predicting vapour pressure of pure components is developed. Figure 4-3 is the flowchart for evaluating a vapour pressure line.

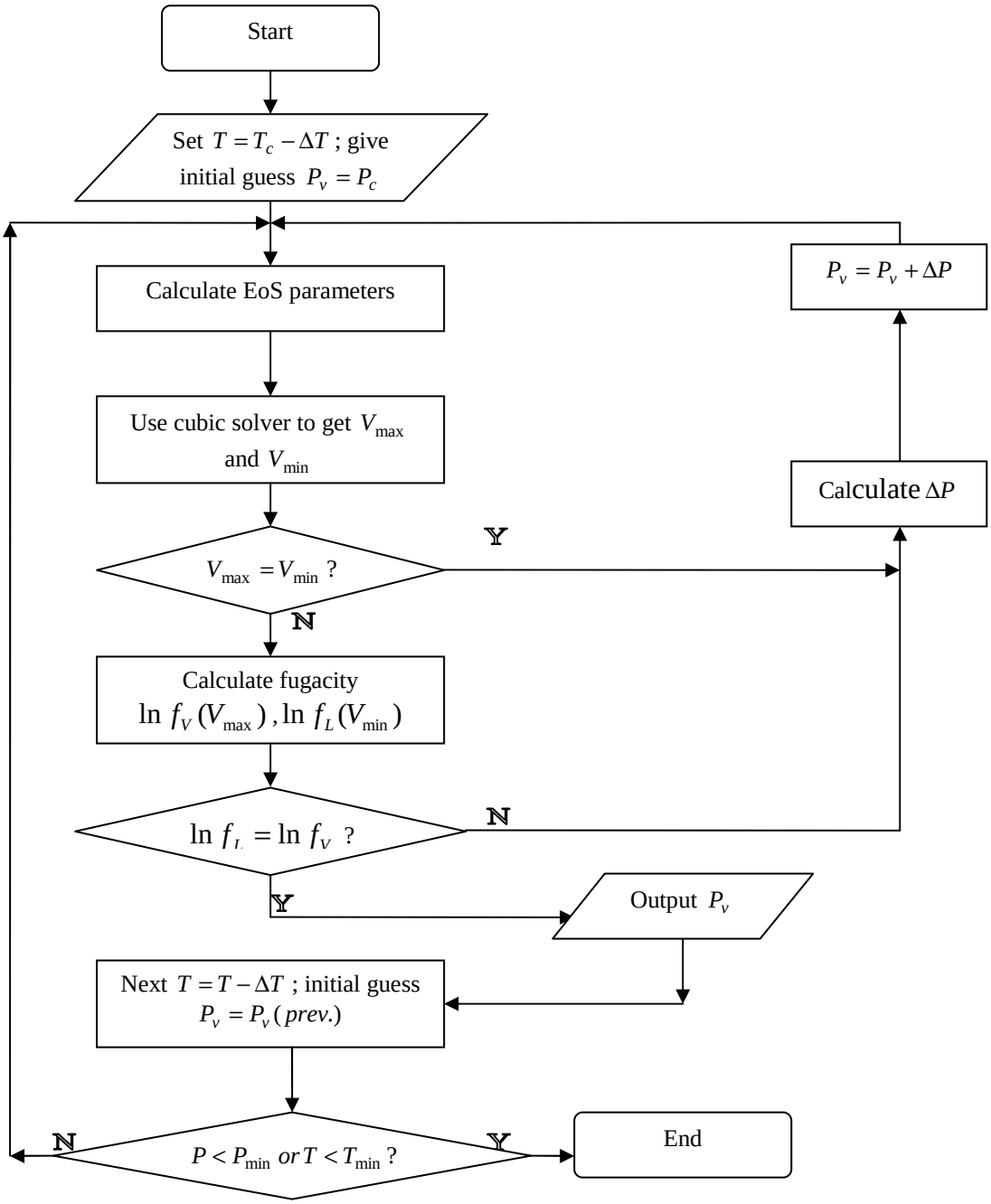

Figure 4-3 Flowchart for the vapour pressure calculation using Peng-Robinson equation of state.

4.2.1 Flowchart

At a specific temperature, *T*, a certain initial guess for the vapour pressure, P_v, is given. Using the cubic solver, one can get two molar volumes by solving the Peng-Robinson equation. In fact, usually three solutions exist. The three solutions are presented in Figure 1-3. One should choose the largest one and the smallest one because only these present the vapour phase and liquid phase, respectively, and are mechanically stable. With these two molar volumes, two fugacity values can be obtained. Then the algorithm in Figure 4-3 is used to calculate the vapour pressure of pure components.

If the two molar volumes obtained are equal, because with the initialization technique presented in Section 4.2.2, the trial vapour pressure is surely larger than the true vapour pressure at the current temperature, the trial vapour pressure is decreased with a certain value, for example, $\Delta P = -0.1$ bar. Two different molar volumes may then be obtained. If the trial pressure is still too large, it will be decreased by that certain value again until two different molar volumes are obtained. Two different molar volumes give two fugacities. These two values are then compared. If they are not equal, the pressure, P_v, is not the true vapour pressure at the temperature and the pressure is updated using the Newton-Raphson method (Section 3.3). The loop is repeated until the two fugacities obtained satisfy the convergence criterion. The corresponding pressure, P_v, is the vapour pressure at that specific temperature. The temperature is varied by a certain value ΔT, which depends on the number of points to be calculated, and the vapour pressure at this next temperature is evaluated. The value of ΔT must also guarantee that the

initial guess at the next temperature is precise enough for the code to converge to the right solution. If the temperature becomes less than T_{min} or the vapour pressure obtained is less than P_{min}, the algorithm exits the code to calculate vapour pressure. The values of T_{min} and P_{min} are read from the data file.

4.2.2 Initialization

The evaluation of this part of phase diagram commences from the critical points of pure components. The vapour pressure at the critical temperature is the critical pressure. The following points have temperatures 5℃ less than the previous point. Each point takes the calculated vapour pressure of the last one as its initial estimate. The algorithm uses the Newton-Raphson method to solve equation (3.13).

4.3 Calculation of Critical Line

Based on the mathematical framework in Section 3.4 to evaluate a critical point, the algorithm for predicting critical points is developed.

4.3.1 Flowchart

First the stability limit is evaluated using equation (3.27). At a given composition, the code uses the flowchart shown in Figure 4-4 to find temperature-volume pairs which make the determinant of *Q* (equation 3.27) equal to zero. This gives the stability limit for the mixture.

Figure 4-4 is the flowchart for evaluating the critical temperature at a specific molar volume. Figure 4-5 is the flowchart for calculating the critical molar

volume at a specific temperature. These two flowcharts do not work separately, but work cooperatively.

First, an initial value is given for the critical molar volume. Then the code uses the flowchart shown in Figure 4-4 to calculate the critical temperature. When the code obtains the critical temperature at the a specific molar volume, it commences the computation shown in the flowchart of Figure 4-5. The flowchart in Figure 4-5 is used to solve equation (3.28). With the temperature calculated in the first flowchart, the corresponding molar volume can be evaluated. Then the code compares that with the initial guess of molar volume; if they satisfy the condition

$$\left|\frac{v_{n+1}-v_n}{v_n}\right| < 1\times10^{-5}, \tag{4.1}$$

the code will output the results. If they do not satisfy the condition, the code goes back to the calculation shown in the flowchart of Figure 4-4. The computation will be continued until the code converges.

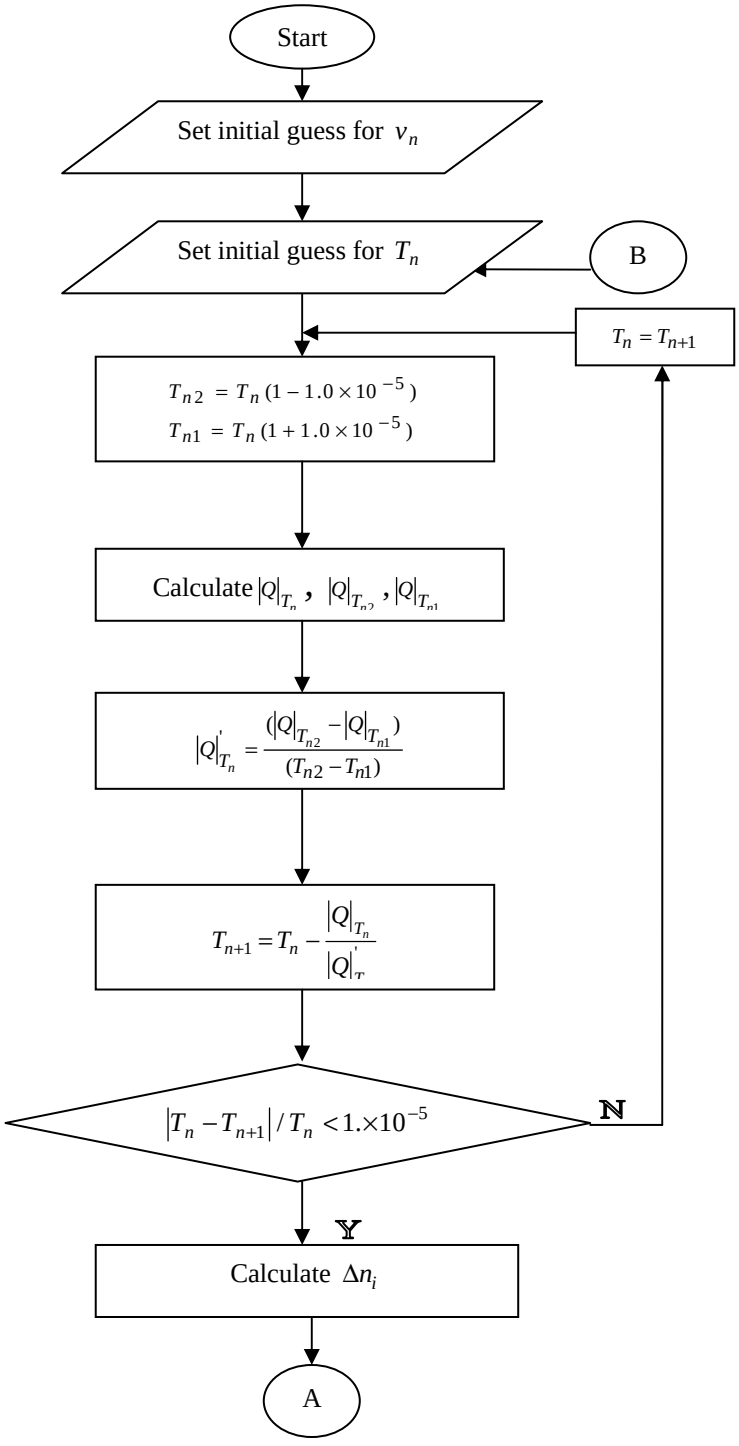

Figure 4-4 Flowchart for calculating the critical temperature at a specific molar volume.

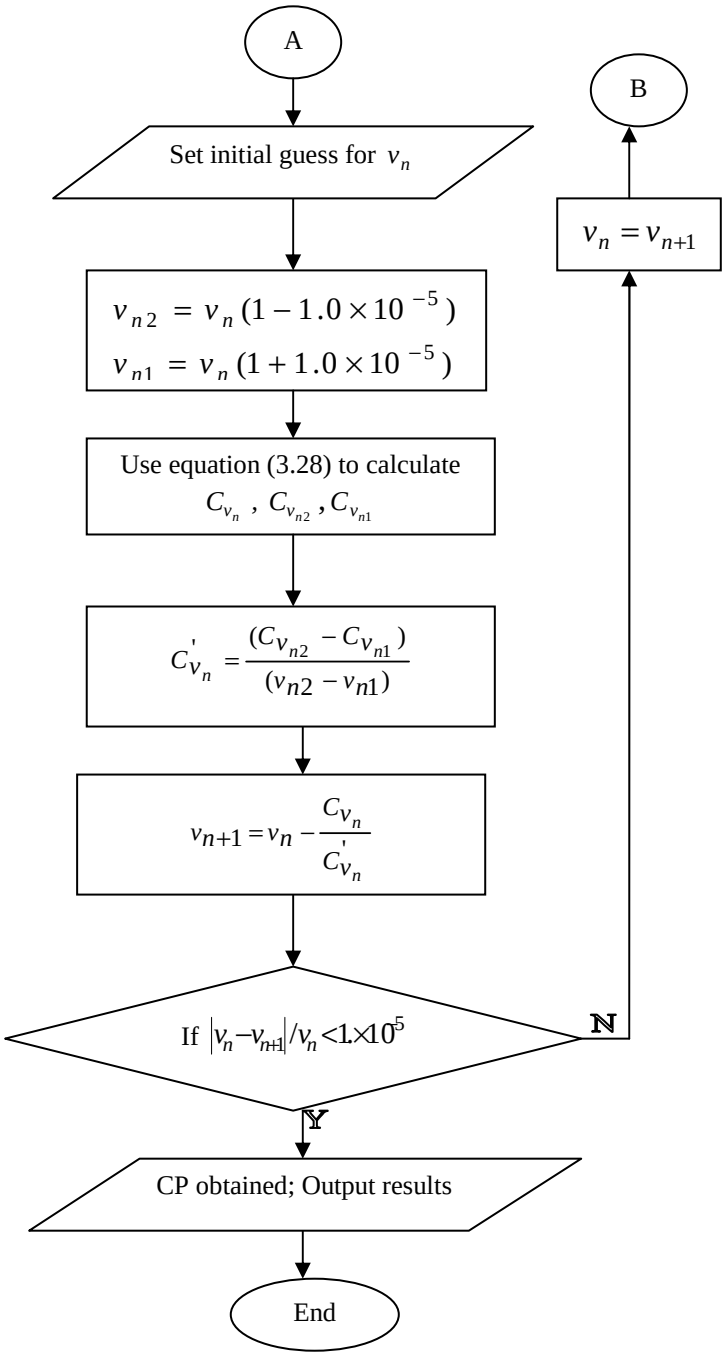

Figure 4-5 Flowchart for calculating the critical molar volume at a specific temperature.

In Figure 4-4, the initial guess for temperature is set as follows (Heidemann and Khalil, 1980):

$$T_0 = 1.5\sum y_i T_{ci}\,, \tag{4.2}$$

where y_i and T_{ci} are the composition and critical temperature of component *i*, respectively.

In the algorithm shown in the flowchart of Figure 4-4, the Newton-Raphson method is used to update the critical temperature:

$$T_{n+1} = T_n - \frac{|Q|_{T_n}}{|Q|'_{T_n}}. \tag{4.3}$$

The code uses a central difference formula to evaluate $|Q|'_{T_n}$:

$$|Q|'_{T_n} = \frac{(|Q|_{T_{n2}} - |Q|_{T_{n1}})}{(T_{n2} - T_{n1})}, \tag{4.4}$$

where

$$T_{n2} = T_n(1 - 1.0\times10^{-5})\,, \tag{4.5}$$

and

$$T_{n1} = T_n(1 + 1.0\times10^{-5})\,, \tag{4.6}$$

In the algorithm shown in the flowchart of Figure 4-5, the Newton-Raphson method is used to update the critical molar volume:

$$v_{n+1} = v_n - \frac{C_{v_n}}{C'_{v_n}} \tag{4.7}$$

where C_{v_n} is the cubic term for the *n*th iteration.

The code uses a central difference formula to calculate C'_{v_n} :

$$C'_{v_n} = \frac{(C_{v_{n2}} - C_{v_{n1}})}{(v_{n2} - v_{n1})} \tag{4.8}$$

where

$$v_{n2} = v_n(1-1.0\times10^{-5}), \tag{4.9}$$

and

$$v_{n1} = v_n(1+1.0\times10^{-5}). \tag{4.10}$$

4.3.2 Initialization

For L = V critical points, the initial estimate for critical temperature is set to $1.5\sum_i T_{ci}$, T_{ci} being the critical temperature of pure component *i*, in the following three cases: if the point to be computed is the first critical point, if the critical pressure obtained of the last point is very high or if the evaluation of that point fails. The initial guess for the critical molar volume is set as $4b_m$, b_m being the size parameter of the equation of state for the binary mixture. In other cases, the initial estimates of critical temperature and critical molar volume are the computed results of the last critical point evaluated. The convergence criterion is $\left|\frac{v_{n+1} - v_n}{v_n}\right| < 1\times10^{-5}$, v_{n+1} and v_n being the molar volumes of this iteration and the last iteration respectively.

For $L_1 = L_2$ critical points, the initial estimate for critical molar volume is set to $1.8b_m$ in all cases. If the critical pressure obtained for the last point is very high ($P > 4.2\sum_i p_{ci}$) or the evaluation of that point fails, the initial estimate for

critical temperature is set to $1.5\sum_i T_{ci}$ and in other cases, the initial guess for critical temperature is the computed results of the last point.

4.4 Computation of Critical Endpoints

In the calculation of phase diagrams, it is essential to learn if a critical endpoint exists. If one critical endpoint is found, the code transfers to the calculation of the three-phase line at the obtained critical endpoint. After each critical point is obtained, the tangent plane criterion is used to determine if the point is unstable. If it is, a critical endpoint is present near the critical point. After a critical endpoint is determined, an equilibrium phase is obtained. It has been discussed in Chapter 1 that at a critical endpoint, a separate phase, called the equilibrium phase, is an incipient phase in equilibrium with the critical phase.

4.4.1 Flowchart

Based upon the mathematical framework presented in Section 3.5, an algorithm is developed to do a global stability test and determine the critical endpoints and the corresponding equilibrium phase compositions. The flowchart for the algorithm is presented in Figure 4-6.

First, two sets of initial guesses for the unnormalized mole fraction of the trial phase are given to avoid missing solutions. Both the Newton-Raphson method and the successive substitution method have been tried. The iteration count for Newton-Raphson method does not differ largely with that for successive substitution method. Only after the trial values of the variables are close enough to the root, will the method converge quadratically. Here the calculated results of the

last point cannot be used as initial guesses. The successive substitution method is simple compared with the Newton-Raphson method and less calculations are needed. Thus, the successive substitution method is employed to solve the equation group (3.39):

$$\ln Y_i + \ln \phi_i - h_i = 0 . \tag{3.39}$$

The code converges to the same solution or two different solutions with the two sets of initial estimates. If both sets of initial estimates converge to a trivial solution, the initial guesses presented in equations (4.9) and (4.10) will be tried. The convergence criterion is $\sum_i (Y_i^{n+1} - Y_i^n)^2 < 10^{-8}$. If two different solutions are obtained, the two values of $\sum_i Y_i$ corresponding to the two solutions are identified and the solution corresponding to the lesser value is discarded because only when the value of $\sum_i Y_i$ is larger than 1 will the system be unstable. The value of θ ($\theta = -\ln \sum_i Y_i$) is evaluated. If $\theta > 0$, the global stability of the system is verified. If $\theta < 0$, the system is unstable. If $\theta < 0$ and $\theta > tol$, a critical endpoint has been found. *tol* represents the convergence criterion for a critical endpoint. The most often employed value for *tol* is -1.0×10^{-3}. If $\theta < 0$ and $\theta \le tol$, the system is unstable but the critical endpoint has not yet been found and the control of the code will automatically transfer to the calculation of another critical point using a shortened step size and tests the stability of that critical point. The detailed algorithm for finding a critical endpoint will be presented in Section 4.4.3.

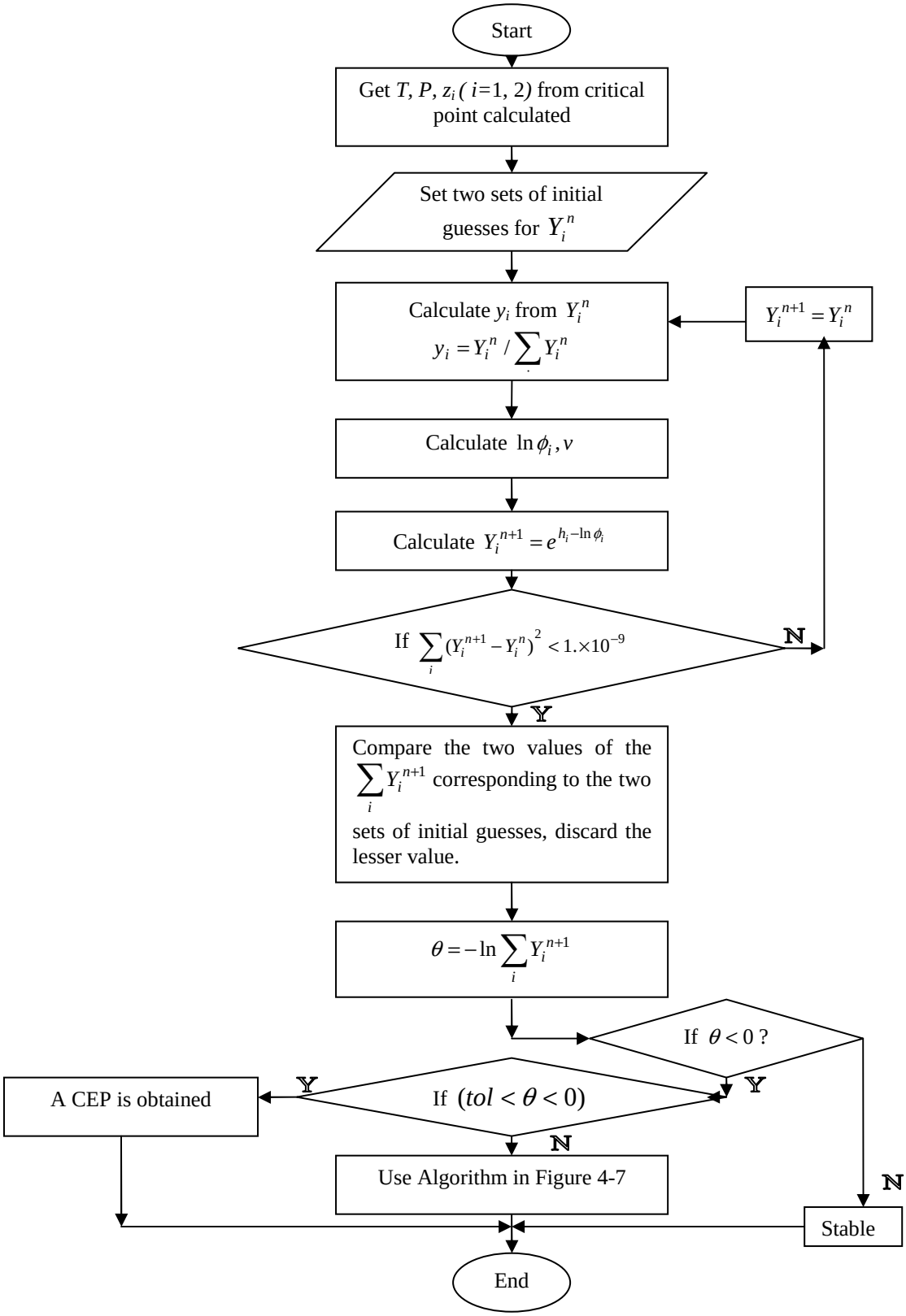

Figure 4-6 Flowchart for stability test and determination of a critical endpoint.

4.4.2 Initialization

To avoid losing roots, two sets of initial estimates are employed. One set is $Y_1 = 10^{-6}, Y_2 = 1 - Y_1$ and the other one is $Y_1 = 1 - 10^{-6}, Y_2 = 1 - Y_1$. A different technique for setting the two sets of initial estimates is as follows (Michelsen, 1982):

$$Y_i = K_i z_i \tag{4.11}$$

$$Y_i = z_i / K_i \tag{4.12}$$

where

$$K_i = \frac{P_{c_i}}{P} \exp\{5.42(1 - \frac{T_{c_i}}{T})\}. \tag{4.13}$$

If the code does not converge to the same solution, two sets of results will be obtained and the composition of the equilibrium phase corresponds to the results with lesser value of θ. This point is very significant for the following evaluation of three-phase line, because the initial estimate for the first three-phase point needs the composition of the equilibrium phase at the critical endpoint.

4.4.3 Critical Endpoints

A critical endpoint is very important for a global phase diagram because at a critical endpoint a critical line and a three-phase line join. If the critical endpoint can not be determined, a smooth global phase diagram cannot be developed. After an unstable critical point is obtained, the control of the code will determine the value of θ. If θ is less than *tol*, the critical point is not a critical endpoint. The control of the code will restore the compositions and corresponding temperature and pressure values of the last stable critical point obtained and decrease the step size

for changing compositions. A new critical point which is closer to that stable critical point will be evaluated and then a stability test at the new point is done. If θ satisfies the conditions $\theta < 0$ and $\theta > tol$, the critical endpoint is obtained. If it does not, the above technique for updating compositions will be employed again until the critical point satisfying the conditions $\theta < 0$ and $\theta > tol$ is obtained and a critical endpoint has been found. The flowchart is presented in Figure 4-7.

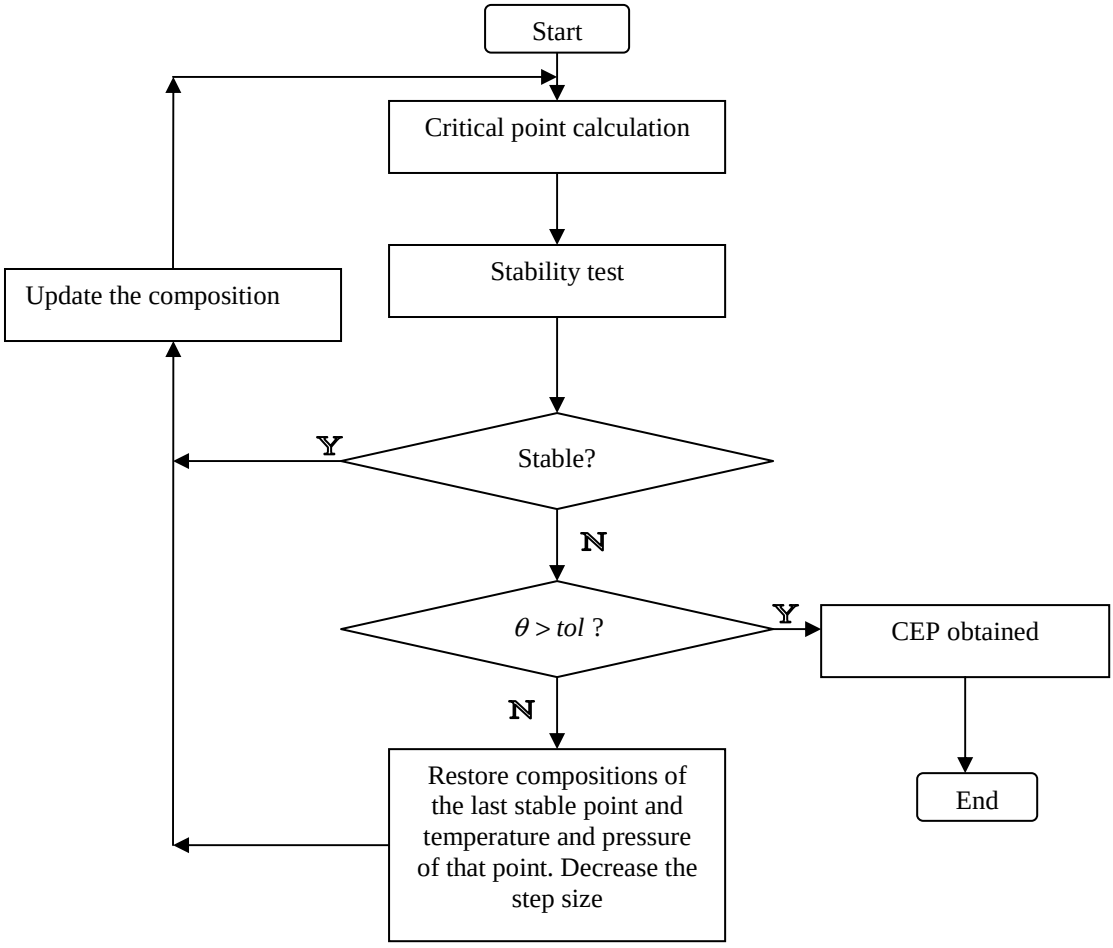

Figure 4-7 Flowchart for determining critical endpoint in the calculation of critical points.

4.5 Calculation of the Three-Phase Lines

A three-phase line is a significant part of a global phase diagram in *PT* space. The code for the calculation of a three-phase line has also been designed.

From Section 3.6, the following four simultaneous equations are obtained to determine the three-phase line points for a binary system:

$$\begin{aligned} g_1 &= \ln f_{11} - \ln f_{ref1} = 0 \\ g_2 &= \ln f_{12} - \ln f_{ref2} = 0 \\ g_3 &= \ln f_{31} - \ln f_{ref1} = 0 \\ g_4 &= \ln f_{32} - \ln f_{ref2} = 0, \end{aligned} \tag{3.49}$$

where

$$\ln f_{ref1} = \ln f_{21}, \tag{3.50}$$

and

$$\ln f_{ref2} = \ln f_{22}. \tag{3.51}$$

The four independent variables are the temperature, pressure of the system and the MVC (most volatile component) mole fractions of phase I and phase III at the three-phase points. Because only the MVC mole fractions of phase II vary smoothly along the three-phase line and the critical endpoint, where phase II is surely to become a critical phase but phase I or phase III is not certain to become a critical phase, phase II is chosen as the reference phase (Figures 4-8 and 4-9).

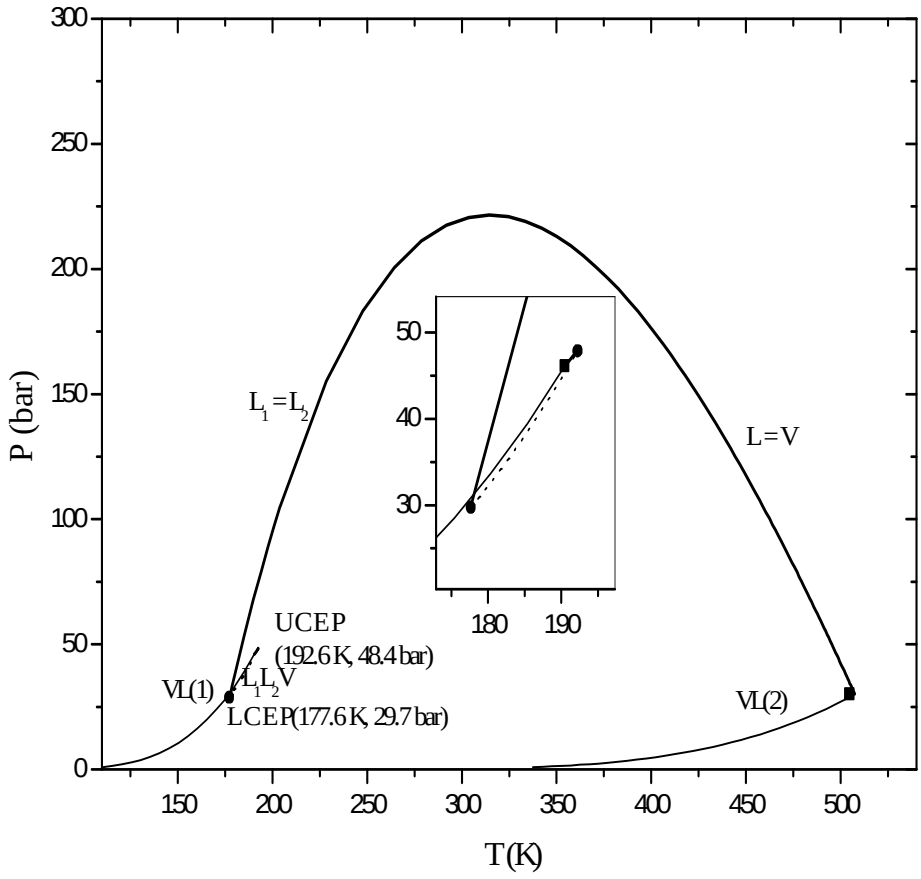

Figure 4-8 Global phase diagram in *PT* space for type V phase behaviour of the methane + n-hexane binary.

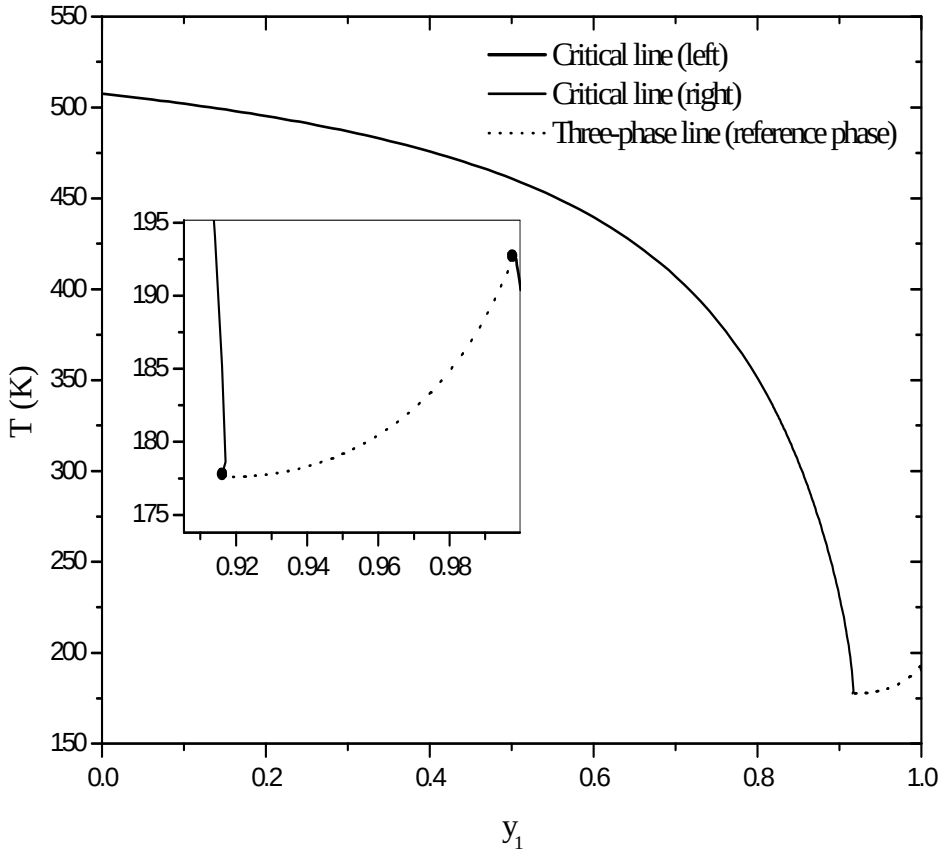

Figure 4-9 *T-y* Projection for the global phase diagram in Figure 4-8: (●) critical endpoint.

4.5.1 Flowchart

The code uses the Newton-Raphson method to solve equation group (3.49). The MVC mole fraction of the reference phase is varied with a step size to evaluate points in the three-phase line continuously. The flowchart is shown in Figure 4-10.

The convergence criterion $\left| y_{21} - y_{31} \right| < 10^{-4}$ is employed to determine if the second critical endpoint is present. If it is, the system is a type V system. The

control of the code then transfers to the calculation of the L = V critical line starting from the pure MVC critical point. If no such critical endpoint is determined, with more and more three-phase points obtained, the MVC mole fraction of phase I or phase III becomes so close to 1 that the division by zero error will certainly occur. The division by zero error occurs when the coefficient matrix for the four simultaneous equations to be solved is decomposed. The technique to handle this exception is presented in Chapter 5.

4.5.2 Initialization

Usually before the evaluation of a three-phase line, a critical endpoint is obtained. At the critical endpoint, a critical phase is in equilibrium with another phase, the equilibrium phase. The initial estimates of temperature and pressure for the first three-phase point is set with the corresponding values at the critical endpoint. Initial guesses for the compositions of the three phases are set as follows: the MVC (most volatile component) mole fraction of the reference phase (phase II) is set to the MVC mole fraction of the critical phase at the critical endpoint. The composition of the first phase is set with the value obtained when the MVC mole fraction of the critical phase is decreased by the current step size for changing composition and the third phase is set with the composition of the equilibrium phase.

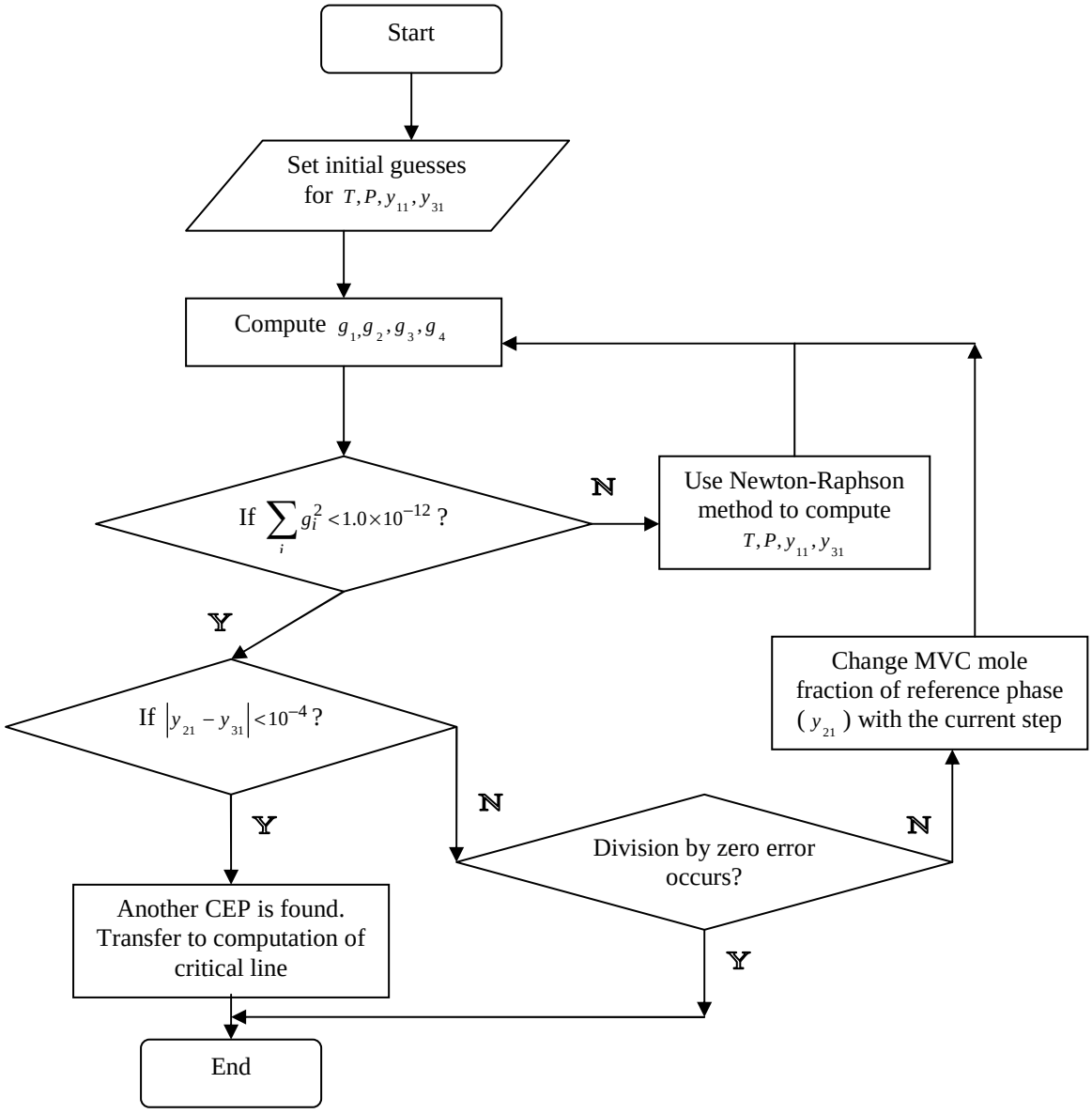

Figure 4-10. Flowchart for calculating three-phase line. CEP stands for the critical endpoint and MVC represents the most volatile component. For y_{ij}, i represents the phase index and j represents the component index.

4.6 Summary

In the chapter, the algorithm for predicting a global phase diagram in PT space automatically is shown. Different algorithms for the computation of different parts of a global phase diagram are then presented. In the next chapter, the calculation results and code performance are presented. The program exceptions are also discussed.

5. RESULTS AND DISCUSSION

Based upon the algorithms presented in Chapter 4, a code in C++ language using MS Visual Studio 7.0 was developed to predict global phase diagrams automatically. The calculated data for a whole global phase diagram are stored automatically in an output file. Phase diagrams for different types of binary systems are computed successfully and the transition states between different types of phase behaviour are also explored.

5.1 Phase Diagrams Calculated for Different Types of Binary Systems

The project focuses on the systems in petroleum processing field. The methane + alkane binary, ethane + alkanol binary and the binary mixture of propane + phenanthrene are explored. Different types of phase behaviours, including type I, type II, type III and type V, are observed. The code performance with respect to these systems is then discussed.

5.1.1 Type I

As presented in Chapter 2, phase diagrams of type I binary systems are simple, so just one phase diagram is presented here. For the methane + propane binary mixture with a binary interaction parameter for the Peng-Robinson equation

of state set to 0.04, the corresponding phase diagram belongs to type I (Figure 5-1). A continuous critical line is observed.

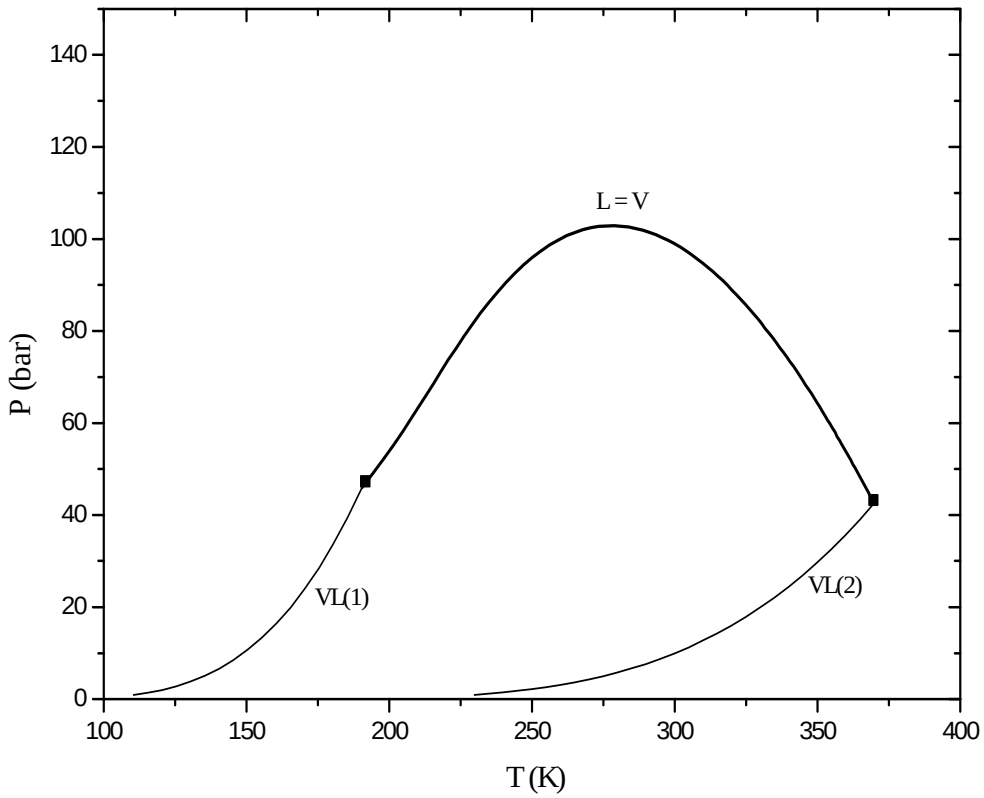

Figure 5-1 *PT* phase diagram of methane(1) + propane(2) with K_{ij} for Peng-Robinson equation of state being 0.04: (■) pure component critical point, K_{ij} stands for binary interaction parameter.

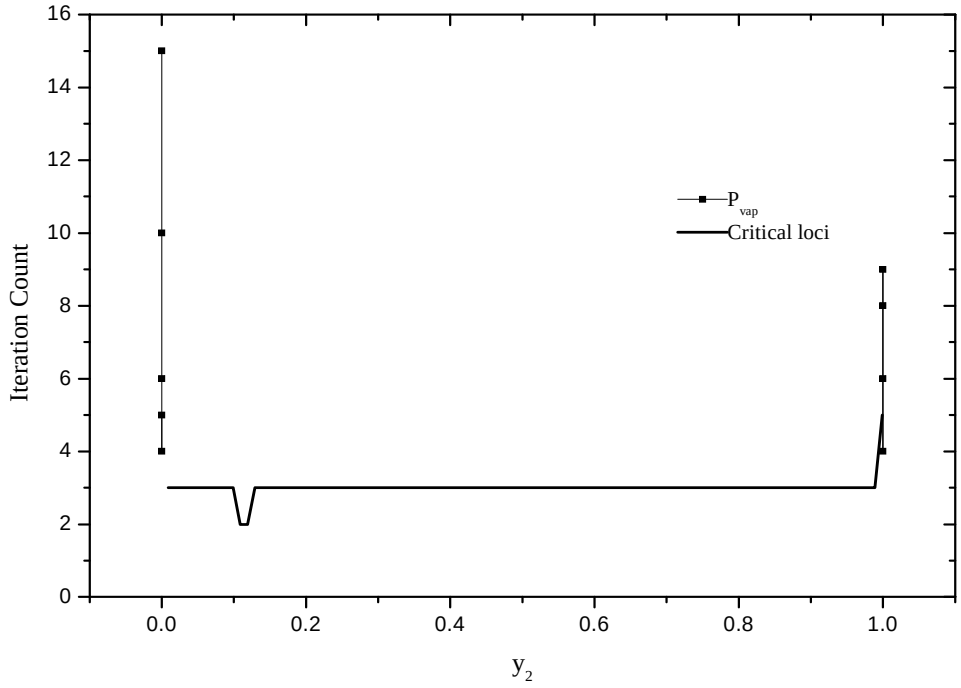

Figure 5-2 The relationship between the iteration count and composition of the solute for the calculation of the phase diagram of methane (1) + propane (2) with $K_{ij} = 0.04$ for the Peng-Robinson equation of state.

From Figure 5-2, it is observed that the first points have a larger iteration counts than the subsequent points of the vapour pressure lines, because the calculation of the first point uses the critical pressure of the pure MVC as the initial guesses, which is not so close to the root compared to the initial estimates for the subsequent points and with the decrease of temperature, the differences in vapour pressure between two neighbor points decrease. The calculation of the subsequent points of the vapour pressure line employs the computed results of the last points obtained as initial guesses.

The calculation of the first critical point uses $1.5\sum_i T_{ci}$ and $4b_m$ as initial estimates for the critical temperature and critical molar volume, respectively. The estimates are not so close to the solutions like the estimates for the computation of the subsequent points, so the iteration count for the first point may be larger than the subsequent points. The initial estimates for the subsequent points are the computed results of the last critical points obtained.

5.1.2 Type II

For type II systems, as presented in Chapter 2, a $L_1 = L_2$ critical line and a three-phase line in addition to the continuous L = V critical line are obtained. For the binary mixture of ethane + ethanol with binary interaction parameter for the Peng-Robinson equation of state being 0.0362, the corresponding phase diagram belongs to type II (Figure 5-3).

From Figure 5-4, it is observed that the first points of the vapour pressure lines have larger iteration counts than the subsequent points. The iteration counts for the points of the $L_1 = L_2$ critical line decrease as the critical pressures of the obtained points decrease because the calculation of all $L_1 = L_2$ critical points uses $1.8b_m$ as initial guesses for critical molar volumes. If the critical pressure is larger, the critical molar volumes will be lower, the difference between the roots and the initial guesses for the critical molar volumes will be larger and more iterations may be needed.

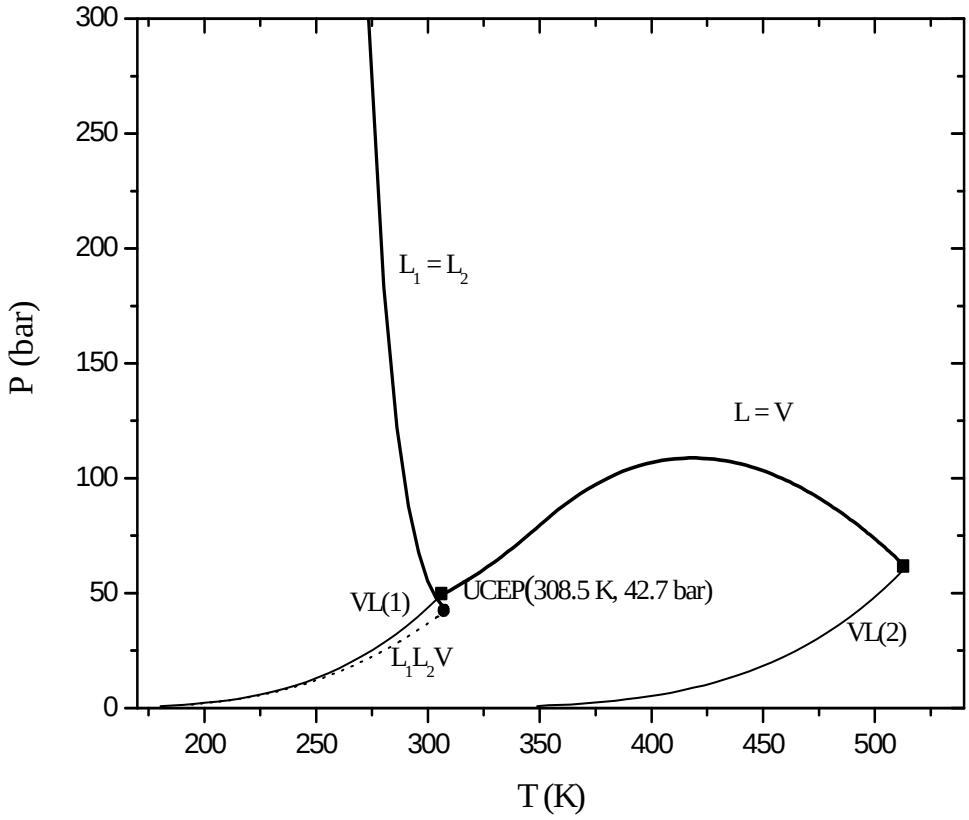

Figure 5-3 *PT* phase diagram of ethane(1) + ethanol(2) with $K_{ij} = 0.0362$ for the Peng-Robinson equation of state: (●) calculated critical endpoint, (■) pure component critical point, K_{ij} stands for binary interaction parameter.

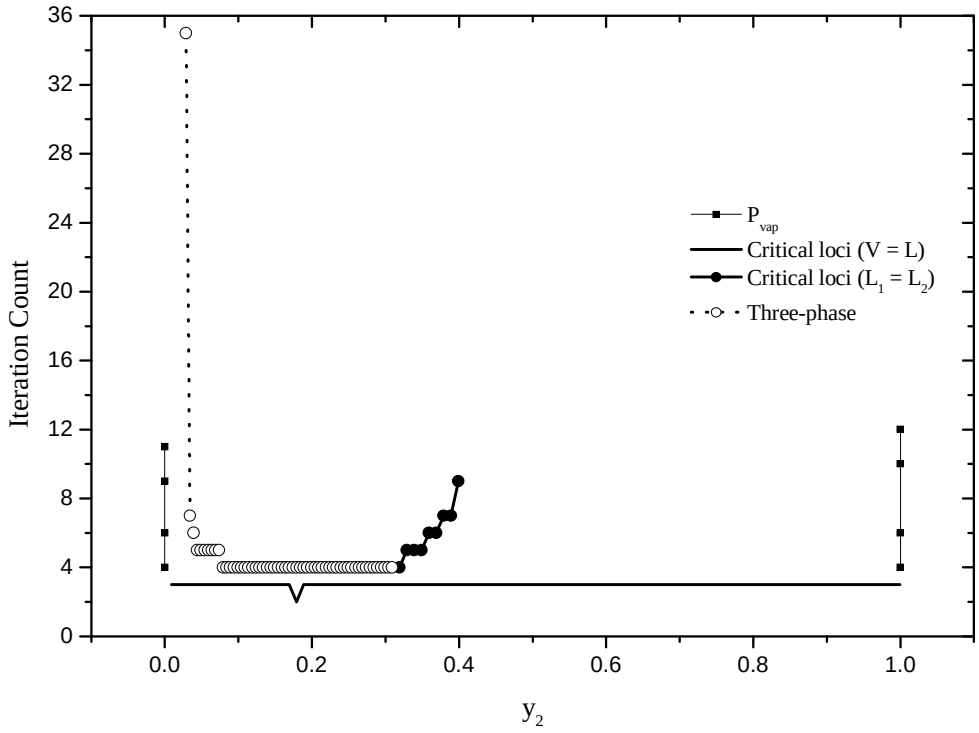

Figure 5-4 The relationship between the iteration count and composition of the solute for the calculation of the phase diagram of ethane (1) + ethanol (2) with $K_{ij} = 0.0362$ for the Peng-Robinson equation of state.

5.1.3 Type III

For type III systems, the L = V critical line becomes two parts. The one commencing from the critical point of the MVC (most volatile component) ends at an upper critical endpoint, where a three-phase line starts. For the binary mixture of propane + phenanthrene with a binary interaction parameter being 0.079 (Figure 5-5), the binary mixture of methane + n-heptane with a binary interaction parameter being 0.082 (Figure 5-7) and the binary mixture of methane + n-hexane with a

binary interaction parameter for the Peng-Robinson equation of state being 0.1 (Figure 5-8), the corresponding phase diagrams are all type III. The code is applicable to all the three binary systems. No $L_1 = L_2$ critical lines are obtained for the three systems. When critical points with very high pressure are found, if no critical endpoint is obtained near the critical points, the critical point calculations have to be restarted from the critical point of the pure MVC.

From Figure 5-6, one can see that with the increase of critical pressure of the L = V critical points on the critical line starting from pure solute critical point, the corresponding iteration count increases. For the evaluation of three-phase line, the first point has a larger iteration count because the initial guesses for it are set with the computed results of the critical endpoint obtained before the calculation of the three-phase line while the subsequent points use the computed results of the last three-phase points obtained as the initial estimates. When the MVC mole fractions of the third phase for the three-phase points approach one, the iteration counts become larger and larger because round off errors increase when the coefficient matrix for the equation system to be solved is decomposed. When the solute mole fraction of the system is under $y_2 = 0.1$, no stable critical points exist.

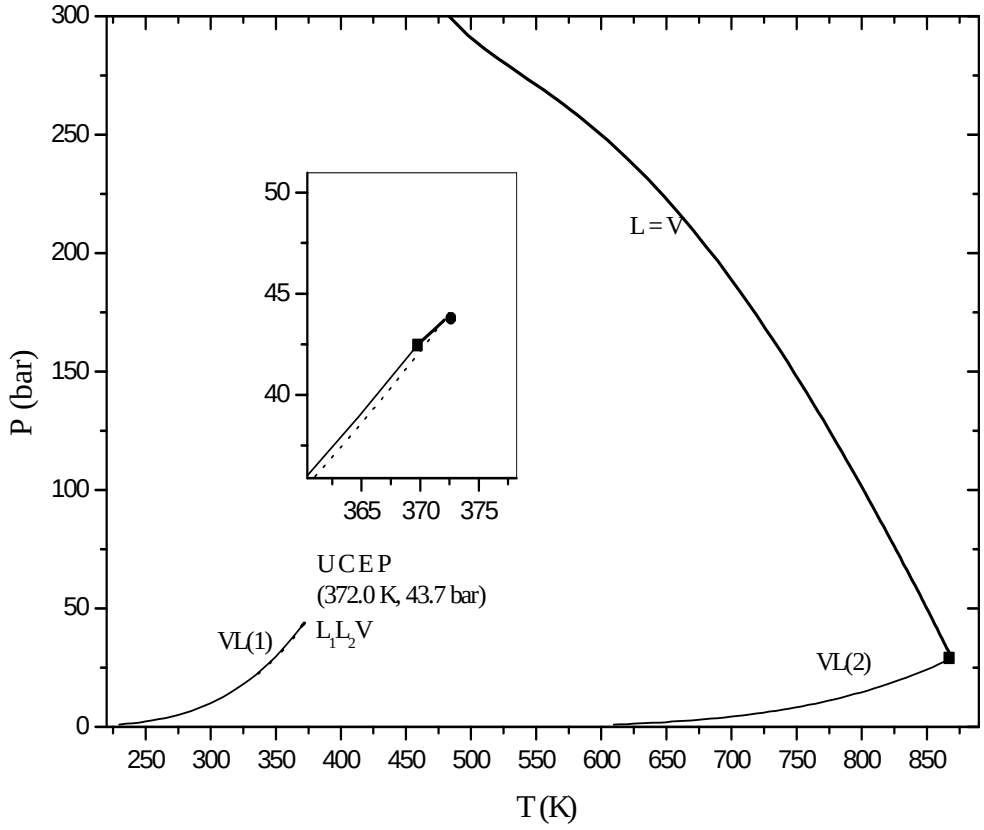

Figure 5-5 *PT* phase diagram of propane(1) + phenanthrene(2) with $K_{ij} = 0.079$ for the Peng-Robinson equation of state: (●) calculated critical endpoint, (■) pure component critical point.

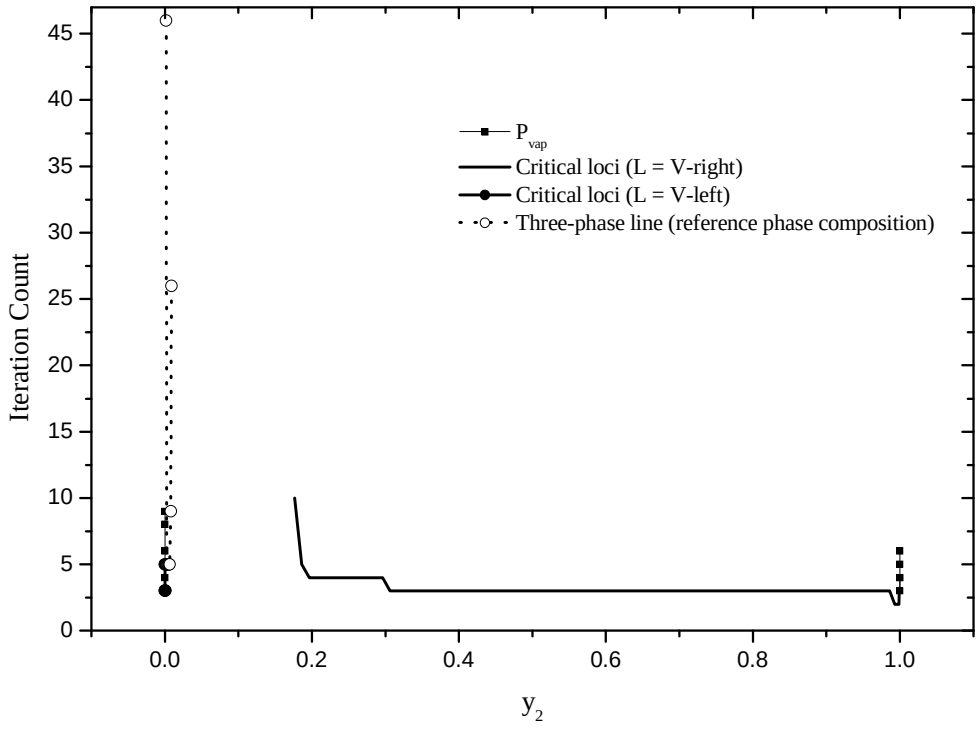

Figure 5-6 The relationship between the iteration count and composition of the solute for the calculation of the phase diagram of propane(1) + phenanthrene(2) with $K_{ij} = 0.079$ for the Peng-Robinson equation of state.

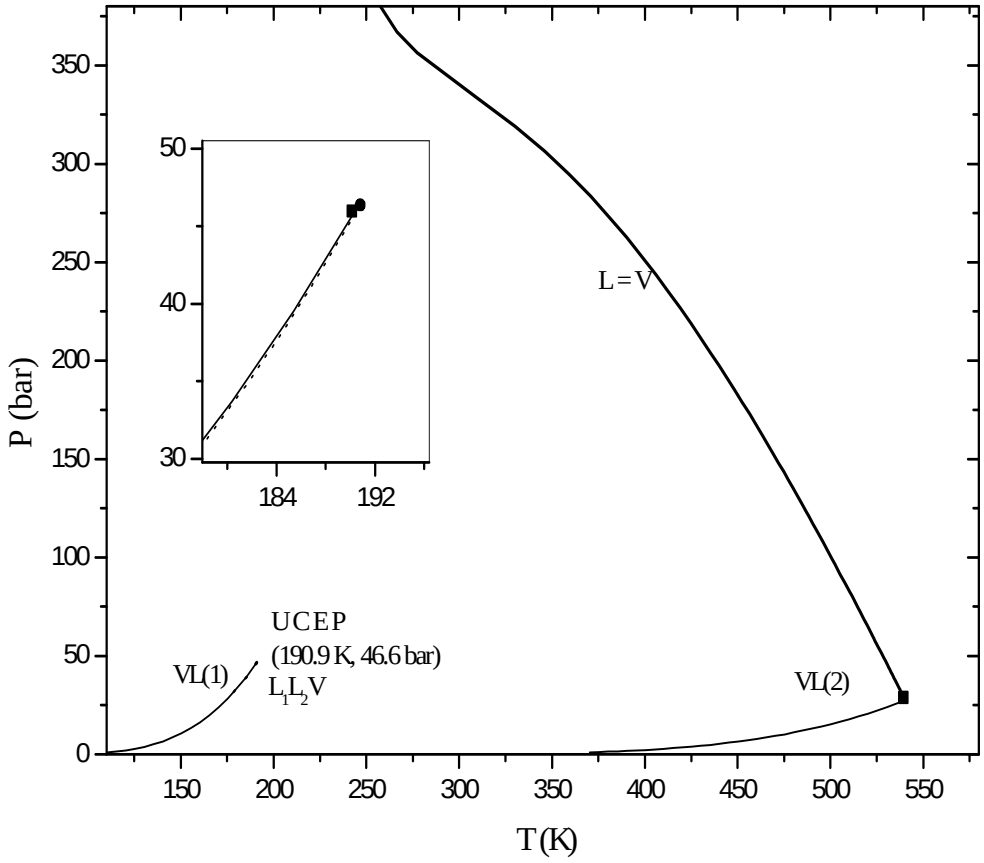

Figure 5-7 *PT* phase diagram of methane(1) + n-heptane(2) with $K_{ij} = 0.082$ for the Peng-Robinson equation of state: (●) calculated critical endpoint, (■) pure component critical point.

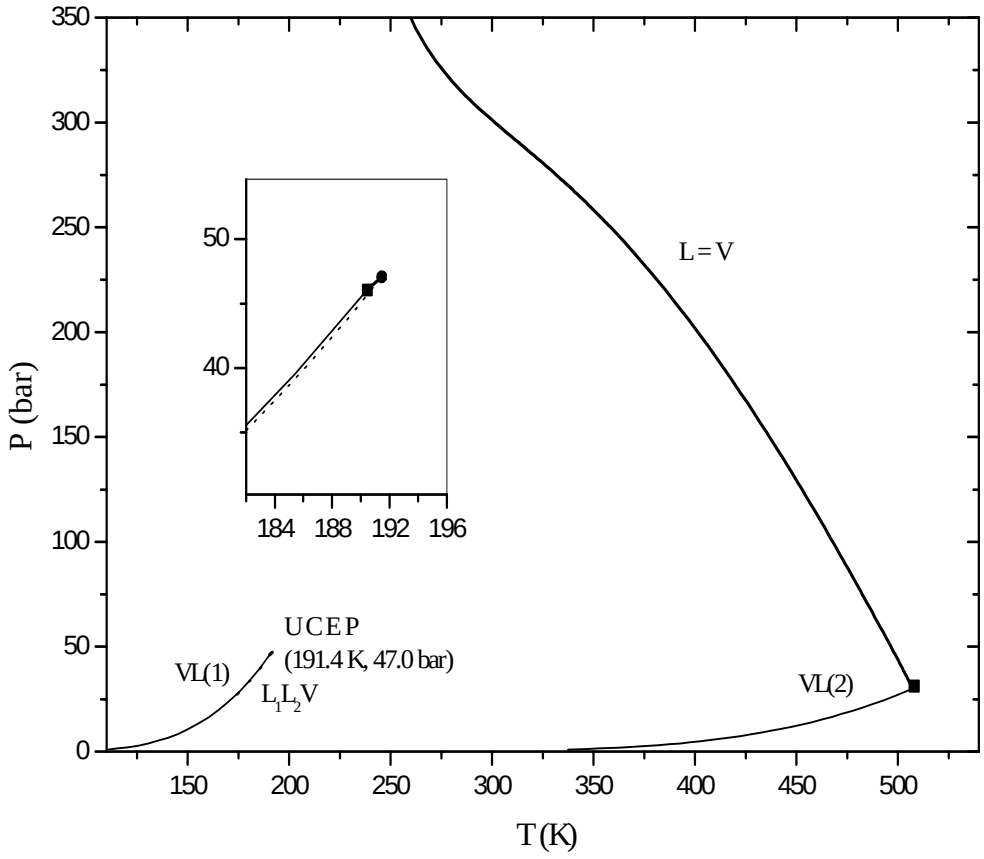

Figure 5-8 *PT* phase diagram of methane(1) + n-hexane(2) with $K_{ij} = 0.1$ for the Peng-Robinson equation of state: (●) calculated critical endpoint, (■) pure component critical point.

5.1.4 Type V

For type V systems, the L = V critical line is separated into two parts as well, but they are connected by a three-phase line with two critical endpoints.

For the binary mixture of methane + n-hexane with a binary interaction parameter of –0.1 (Figure 5-9), the methane + n-heptane mixture with a binary interaction parameter of –0.01 (Figure 5-11) and the binary mixture of propane + phenanthrene with a binary interaction parameter of –0.1 (Figure 5-12), the corresponding phase diagrams all belong to type V. The code developed is applicable to these binary systems.

From Figure 5-10, one can see that for the evaluation of three-phase line, the first point has a larger iteration count because the initial guesses for it are set with the computed results of the critical endpoint obtained before the calculation of the three-phase line while the subsequent points use the computed results of the last three-phase points obtained as the initial estimates. When the computed three-phase points become close to the upper critical endpoint, the MVC mole fractions of the third phase for the three-phase points approach one, and the iteration counts become larger and larger because round off errors increase when the coefficient matrix for the equation system to be solved is decomposed.

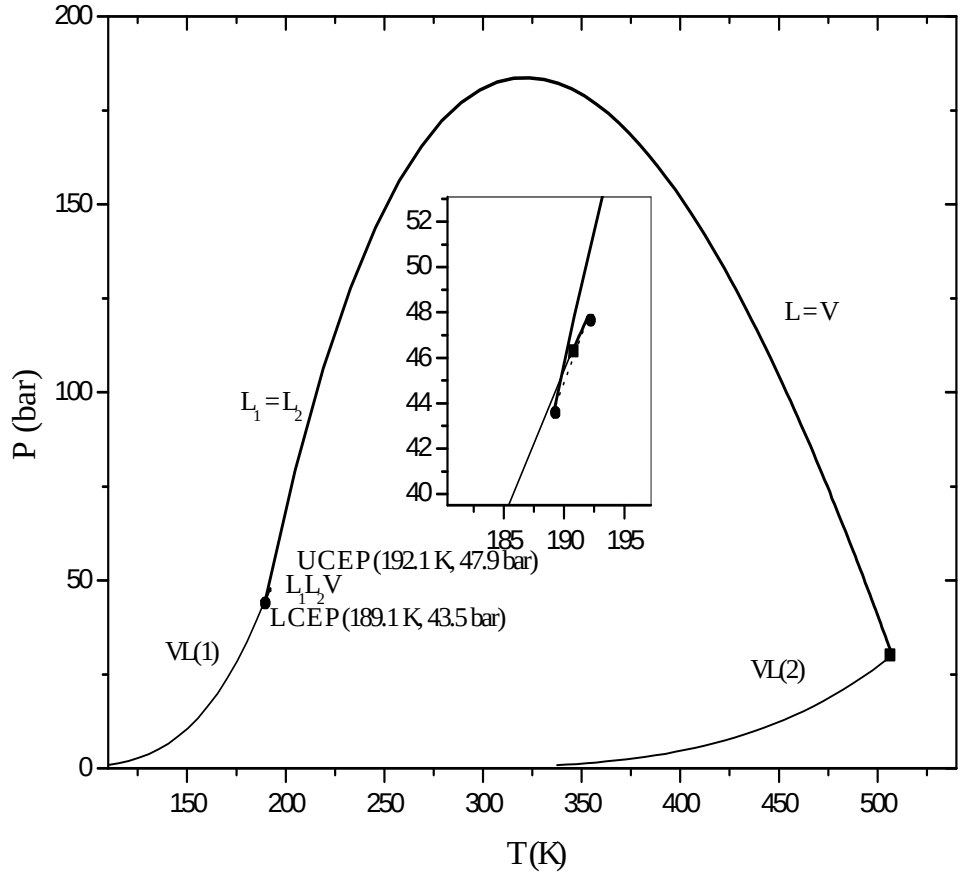

Figure 5-9 *PT* phase diagram of methane(1) + n-hexane(2) with $K_{ij} = -0.10$ for the Peng-Robinson equation of state: (●) calculated critical endpoint, (■) pure component critical point.

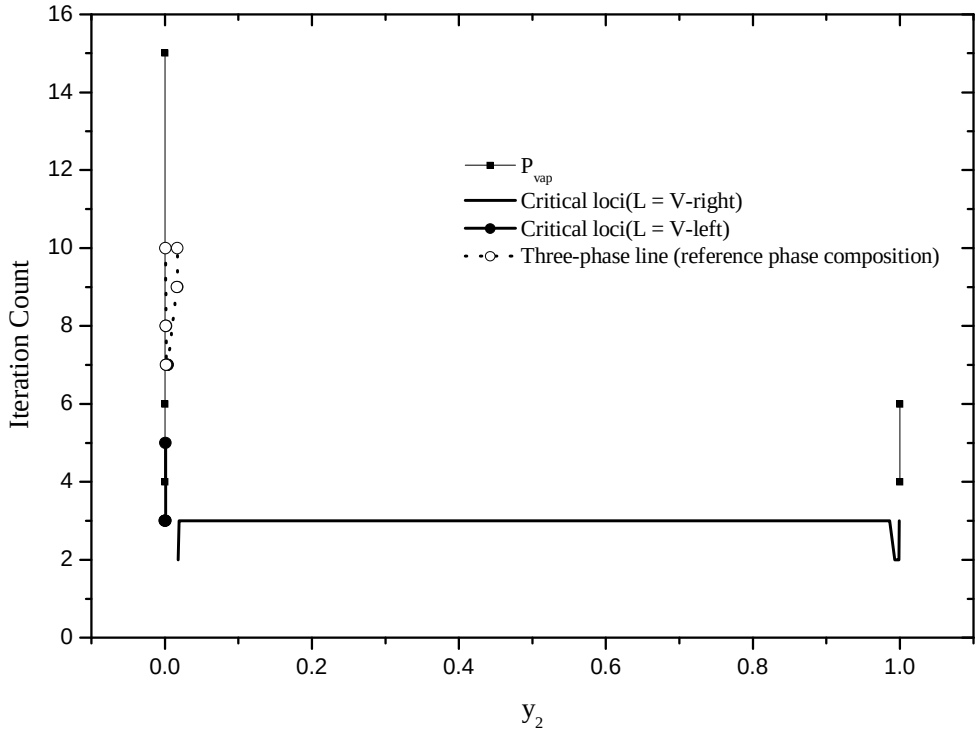

Figure 5-10 The relationship between the iteration count and composition of the solute for the calculation of the phase diagram of methane(1) + n-hexane(2) with $K_{ij} = -0.10$ for the Peng-Robinson equation of state.

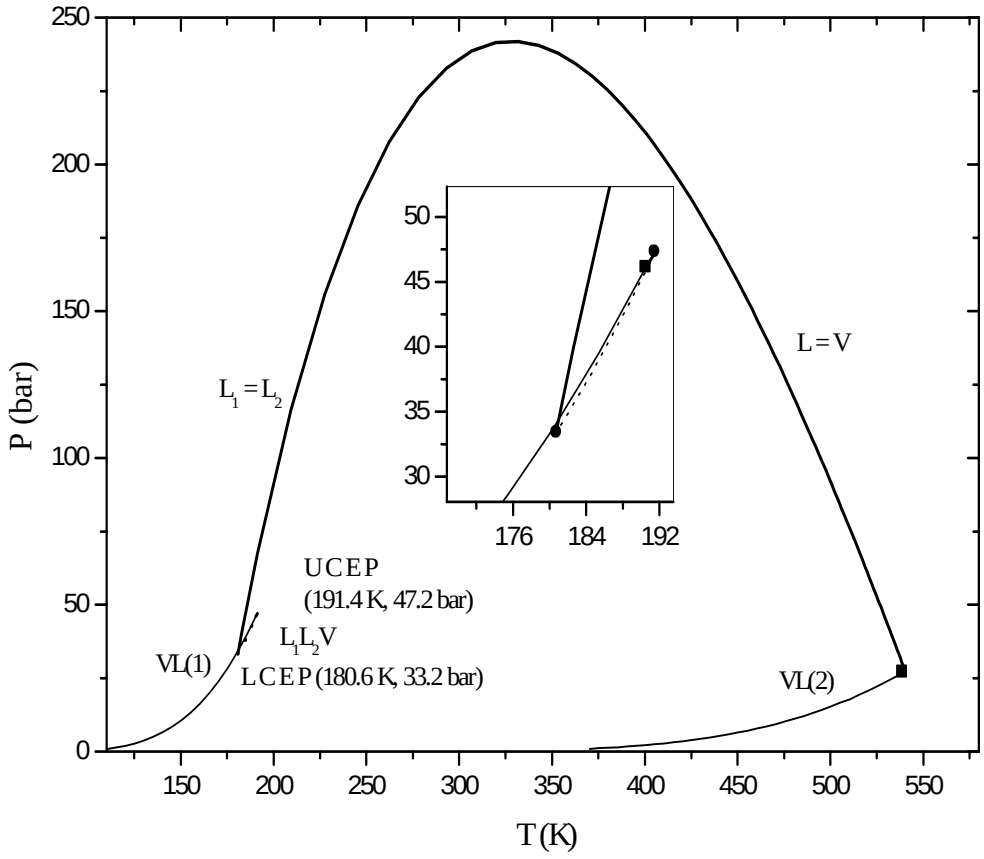

Figure 5-11 *PT* phase diagram of methane(1) + n-heptane(2) with $K_{ij} = -0.01$ for Peng-Robinson equation of state: (●) calculated critical endpoint, (■) pure component critical point.

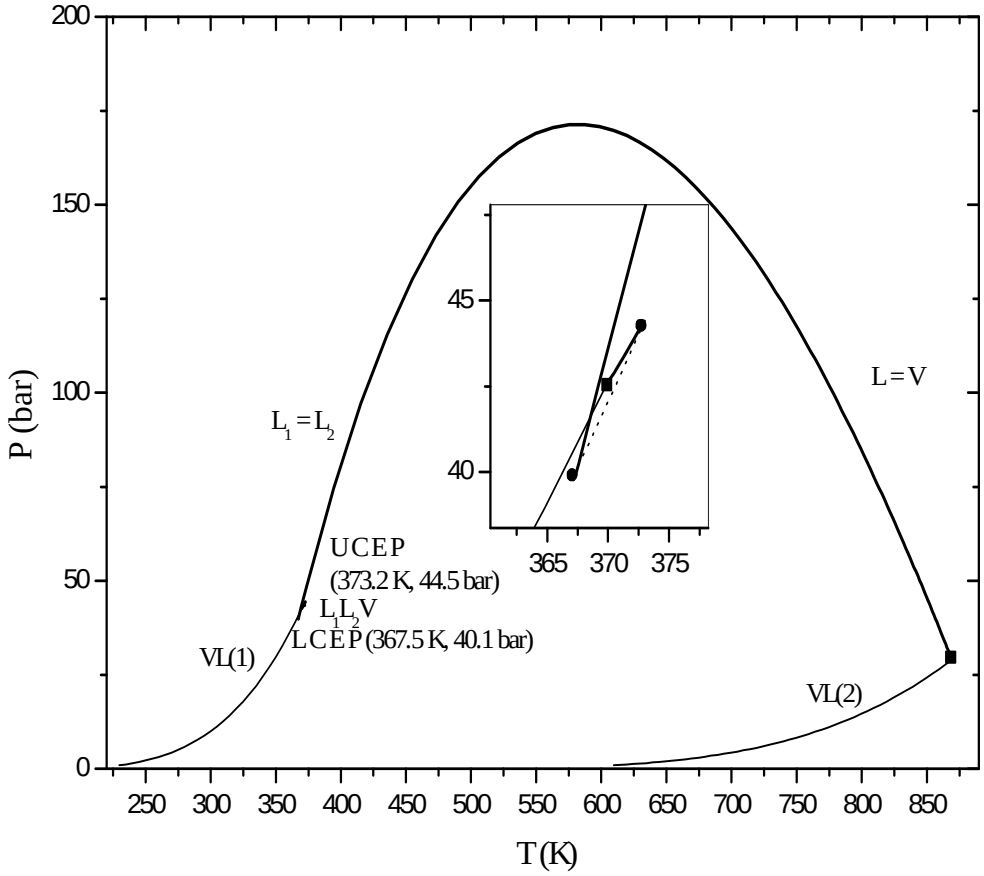

Figure 5-12 *PT* phase diagram of propane(1) + phenanthrene(2) with $K_{ij} = -0.10$ for the Peng-Robinson equation of state: (●) calculated critical endpoint, (■) pure component critical point.

Different types (I, II, III and V) of phase diagrams can be computed continuously and automatically using the developed code. Before the computation, the code needs no information about the types of the binary system, because the code can determine that while doing the calculation.

If in the computation of the L = V critical line, some points with very high pressure are obtained and a three-phase line is obtained and it has only one critical endpoint, it is type III phase behaviour. If the three-phase line obtained has two critical endpoints, the corresponding system belongs to type V (here type IV is not taken into consideration). If in the computation of the L = V critical line no critical endpoints or points with very high pressure ($P > 4.2\sum_i p_{ci}$) are found, the system is type I or II. If an UCST (upper critical solution temperature) line is obtained in the calculation of $L_1 = L_2$ critical line and a three-phase line with one critical endpoint is obtained, the phase behaviour will be determined by the code as type II. Otherwise, it is type I phase behaviour.

When the type is determined, algorithms for the specific type are employed and a global phase diagram is computed successfully.

5.2 Exploring the Transition between Different Types of Phase Behaviour

After the code is developed, the changing trend of the phase diagrams for binary systems with the same components is explored when the binary interaction parameter changes. For binary mixtures, with the increase of the binary interaction parameter, the energy of attraction between unlike molecules decreases because in the mixing rule, $a_{ij} = (1 - K_{ij})\sqrt{a_{ii} a_{jj}}$, with K_{ij}, a_{ij} and a_{ii} being the binary interaction parameter, the attraction cross-parameter for the mixture and the attraction parameter for pure component, respectively. When the interaction between molecules of different components decreases, the Λ parameter (equation

2.3) defined by van Konynenburg increases as well and the binary system has a trend to become more immiscible. The corresponding phase behaviour may transfer from type I to type II to type III or from type V to type III.

5.2.1 Binary Mixture of Ethane and Ethanol

For the binary mixture of ethane + ethanol, with the increase of binary interaction parameter, the phase behaviour transfers from type I to type II and then to type III. The variation trend is shown in a composite figure, Figure 5-13.

It is observed that with the increase of binary interaction parameter, the attractive force between molecules of different components decreases and the phase behaviour changes from type I to type II and then to type III. The trend matches the results of van Konynenburg and Scott (1980).

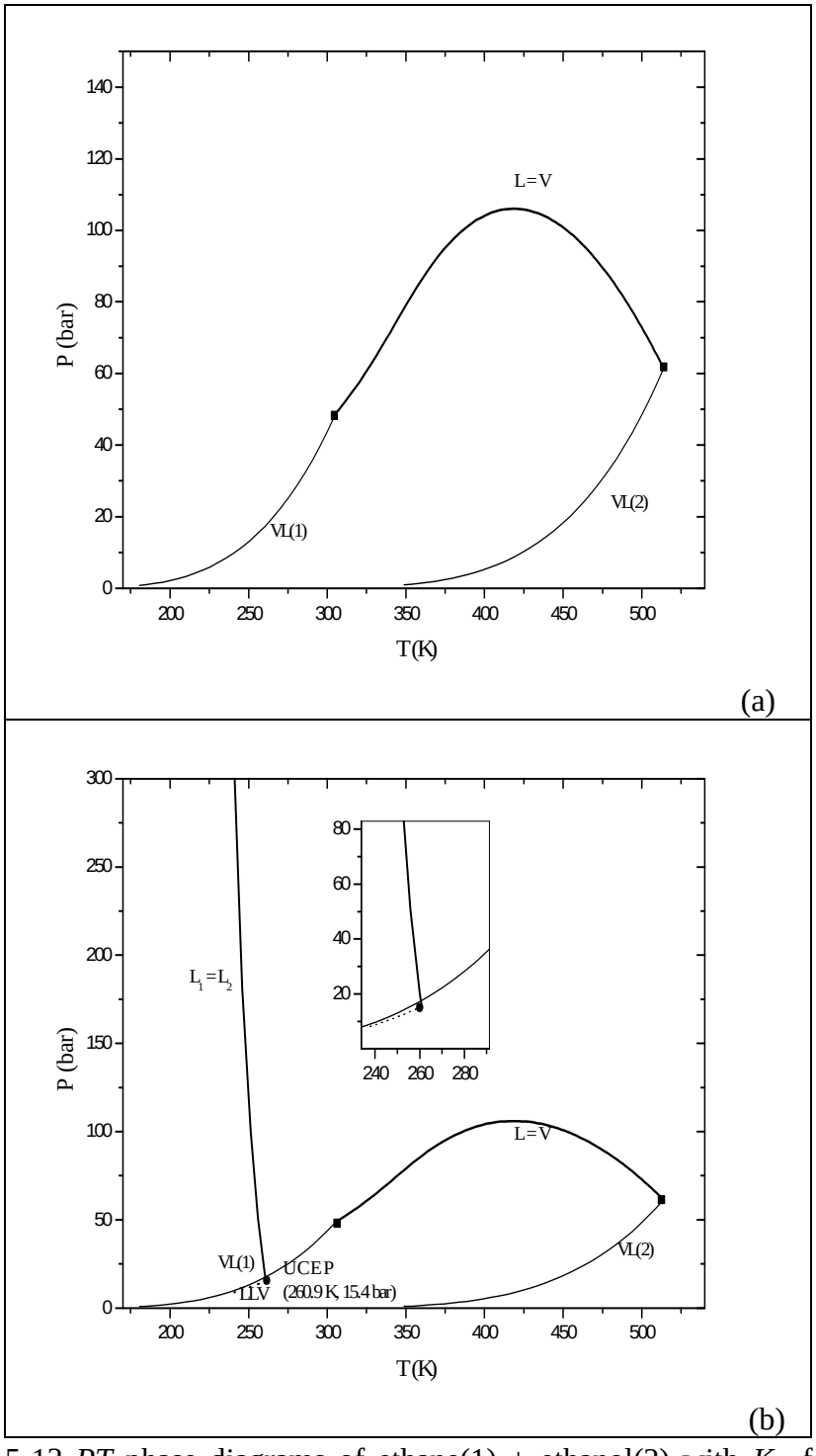

Figure 5-13 *PT* phase diagrams of ethane(1) + ethanol(2) with K_{ij} for the Peng-Robinson equation of being 0.0090 (a), 0.0091 (b): (●) calculated critical endpoint (■) pure component critical point.

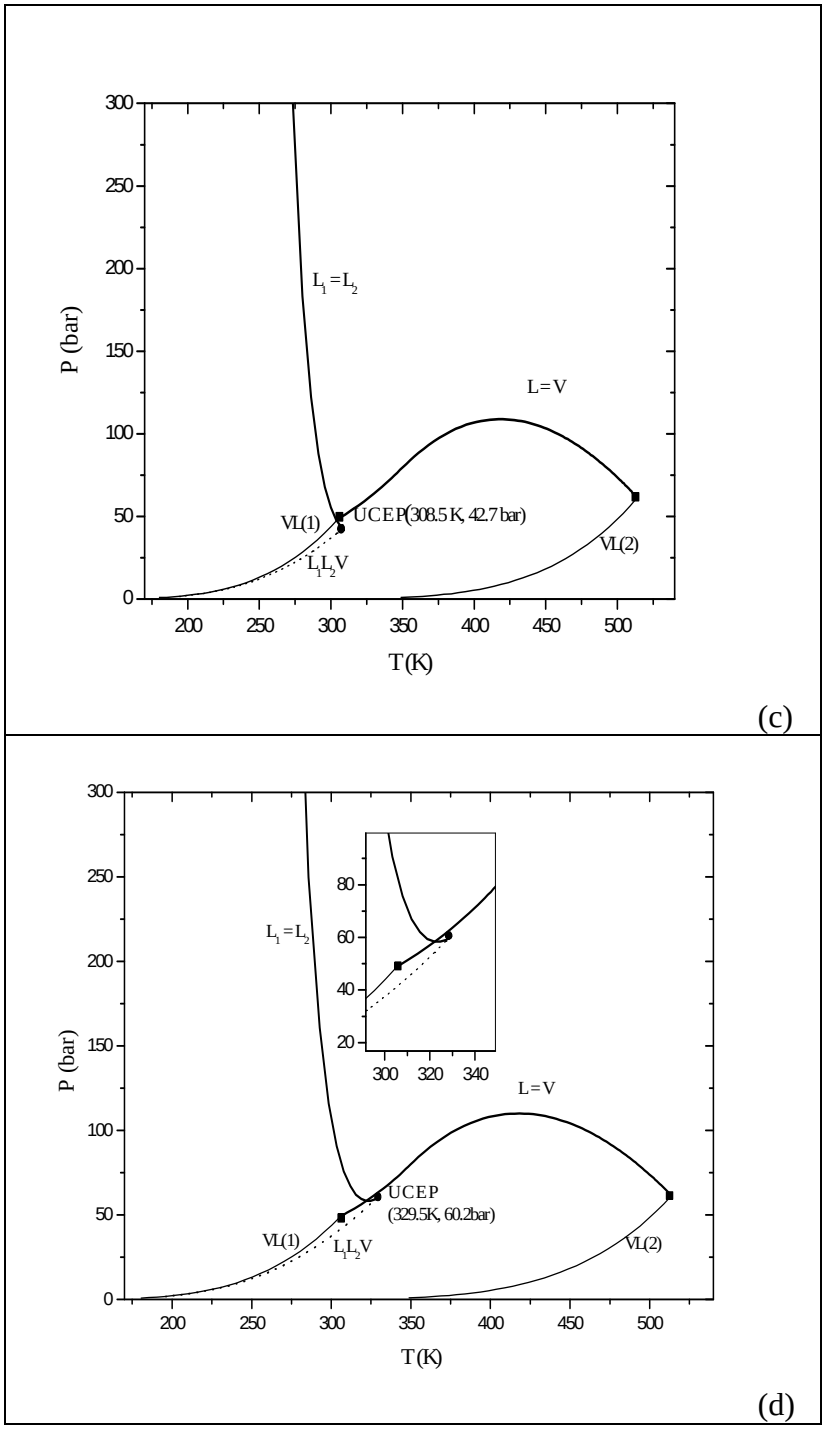

Figure 5-13 *PT* phase diagrams of ethane(1) + ethanol(2) with K_{ij} for the Peng-Robinson equation of being 0.0362 (c) and 0.0449 (d): (●) calculated critical endpoint (■) pure component critical point.

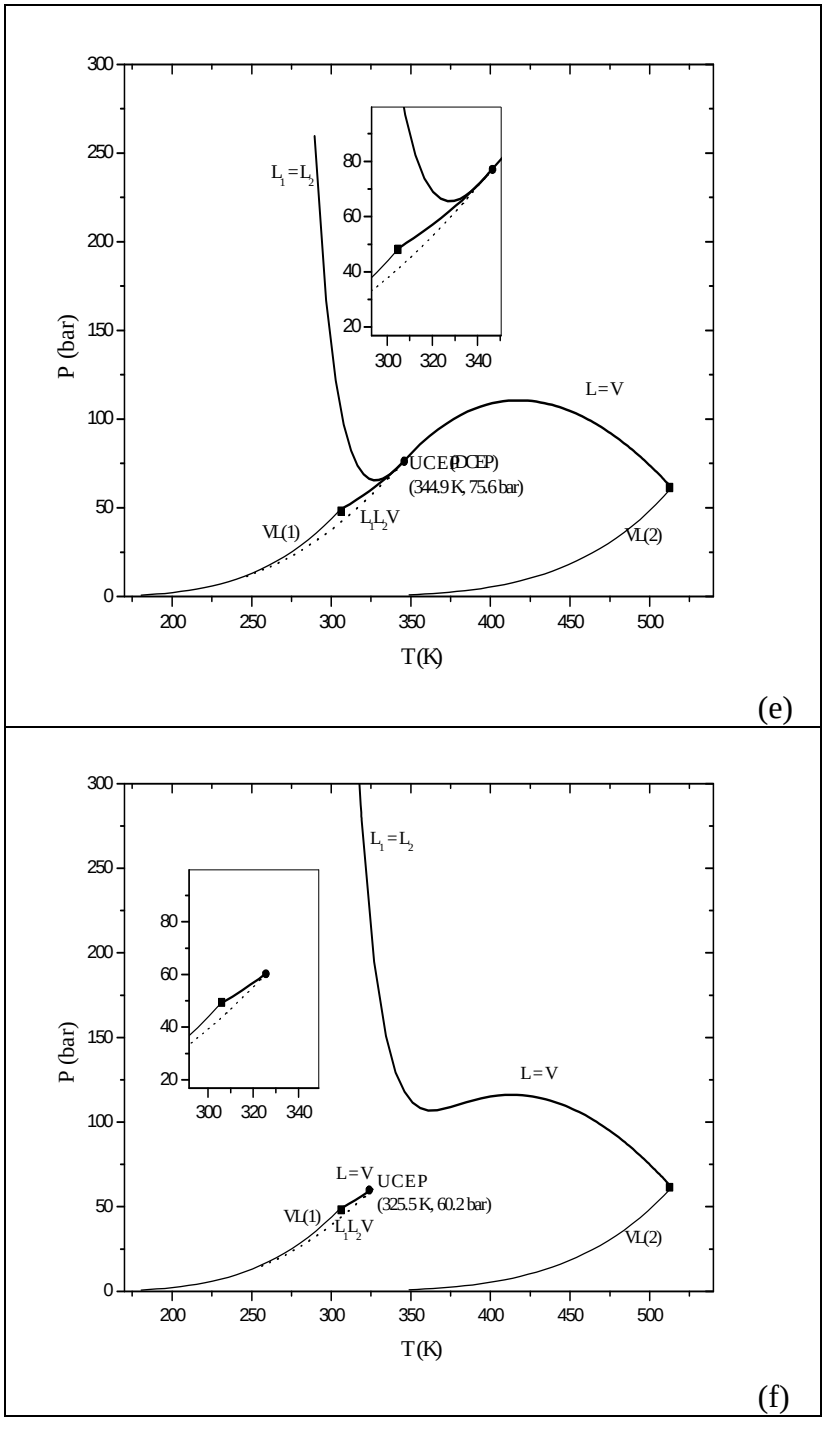

Figure 5-13 *PT* phase diagrams of ethane(1) + ethanol(2) with K_{ij} for the Peng-Robinson equation of being 0.049(e) and 0.08(f): (●) calculated critical endpoint (■) pure component critical point.

The qualitative T_r, y_2 isobars ($T_r = T/T_{c1}$) for type I, type II and type III phase behaviour of the binary system ethane + ethanol are presented in Figures 5-14, 5-15 and 5-16. It is observed that from type I to type II to type III phase behaviour of the ethane + ethanol binary, the system has a trend to become more immiscible over larger and larger temperature and composition ranges, giving rise to more multiphase behaviour.

The boundary state between type I (Figure 5-13 (a)) and type II (Figure 5-13 (b)) phase behaviour corresponds to a phase diagram with an imaginary zero Kelvin point (ZKP). A ZKP is a double critical endpoint with a temperature of zero Kelvin (Deiters and Pegg, 1989). It is observed that the upper critical endpoint in Figure 5-13 (b) has relatively low temperature. A double critical endpoint is a point where a critical line and a three-phase line intersect and the slopes of both lines are equal at the point. A double critical endpoint is also a critical endpoint. At a double critical endpoint, a critical phase is in equilibrium with a non-critical phase. In Figure 5-13 (e), the critical endpoint is a double critical endpoint; the state corresponding to Figure 5-13 (e) is a boundary state between type II and type III phase behaviour.

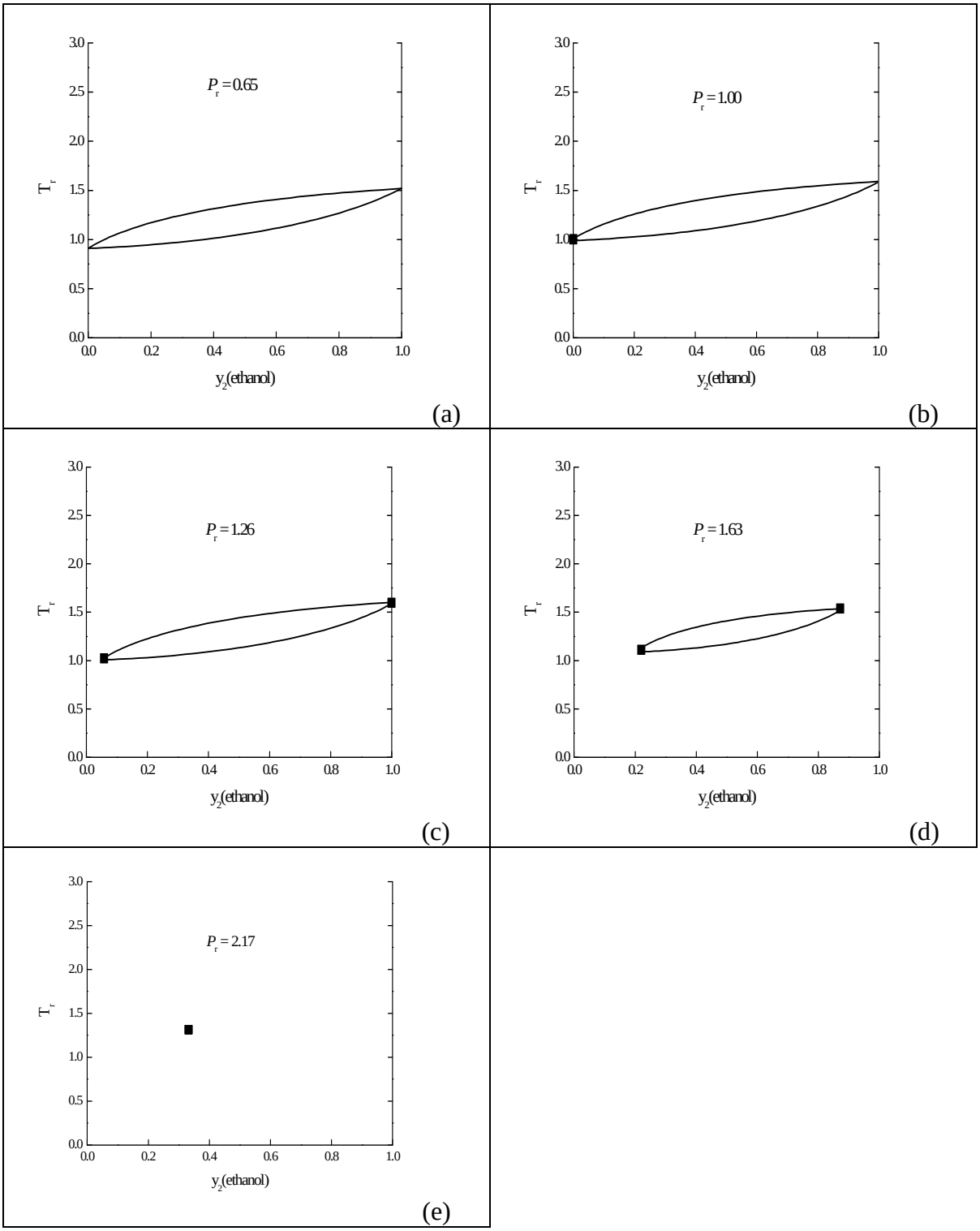

Figure 5-14 T_r, y_2 isobars for type I phase behaviour (Figure 5-13 (a)) of the binary mixture of ethane(1) + ethanol(2): (■)critical point.

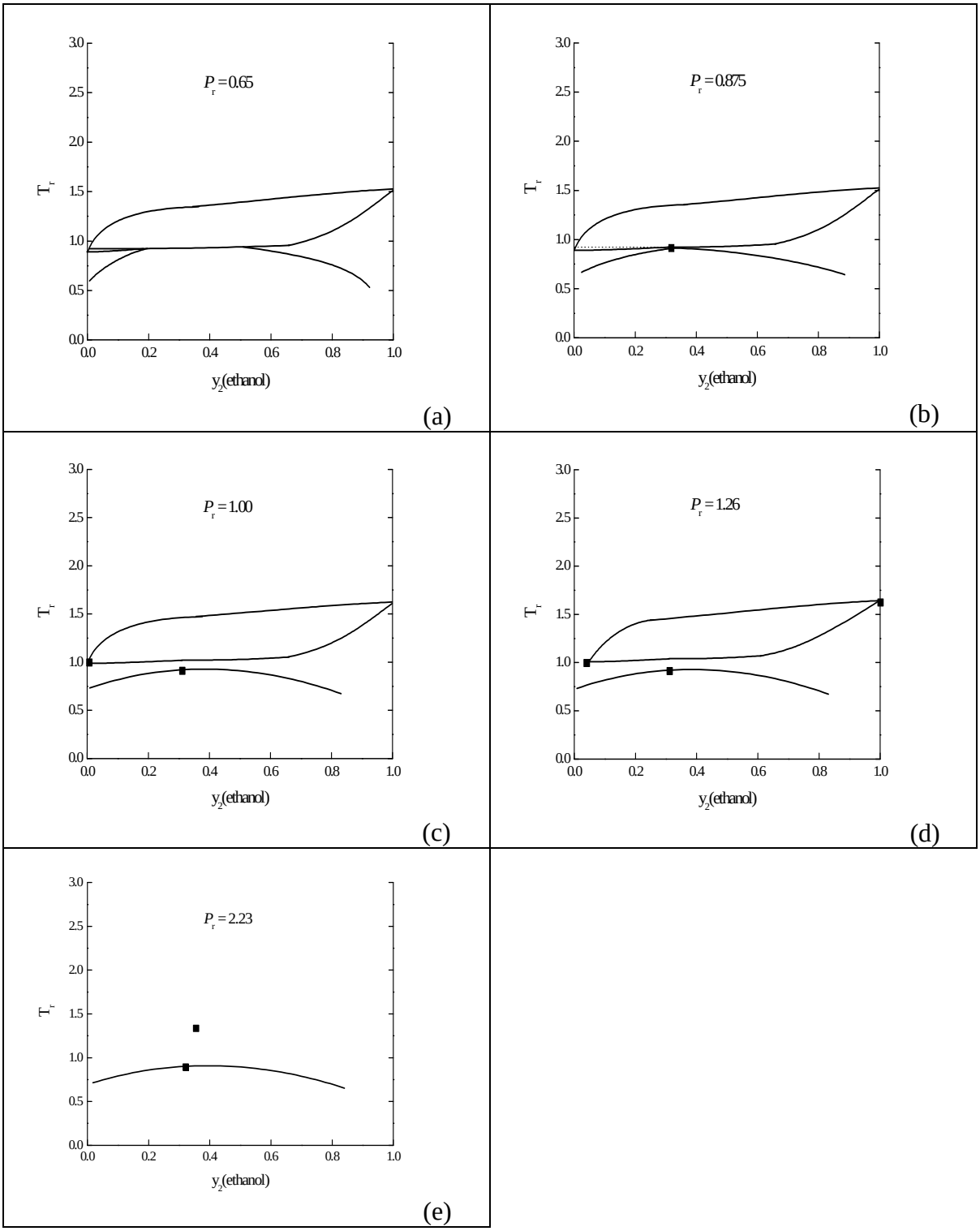

Figure 5-15 T_r, y_2 isobars for type II phase behaviour (Figure 5-13 (c)) of the binary mixture of ethane(1) + ethanol(2): (■) critical point.

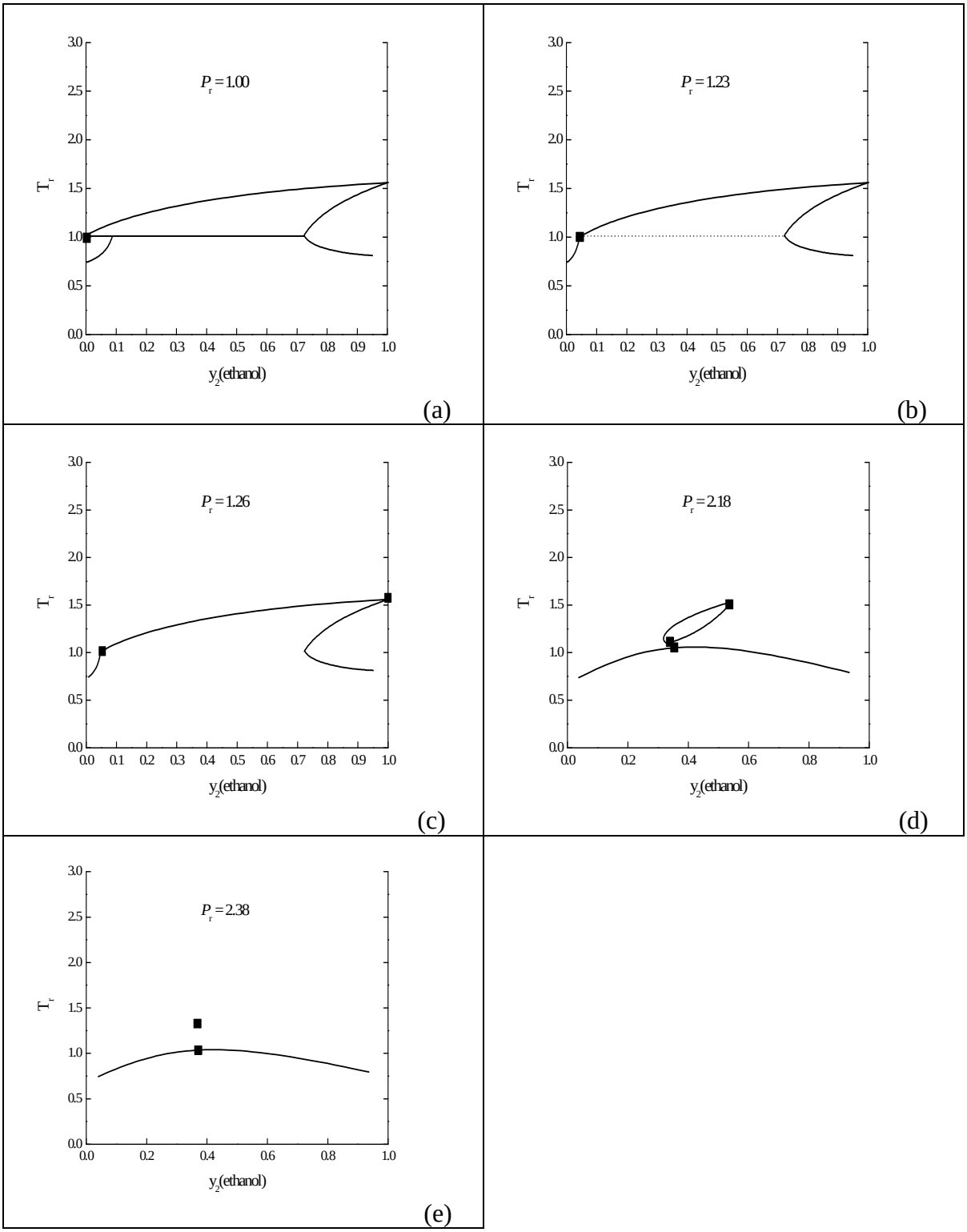

Figure 5-16 T_r, y_2 isobars for type III phase behaviour (Figure 5-13 (f)) of the binary mixture of ethane(1) + ethanol(2): (■) critical point.

5.2.2 Binary Mixture of Methane and n-Hexane

For the binary mixture of methane and n-hexane, with the increase of binary interaction parameter, the phase behaviour changes from type V to type III. The variation trend is shown in a composite figure, Figure 5-17. In Figure 5-17 (a-c), two critical endpoints are obtained, but in Figure 5-17 (d), only one critical endpoint is obtained. The phase behaviour is showing the feature of a type III binary system.

The qualitative T_r, y_2 isobars for type V phase behaviour of the binary system methane + n-hexane are presented in Figures 5-18. It is observed that from type V to type III (Figure 5-16) phase behaviour, the system has a trend to become more immiscible over larger and larger temperature and composition ranges.

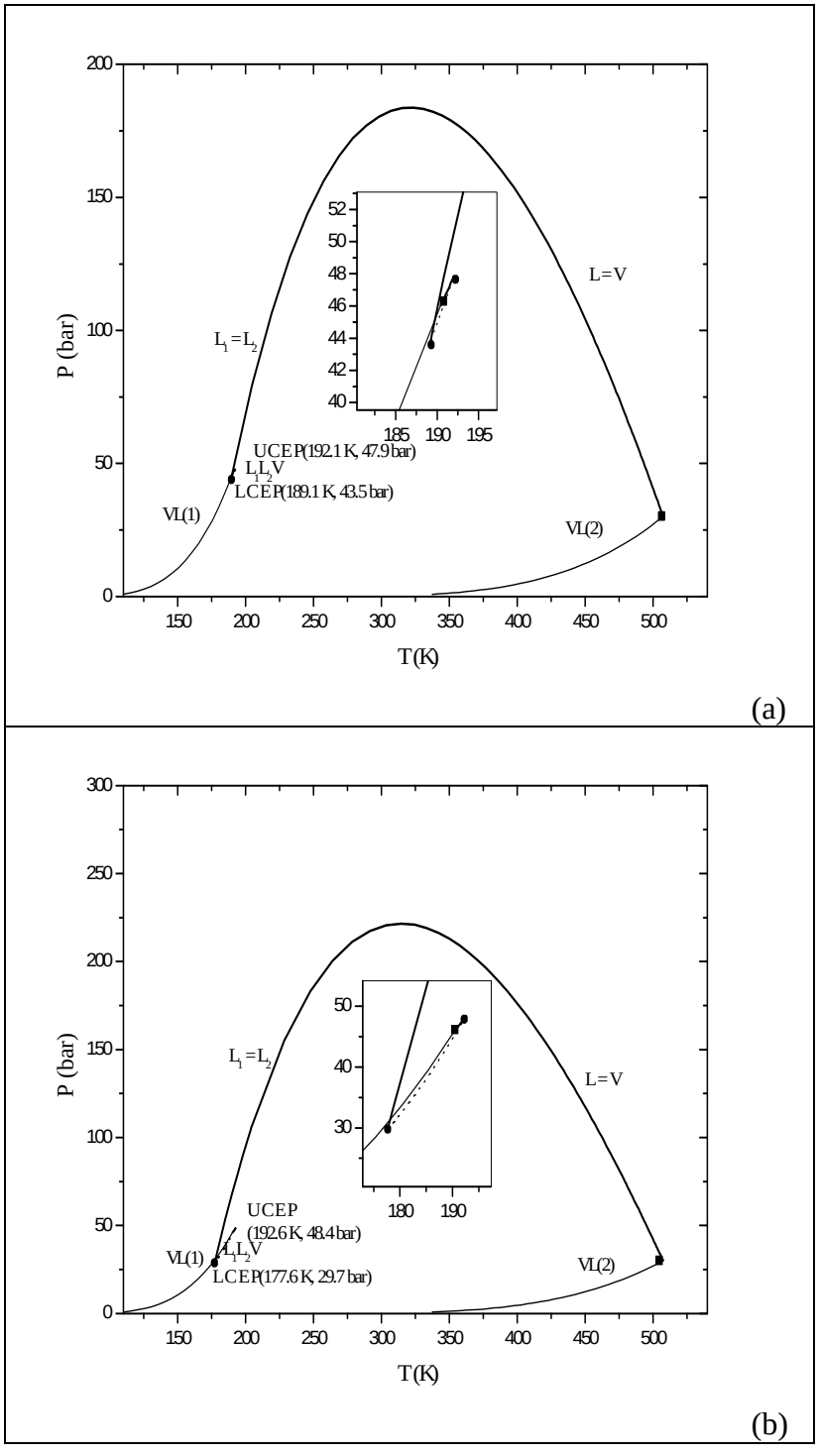

Figure 5-17 *PT* phase diagram of methane(1) + n-hexane(2) with K_{ij} for the Peng-Robinson equation of state being -0.1(a), 0.022(b): (●) calculated critical endpoint, (■) pure component critical point.

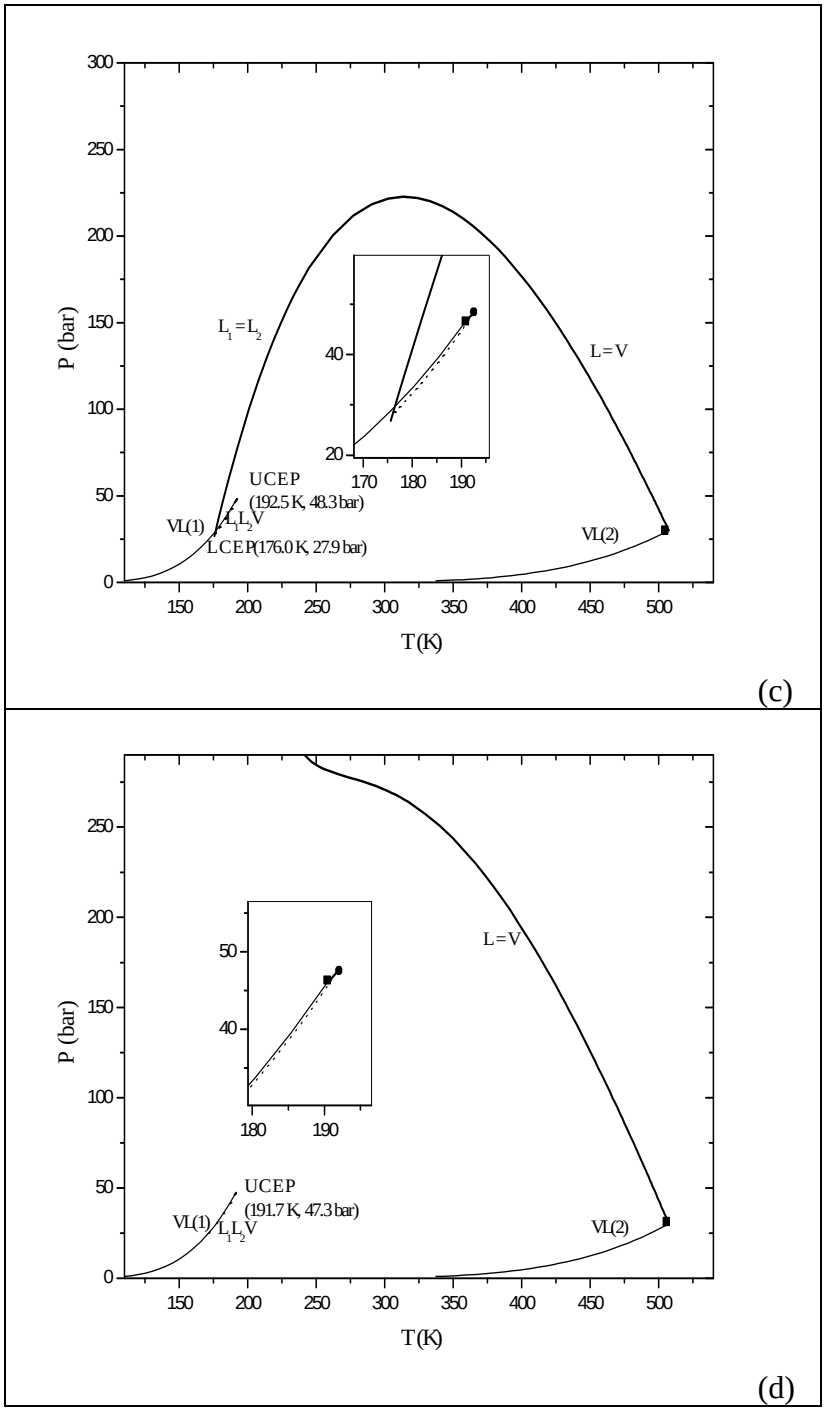

Figure 5-17 *PT* phase diagram of methane(1) + n-hexane(2) with K_{ij} for the Peng-Robinson equation of state being 0.0242(c), 0.08(d): (●) calculated critical endpoint, (■) pure component critical point.

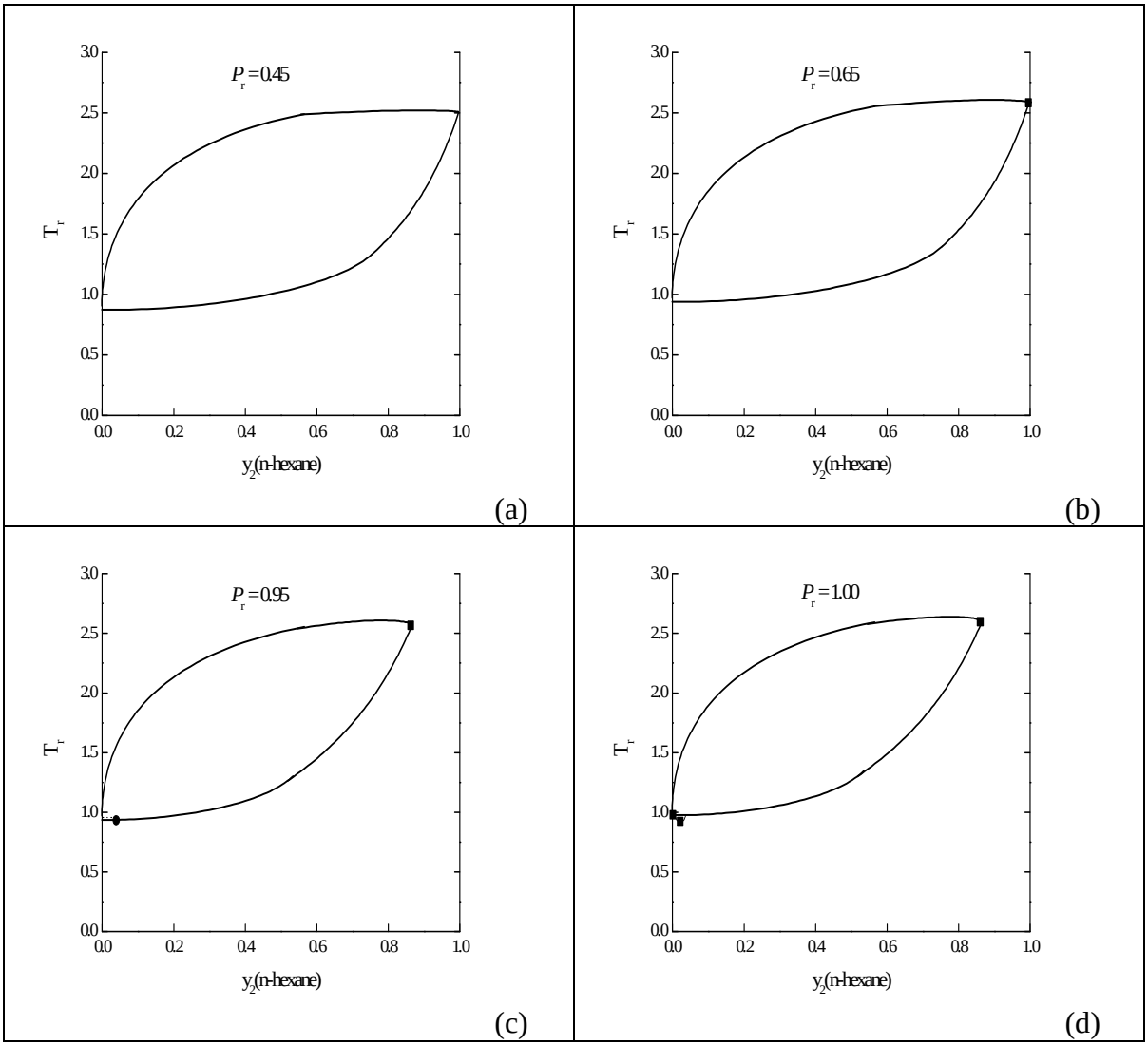

Figure 5-18 T_r, y_2 isobars for type V phase behaviour (Figure 5-17 (a)) of the binary mixture of methane(1) + n-hexane(2): (■) critical point.

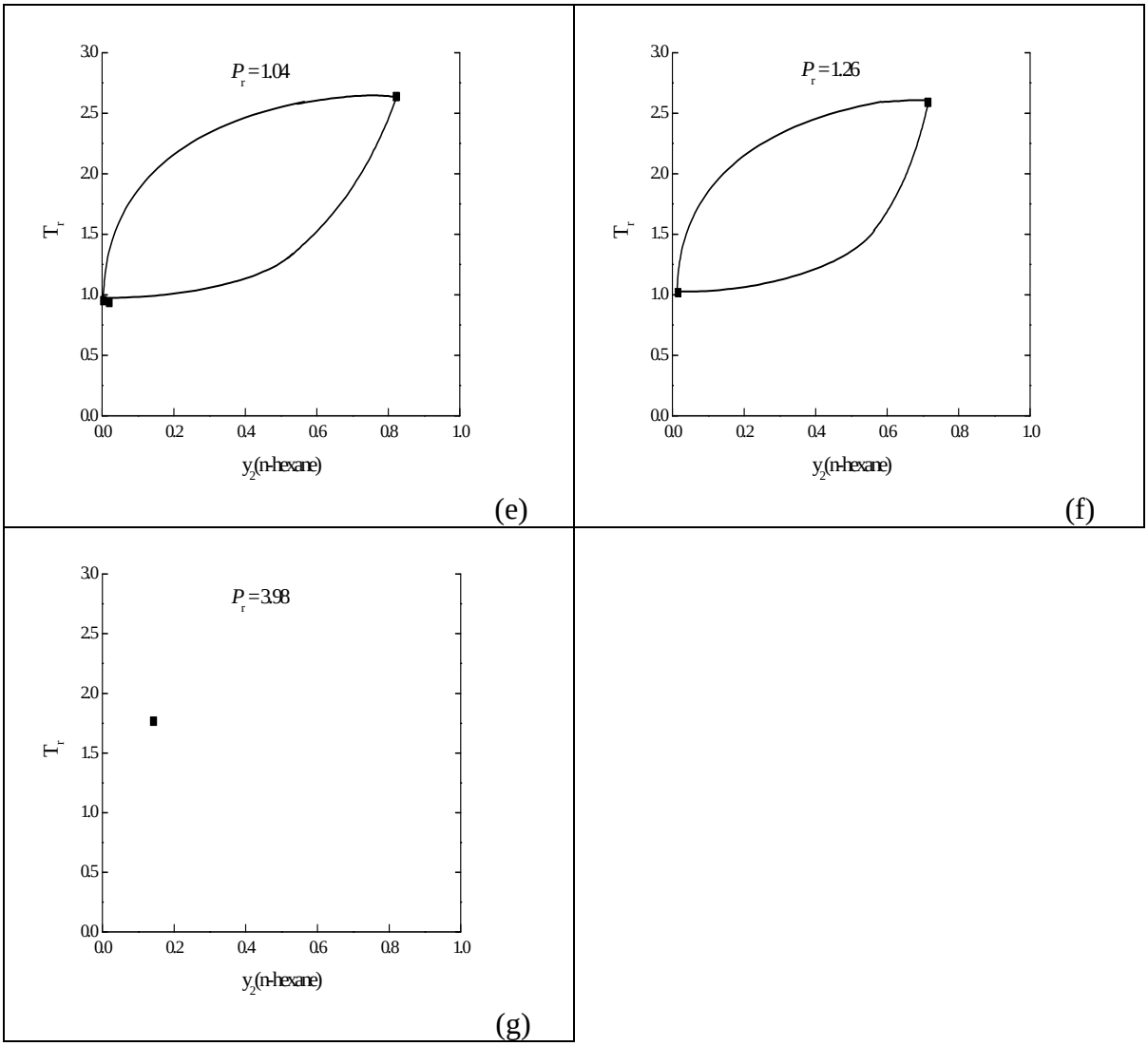

Figure 5-18 T_r, y_2 isobars for type V phase behaviour (Figure 5-17 (a)) of the binary mixture of methane(1) + n-hexane(2): (■) critical point.

The variation trend also matches the results of van Konynenburg and Scott (1980). In Figure 2-8 and 2-9, when the binary interaction parameter increases, λ increases and the phase behaviour changes from type V to type III as well. In Figure 5-17, the corresponding phase behaviour belongs to type III or V. Van

Konynenburg and Scott (1980) noted that the system was probably really type IV with a upper critical solution temperature (UCST) line, which was hard to find because it was hidden below the melting line. The boundary state between type III and type IV phase behaviour is a state with a double critical endpoint as shown in Figure 5-19 (Deiters and Pegg, 1989) and the boundary state between type IV and type V is a state with a ZKP. Because phase diagrams of type IV binary mixtures cannot be predicted with the developed code, such boundary states are not observed with the algorithm as written.

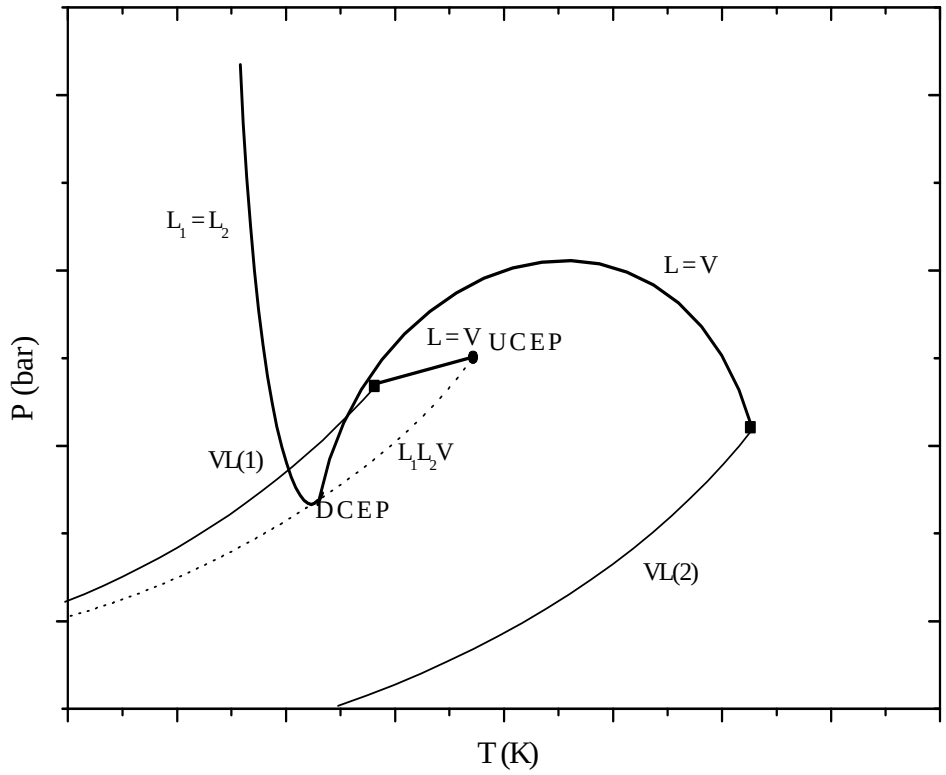

Figure 5-19 The boundary state between type III and type IV phase behaviour: (●) calculated critical endpoint, (■) pure component critical point.

5.3 Code Performance

The convergence criterion, the sensitivity and the corresponding iteration times for evaluation of different component parts in a global phase diagram are presented in this section.

5.3.1 Computing Vapour Pressure of Pure Components

The evaluation of this part of a phase diagram commences from the temperature of the pure component critical point. The subsequent points have a temperature 5℃ lower than the last point. The temperature can also be decreased by other values, which depends on the number of points to be computed. The algorithm uses the Newton-Raphson method to solve equation (3.13). When the convergence criterion is $\left|\ln f_V - \ln f_L\right| < 10^{-6}$, f_V and f_L being the fugacity of pure component in the vapour and liquid phases, respectively, the program iterates 3 to 4 times before it converges. When the vapour pressure obtained at a temperature becomes less than $P_{\min}$, the value of which is read from the data file, the control of the code terminates evaluating the vapour pressure and starts evaluation of other parts of the global phase diagram.

For the binary mixture of ethane and ethanol, when the convergence criterion is changed to $\left|\ln f_V - \ln f_L\right| < 10^{-10}$, the same results as that when the criterion is $\left|\ln f_V - \ln f_L\right| < 10^{-6}$ are obtained except that the iteration count is increased by one for most of the points evaluated. Thus, the algorithm is not sensitive to the convergence criterion.

5.3.2 Evaluating Critical Lines

For L = V critical points, when the convergence criterion is $\left|\frac{v_{n+1}-v_n}{v_{n+1}}\right| < 10^{-5}$, v_{n+1} and v_n being the molar volumes of this iteration and the last iteration, respectively, the code converges after 15 to 17 iterations for critical points with very high pressure ($P > 4.2\sum_i p_{ci}$) for the binary system of methane and n-heptane and the binary system of ethane and ethanol. The value 4.2 was chosen after many calculations according to the pressure values of the most often obtained high pressure critical points and it can also be set larger. The transition to a critical point at a very high pressure is usually a jump. During the 15 to 17 iterations, the pressure jump to high pressure from a lower pressure occurs after 11 iterations. The high pressure critical points obtained are not necessarily valid because, for some compositions of the system, no $L_1 = L_2$ critical point exists, but a $L_1 = L_2$ critical point calculation at such composition may obtain a solution due to false convergence from round off error. Usually such false $L_1 = L_2$ critical point has very large pressure even compared to valid $L_1 = L_2$ critical point. The false results can be determined by drawing the corresponding global phase diagram. At a critical point with very high pressure, the iteration count is relatively large. In the above case, for the first 11 iterations the trial pressure is at a lower value. The trial pressure then jumps to a very high value and the code iterates 4-6 times before it converges. For points at a lower pressure, the number of iterations before convergence is 3 to 4 for the binary system of methane + n-heptane and the ethane + ethanol binary mixture.

For $L_1 = L_2$ critical points, when the convergence criterion is set to $\left|\frac{v_{n+1}-v_n}{v_{n+1}}\right| < 10^{-5}$, for obtained points with very high pressures ($P > 4.2\sum_i p_{ci}$) and with lower pressures, the numbers of iterations for converging are 15 to 17 and 5 to 6, respectively, for binary mixtures of methane + n-heptane and ethane + ethanol.

The numbers of iterations for different types of critical points are summarized in Table 5-1.

Table 5-1: The numbers of iterations for evaluation of different types of critical points. CP represents critical point.

Types of CPs	L = V CPs	$L_1 = L_2$ CPs
CPs at a lower pressure	3-4	5-6
CPs with very high pressure	15-17	15-17

For the above system, when the convergence criterion is changed to $\left|\frac{v_{n+1}-v_n}{v_{n+1}}\right| < 10^{-9}$, the same results as that when the criterion is $\left|\frac{v_{n+1}-v_n}{v_{n+1}}\right| < 10^{-5}$ are obtained except that the number of iterations is increased by 1 for most of the points evaluated. Thus, the algorithm is not sensitive to the convergence criterion.

5.3.3 Calculation of the Critical Endpoint

To increase the chances of finding a non-trivial solution of equation 3.39, two sets of initial estimates are employed here. One is $Y_1 = 10^{-6}, Y_2 = 1 - Y_1$ and the other one is $Y_1 = 1 - 10^{-6}, Y_2 = 1 - Y_1$. When the equilibrium phase of the computed

critical endpoint is a vapour phase, the second set of initial guess is more successful than the first one. When the equilibrium phase is a liquid phase, the first set of initial guesses are more successful. With the two sets of initial guesses, two sets of results will be obtained and the composition of the equilibrium phase corresponds to the results with a smaller value of θ (equation 3.43). This point is very significant for the subsequent evaluation of a three-phase line, because the composition of the incipient equilibrium phase is needed to initialize the three-phase calculation. The convergence criterion is $\sum_i g_i^2 < 10^{-8}$, where $g_i = Y_i^{n+1} - Y_i^n$. The value of $\sum_i g_i^2$ decreases smoothly until the convergence criterion is met. The number of iterations for achieving convergence ranges from 3 to 100. For a binary system of methane + n-heptane with a binary interaction parameter of –0.037, when $\theta < 0$, the number of iterations is 2 before the code achieves convergence.

For the above system with the methane mole fraction being 0.9711, when the convergence criterion is changed, different results from that when the criterion is $\sum_i g_i^2 < 10^{-8}$ are obtained. When the convergence criterion is $\sum_i g_i^2 < 10^{-8}$, the θ obtained is 7.767×10^{-6} . When the convergence criterion is $\sum_i g_i^2 < 10^{-14}$, the θ obtained is 9.019×10^{-10} . When the convergence criterion is set to $\sum_i g_i^2 < 10^{-18}$, the θ obtained equals 1.962×10^{-12} but when the criterion is decreased to $\sum_i g_i^2 < 10^{-20}$, the code converges to a trivial solution because the criterion is so small that it cannot be met at a stationary point because of round off errors.

Therefore the algorithm is sensitive to the convergence criterion. The relationship between convergence criterion and the value of θ is summarized in Table 5-2.

Table 5-2: The relationship between convergence criterion and the value of θ

Convergence criterion	θ
10^{-8}	7.767×10^{-6}
10^{-14}	9.019×10^{-10}
10^{-18}	1.962×10^{-12}
10^{-20}	0

5.3.4 Calculation of Three-Phase Line

Usually before the evaluation of a three-phase line, a critical endpoint is obtained. At the critical endpoint, a critical phase is in equilibrium with another phase, the equilibrium phase. The initial estimates of temperature and pressure for the first three-phase point are set with the corresponding values at the critical endpoint.

When the convergence criterion is $\sum_i g_i^2 < 10^{-12}$, the program usually converges after 4 to 5 iterations. Along the three-phase line, different points usually have iteration counts that differ less, but when the highest MVC mole fraction in the three phases of a three-phase point obtained is larger than 0.99999, the number of iterations increases to nearly 30 to 100. At such points, the deviation decreases very slowly at first. For example, for the binary mixture of ethane + ethanol, when the value of the binary interaction parameter is 0.0362, the number of iterations is

38. For the first 34 iterations, the error $\sum_i g_i^2$ is close to 0.02 and decreases by 0.0002 each time. After the 35th iteration, the code converges very fast because only after the trial value of the solution is close enough to the root, will the Newton-Raphson method converge quadratically.

For the above system, when the convergence criterion is changed to $\sum_i g_i^2 < 10^{-26}$, the same results as that when the criterion is $\sum_i g_i^2 < 10^{-12}$ are obtained except that the number of iterations is increased by 2 for most of the points evaluated. Therefore the algorithm is not sensitive to the convergence criterion.

All in all, a code with good performance to predict different types (I, III, V and II) of phase behaviour has been successfully developed. With the code, different types of phase behaviour are explored and a good insight into the phase behaviour of binary mixtures has been obtained.

5.4 Program Exceptions

5.4.1 Identifying Type V Phase Behaviour Wrongly Taken as Type III (Pressure Exceptions)

The developed program converges fast and can determine the types of binary mixtures automatically. But, when it calculates the phase behaviour of the methane + n-hexane binary mixture, it is observed that the program may mistake a type V system as type III. For example, when the binary interaction parameter of the binary system of methane + n-hexane becomes 0.02418, critical points with very high pressure (the criterion for very high pressure is $P > 4.2\sum_i P_{ci}$; the value is

too low in this case, because the very high pressure obtained will be much larger than this value) is obtained in the evaluation of L = V critical line. The control of the code will determine that this critical line being evaluated is one extending to very high pressure and because no three-phase line connects it with the other one commencing from the critical point of the pure MVC, the control of the code then suspends the computation of the above critical line and starts evaluation of the other one. The calculation sequence is changed, starting from the point with MVC mole fraction as 0.99999. The following points have decreasing MVC mole fractions. Then the upper critical endpoint is determined and computation of the three-phase line begins. Finally two critical endpoints are obtained. This is a sign of the type V system. It is difficult to determine now which type, type III or V, the binary system belongs to.

A technique was found to solve the above exception. When a point with very high pressure is found, the control of the code does not transfer to computation of the critical line on the other side immediately, but returns to the last lower pressure stable point, decreases the step size and continues the computation. If critical points with very high pressure are found again, the control of the code also returns to the last lower pressure stable point, decreases the step size and continues the computation If a critical endpoint satisfying the convergence criterion is obtained, the control of the code will transfer to the evaluation of three-phase line. Then the second critical endpoint will be determined and the control transfers to the evaluation of the critical line on the other side with MVC mole fraction increasing. Thus, a type V phase diagram for the binary system is obtained.

In the above computation, the critical points in the zone near the point with very high pressure are difficult to handle because many points in the zone have very high pressure and evaluation of the critical points fail because the number of iterations exceeds the pre-defined maximum value or the molar volumes obtained are less than b_m , or the temperature obtained is less than zero. After much debugging and modification work, the code section to determine the critical endpoint in the above zone has been finished and added to the former version of the code. Figure 4-16 shows the flowchart of the algorithm. It should be noted that this part of code is only for determining critical endpoints in the above zone.

The code is employed to predict the phase behaviour of methane binary mixture of n-hexane and binary system of ethane + ethanol. The computation results show the transition between one type of phase behaviour and another. Usually the evaluation of phase behaviour of the binary system near a boundary state is difficult because the type of the phase behaviour may be wrongly determined. The newly modified program is capable to obtain true results for binary mixtures near that state. It can identify type V phase behaviour wrongly taken as type III phase behaviour with the former version of the code.

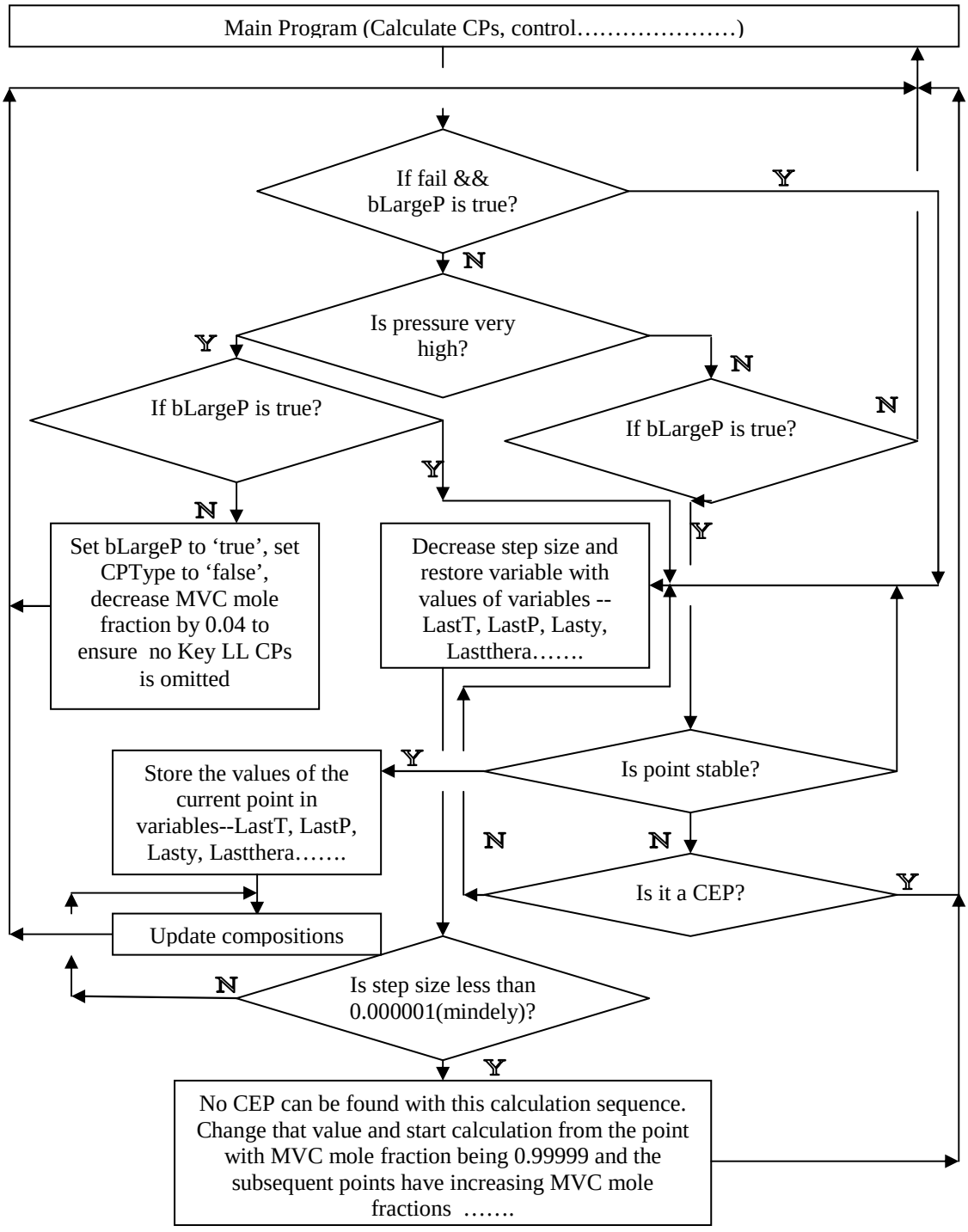

Figure 5-20: Flowchart for determining the critical endpoint in the zone near points with very high pressure. bLargeP is a variable to show if a critical point with very high pressure has been obtained. If obtained, bLargeP is changed to TRUE from FALSE. CPType is a boolean variable showing the type of critical point. LastT, Last P, etc. are used to store the data of the last critical point.

5.4.2 Other Exceptions

In the function to evaluate the fugacity of components of a mixture, a "divide by zero" or "logarithm of zero" exception will occur if the fugacity of a pure component or the fugacity of a component whose composition is very small is computed with the function. In these cases, the divisor may be zero or rather small, for example, less than 10^{-30}. After plenty of calculations were done, the value 10^{-30} was chosen. When a numerator in the function to calculate fugacity of components is smaller than 10^{-30}, the program determines that a exception occurs. The technique employed to handle the exception is to set the value of these quotients in the case of division by zero exception and the value of the logarithm in the case of logarithm of zero error, with a pre-defined constant to indicate an exception has occurred. The value of the variable set with the pre-defined constant will not be used in calculation afterwards. Using the technique, the code can run properly when it evaluates the fugacity of a pure component or the fugacity of a component whose composition is small.

Another exception occurs in the function to decompose the coefficients matrix of equation groups using the linear solver. When the largest absolute value of the data in one line of the matrix is close to zero, the exception takes place. To deal with the exception, when the largest absolute value of the data in one line of the matrix is less than a rather small value, for example, 10^{-30}, a variable is set with a pre-defined constant and the control exits the function. When the code needs to use the returned results of the function, it is essential to determine the value of the

variable mentioned above. If it is not equal to the pre-defined constant, execution will proceed normally. If it is equal to the pre-defined constant, the control of the code will skip the evaluation of the current point and commence computation of the next point until a point with no exception encountered in the calculation is obtained. If no such points are obtained over the entire composition range, the program will exit or transfer to computation of the other parts of a global phase diagram. The code is ensured not to crash with this technique to handle the exception.

5.5 Type IV, VI and VII Phase Behaviour

The global phase diagrams of type I, II, III and V have been obtained. From the global phase diagrams developed by van Konynenburg and Scott (1980), it is observed that the region for type IV phase behaviour is rather small, which indicates that the exploration of type IV phase behaviour will be difficult. In Chapter 2, it is presented that one additional $L_1 = L_2$ critical line and one additional three-phase line are present in type IV phase diagrams in addition to the lines in type V phase diagrams. Phase diagrams of type V phase behaviour have been computed successfully. The $L_1 = L_2$ critical phenomenon has been carefully explored with the developed code for binary mixtures researched, especially the binary mixture of methane + n-hexane. No additional $L_1 = L_2$ critical line was found.

The binary systems explored in the project are from the petroleum processing field. Type VI and VII phase behaviour are associated with aqueous or strongly polar mixtures (Wang and Sadus, 2000). Such kinds of phase behaviour

can be developed with equations of state that incorporate a temperature related term or consider the effects of hydrogen bonding (Wang and Sadus, 2000). The Peng-Robinson equation can be employed to predict type VI and VII phase behaviour, but the results may have large deviations (Polishuk et al. 2002) from experimental data. However, comparison to experimental results was not within the scope of this work.

6. CONCLUSIONS AND RECOMMENDATIONS

Global phase diagrams of binary systems in *PT* space are useful. Many researchers do research on phase diagrams. In this study, an algorithm capable of determining the types of the explored binary mixtures was developed to predict global phase diagrams automatically. To evaluate a global phase diagram, algorithms to compute different parts of a global phase diagrams were developed first. Those algorithms were then incorporated and an algorithm and the corresponding code for developing global phase diagrams of binary systems in *PT* space were developed successfully.

The Newton-Raphson method was employed to determine critical lines, three-phase lines and vapour pressure lines, but in the evaluation of the equilibrium phase, the successive substitution method was used. The setting of initial estimates for calculation of different parts, especially three-phase lines, of a global phase diagram is difficult. The algorithm developed in the project is capable of solving the problem. After a critical endpoint is obtained in the calculation of critical lines, the code commences the evaluation of a three-phase line. The initial guesses for the first three-phase point are set with data of the critical endpoint. The subsequent

three-phase points are all set with the corresponding data of the last three-phase point.

6.1 Evaluating Type I, II, III and V Phase Diagrams

Using the developed code, one can generate phase diagrams corresponding to type I, II, III and V phase behaviour.

If in the evaluation of the L = V and $L_1 = L_2$ critical points, no critical endpoints or critical point with very high pressure are found, the binary system belongs to type I system, for example, the binary mixture of ethane + ethanol with binary interaction parameter being 0.0090. In type I phase diagrams, no three-phase lines are present. The computation is relatively straightforward.

If a critical endpoint and thus a three-phase line is obtained in the $L_1 = L_2$ critical point evaluation, the system is a type II system, for example, the binary mixture of ethane + ethanol with the binary interaction parameter being 0.0362. The critical endpoint of type II phase diagram is obtained in the calculation of the $L_1 = L_2$ critical points with algorithm to evaluate equilibrium phase. Then the control of the code commences evaluation of the three-phase line.

If in the calculation of the L = V critical line, critical points with very high pressure are obtained, and a critical endpoint is then obtained in the calculation of the L = V critical line starting from the critical point of the pure MVC, then the system is type III system, for example, the binary mixture of ethane + ethanol with the binary interaction parameter being 0.08.

If two critical endpoints are obtained in L = V critical point computation and no critical endpoint is found in the $L_1 = L_2$ critical point calculation, the corresponding system belongs to type V according to the classification scheme of van Konynenburg and Scott (1980). For example, the binary mixture of n-heptane + methane with binary interaction parameter being –0.037 was found to be a type V system. In the calculation of the critical line commencing from the pure solute critical point, the first critical endpoint, a lower critical endpoint, is obtained. Then the control of the code transfers to evaluation of the three-phase line. After the second critical endpoint is determined, the control of the code commences the evaluation of the critical line starting from the pure MVC critical point.

6.2 Transitions between Different Types of Phase Behaviour

For the same binary mixture with different binary interaction parameters for the Peng-Robinson equation of state, different types of phase behaviours are observed.

The changing trend of the phase behaviour for binary systems with the same components was explored when the binary interaction parameter changes. It was observed from the calculation results that with the increase of the binary interaction parameter, the phase behaviour may transfer from type I to type II to type III or from type V to type III. The trend matches the results of van Konynenburg and Scott (1980).

The boundary state between type I and type II phase behaviours is a state with a ZKP. The boundary state between type II and type III, and that between type V and type III, is a state with a double critical endpoint.

6.3 Future Work

- It is difficult to predict type IV phase behaviour, because $L_1 = L_2$ critical lines are hard to find. If the homotopy-continuation method (Section 2.4.3) is employed to evaluate the critical line, a single initial guess can obtain multiple solutions. Using the homotopy-continuation method, if a $L_1 = L_2$ critical point is present except the L = V critical point, one is more likely to find out the $L_1 = L_2$ critical point. This avoids missing any $L_1 = L_2$ critical lines in the evaluation of a global phase diagram and different types of phase behaviour can be obtained.
- The Peng-Robinson equation of state can be employed to predict type VI and type VII phase diagrams. The homotopy-continuation method (Section 2.4.3) should also be employed to ensure the finding of all $L_1 = L_2$ critical lines.

REFERENCES

Antoine, C. Vapour pressures: new relation between pressures and temperatures. *C. R. Hebd. Seances Academic Science* (*Comptes rendus hebdomadaires des sèances de l´ Acadèmie des Sciences*). 107, 1888, 681-684.

Baker, L. E.; Pierce, A. C.; Luks, K. D. Gibbs energy analysis of phase equilibria. *Society of Petroleum Engineers Journal*. 22(5), 1982, 741-742.

Chang, H. L.; Hurt, L. J.; Kobayashi, R. Vapour-liquid equilibria of light hydrocarbons at low temperatures and high pressures: the methane-n-heptane system. *AICHE Journal*. 12, 1966, 1212-1216.

Choi, E. J. and Yeo S. D. Critical properties for carbon dioxide plus n-alkane mixtures using a variable-volume view cell. *Journal of Chemical Engineering Data*. 43(5), 1998, 714-716.

Christov, M. and Dohrn, R. Review-High-pressure fluid phase equilibria Experimental methods and systems investigated (1994–1999). *Fluid Phase Equilibria*. 202, 2002, 153-218.

Chueh, P. L. and Prausnitz, J. M. Vapour-liquid equilibria at high pressures: vapour-phase fugacity coefficients in non-polar and quantum-gas mixtures. *Industrial Engineering Chemistry Fundamentals*. 6(4), 1967, 492-498.

Degance, A. E. Ab initio equation of state phase equilibria computation via path continuation. *Fluid phase Equilibria*. 89(2), 1993, 89-303.

Deiters, U. K. and Pegg, I. L. Systematic investigation of the phase behaviour in binary mixtures: I. Calculations based on the Redlich-Kwong equation of state. *Journal of Chemical Physics*. 90(11), 1989, 6632-6641.

Gauter, K.; Heidemann, R. A. and Peters C. J. Modeling of fluid multiphase equilibria in ternary systems of carbon dioxide as the near-critical solvent and two low-volatile solutes. *Fluid Phase Equilibria*. 158, 1999, 133-141.

Gubblns, K. E.; Shlng, K. S. and Streett, W. B. Fluid phase equilibria: experiment, computer simulation and theory. *Journal of Physical Chemistry*. 87(23), 1983, 4573-4585.

Heidemann, R. A. and Khalil, A. M. The calculation of critical points. *AICHE Journal*. 26(5), 1980, 769-780.

Heidemann, R. A. and Michelsen, M. L. Instability of successive substitution. *Industrial Engineering Chemistry Resarch*. 34, 1995, 958-966.

Huckaby, D. A.; Shinmi, M.; Ausloos, M. and Clippe, P. Enantiomeric phase-separation in a lattice gas-model - Guggenheim approximation. *Journal of Chemical Physics*. 84(9), 1986, 5090-5094.

Kraska, T. and Deiters U. K. Systematic investigation of the phase behaviour in binary fluid mixtures. II. Calculations based on the Carnahan-Starling-Redlich-Kwong equation of state. *Journal of Chemical Physics*. 96(1), 1992, 539-547.

Kordikowski, A.; Robertson, D. G.; AguiarRicardo, A. I.; Popov, V.K.; Howdle, S.M. and Poliakoff, M. Probing vapour/liquid equilibria of near-critical binary gas mixtures by acoustic measurements. *Journal of Physical Chemistry*. 100(22), 1996, 9522-9526.

Kordikowski, A.; Robertson, D. G.; Poliakoff, M.; DiNoia, T. D.; McHugh, M.; and AguiarRicardo, A. Acoustic determination of the critical surfaces in the ternary systems CO_2 + CH_2F_2 + CF_3CH_2F and CO+C_2H_4+CH_3CHCH_2 and in their binary subsystems. *Journal of Physical Chemistry B*. 101(30), 1997, 5853-5862.

Lin, W. -J. and Seader, W. D. Computing multiple solutions to systems of interlinked separation columns. *AICHE Journal*. 33(6), 1987, 886-897.

Luszczyk, M. Vapour-liquid-liquid equilibria for the system 3-methoxypropionitrile plus water in the vicinity of the upper critical endpoint. *Physical Chemistry Chemical Physics*. 4(19), 2002, 4724-4731.

Michelsen, M. L. The isothermal flash problem. part I: stability. *Fluid Phase Equilibria*. 9, 1982, 1-19.

Michelsen, M. L. Calculation of critical points and of phase boundaries in the critical region. *Fluid Phase Equilibria*. 16, 1984, 57-76.

Redlich, O. and Kwong, J. N. S. On the thermodynamics of solutions. V. an equation of state - fugacities of gaseous solutions. *Chemical Reviews*. 44, 1949, 233-244.

Reid, R. C.; Prausnitz, J. M. and Poling, B. E. *The Properties of Gases & Liquids*, McGraw-Hill Book Company, Fourth edition, New York, 1987.

Peng, D. -Y. and Robinson, D. B. A New Two Constant Equation of State. *Industrial Engineering Chemistry Fundamentals*. 15(1), 1976, 59-64.

Peng, D. -Y. and Robinson, D. B. A rigorous method for predicting the critical properties of multi-component mixtures from an equation of state. *AICHE Journal*. 23, 1977, 137-144.

Plybon, B. F. *An Introduction to Applied Numerical Analysis*. PWS-KENT Publishing Company, Boston, 1992.

Polishuk, I.; Wisniak, J. and Segura H. Closed loops of liquid–liquid immiscibility predicted by semi-empirical cubic equations of state and classical mixing rules. *Physical Chemistry Chemical Physics*. 4, 2002, 879-883.

Ribeiro, N. and Aguiar-Ricardo, A. A simple acoustic probe for fluid phase equilibria: application to the CO_2+$N(C_2H_5)_3$ system. *Fluid Phase Equilibria*. 185(1-2), 2001, 295-303.

Scalise, O. H.; Gianotti, R. D. and Zarragoicoechea G. J. Azeotropic states in the CO_2-C_2H_6 mixture from the hard sphere Lennard-Jones quadrupolar molecular model. *Journal of Chemical Physics*. 91(7), 1989, 4273-4277.

Specovius, J.; Leiva, M. A.; Scott, R. L. and Knobler, C. M. Tricritical phenomena in "quasi-binary" mixtures of hydrocarbons. 2. Binary Ethane Systems. *Journal of Physical Chemistry*. 85(16), 1981, 2313-2316.

Straver, E. J. M.; de Roo, J. L., Peters, C. J. and Arons J. D. 3-phase behaviour in binary-mixtures of near-critical propane and triglycerides. *ACS Symposium Series*, 514, 1993, 46-54.

Straver, E. J. M.; de Roo, J. L.; Peters, C. J. and Arons, J. D. Phase behaviour of the binary system propane and tristearin. *Journal of Supercritical Fluids*. 11(3), 1998, 139-150.

Stryjek, R. Critical properties of the N_2 ,CH_4 and C_2H_6+n-alkane mixtures, *Fluid Phase Equilibria*, 87(1), 1993, 99-114.

Suleimenov, O. M.; Panagiotopoulos, A. Z. and Seward T. M. Grand canonical Monte Carlo simulations of phase equilibria of pure silicon tetrachloride and its binary mixture with carbon dioxide. *Molecular Physics*. 101(21), 2003, 3213-3221.

Sun, A. C. and Seider, W. D. Homotopy-continuation method for stability analysis in the global minimization of the Gibbs free energy. *Fluid Phase Equilibria*, 103, 1995, 213-249.

van Konynenburg, P.H. and Scott, R. L. Critical lines and phase equilibriu in binary Van Der Waals mixtures. *Philosophical Transactions of the Royal Society of London*. Series A, *Mathematical and Physical Sciences*. 298(9), 1980, 495-540.

Wagner, W.; Evers, J. and Pentermann, W. New vapor-pressure measurements and a new rational vapor-pressure equation for oxygen, *Journal of Chemical Thermodynamics*, 8(11), 1976, 1049-1060.

Wang J. -L. and Sadus R. J. Phase behaviour of binary fluid mixtures: a global phase diagram solely in terms of pure component properties. *Fluid Phase Equilibria*. 214, 2003, 67–78.

Yaws C. L. Chemical properties handbook, *McGraw Hill Publishers*, New York, 1999.

APPENDIX

Table A1: Critical properties, mole weight (M) and acentric factors (ω) of pure components studied in the project (Yaws, 1999)

Formula	Name	M (kg/kmol)	T_c (K)	P_c (bar)	V_c (cm^3/mol)	ω
CH_4	methane	16.043	190.4	46	99.2	0.0109
C_2H_6	ethane	30.07	305.4	48.8	148.3	0.0979
C_3H_8	propane	44.094	369.8	42.5	203.0	0.1518
C_6H_{14}	n-hexane	86.178	507.5	30.1	370.0	0.299
C_7H_{16}	n-heptane	100.205	540.3	27.4	432.0	0.3494
C_2H_6O	ethanol	46.069	513.9	61.4	167.1	0.643
$C_{14}H_{10}$	phenanthrene	178.233	869.3	29.0	584.0	0.495